
# BRNO UNIVERSITY OF TECHNOLOGY

VYSOKÉ UČENÍ TECHNICKÉ V BRNĚ

## FACULTY OF ELECTRICAL ENGINEERING AND COMMUNICATION

FAKULTA ELEKTROTECHNIKY
A KOMUNIKAČNÍCH TECHNOLOGIÍ

## DEPARTMENT OF ELECTRICAL POWER ENGINEERING

ÚSTAV ELEKTROENERGETIKY


# CLASSIFICATION AND MODELLING OF LED LIGHT SOURCES IN TERMS OF SENSITIVITY TO SUPPLY VOLTAGE FLUCTUATIONS

KLASIFIKACE A MODELOVÁNÍ LED SVĚTELNÝCH ZDROJŮ Z HLEDISKA CITLIVOSTI NA KOLÍSÁNÍ NAPÁJECÍHO NAPĚTÍ

MASTER'S THESIS
DIPLOMOVÁ PRÁCE


AUTHOR
AUTOR PRÁCE

**Tomáš Hudáč**

SUPERVISOR
VEDOUCÍ PRÁCE

**prof. Ing. Jiří Drápela, Ph.D.**



BRNO 2023

VYSOKÉ UČENÍ TECHNICKÉ V BRNĚ
FAKULTA ELEKTROTECHNIKY A KOMUNIKAČNÍCH TECHNOLOGIÍ

# Diplomová práce

magisterský navazující studijní program **Elektroenergetika**

Ústav elektroenergetiky

***Student:*** Tomáš Hudáč ***ID:*** 214378

***Ročník:*** 2 ***Akademický rok:*** 2022/23

**NÁZEV TÉMATU:**

## Klasifikace a modelování LED světelných zdrojů z hlediska citlivosti na kolísání napájecího napětí

**POKYNY PRO VYPRACOVÁNÍ:**

1. Příčiny blikání světelných zdrojů, klasifikace kolísání napětí způsobující blikání světelných zdrojů, včetně reálných kolísání napětí; charakterizace a přehled citlivosti a odolnosti světelných zdrojů na kolísání a změny napětí
2. Průzkum trhu LED světelných zdrojů, metodika selekce zkušebních vzorků
3. Realizace souboru zkoušek charakterizující vlastnosti vybraného souboru LED a jejich vyhodnocení
4. Klasifikace LED/LED driverů podle jejich citlivosti na kolísání napětí
5. Vývoj modelu vybraného LED zdroje
6. Ověření modelu simulacemi

**DOPORUČENÁ LITERATURA:**

doporučená literatura podle pokynů vedoucího závěrečné práce

***Termín zadání:*** 6.2.2023 ***Termín odevzdání:*** 22.5.2023

***Vedoucí práce:*** prof. Ing. Jiří Drápela, Ph.D.

**prof. Ing. Petr Toman, Ph.D.**
předseda rady studijního programu

# Abstract

The aim of this thesis is to investigate and characterise the flicker performance of retrofit LED lamps currently available on the market, and to develop a model of an LED lamp. To find representative samples of LED lamps, market analyses has been carried out which shows the bestselling types. The results of the analysis have been obtained 31 samples. With different LED technologies and different power control options, such as wireless or triac. By performing measurements under the ideal power supply conditions and by disassembling certain samples have been overall identified 4 main classes with different driver topologies. Further were conducted tests on their flicker sensitivity and flicker immunity. By acquiring results from tests each driver topology has been rated by its overall flicker performance. In the end of a thesis Simulink is proposed model of a lamp which successfully simulated IH GF curves in comparison with measured values.

# Keywords

Flicker, LED lamp, Incandescent bulb, gain, sensitivity, immunity, IH,

# Abstrakt

Cieľom tejto práce je preskúmať a charakterizovať celkovú odolnosť voči flickru v LED svetelných zdrojoch dostupných na súčasnom trhu, a vytvoriť modelu LED svetelného zdroja. Na nájdenie reprezentatívnych vzoriek LED svetelných zdrojov, bola prevedená analýza online trhu, ktorá ukazuje najpredávanejšie typy. Na základe výsledkov z analýzy sa získalo 31 vzoriek. S rôznymi LED technológiami a rôznymi možnosťami regulácie výkonu, napríklad bezdrôtovo alebo triakom. Vykonaním meraní za ideálnych podmienok napájania a rozobraním niektorých vzoriek boli celkovo identifikované 4 hlavné triedy s rôznymi topológiami napájacích obvodov. Ďalej sa vykonali testy ich citlivosti na blikanie a imunitou voči blikaniu. Na základe získaných výsledkov testov bola každá topológia ovládača ohodnotená podľa jej celkovej odolnosti voči blikaniu. V závere práce bol navrhnutý model v Simulinku, ktorý úspešne simuloval IH GF krivky v porovnaní s nameranými hodnotami

# Klíčová slova

Flicker, LED zdroj, žiarovka, citlivosť, odolnosť, IH

# Bibliographic citation

HUDÁČ, Tomáš. Classification and modelling of LED light sources in terms of sensitivity to supply voltage fluctuations. Brno, 2023. Available also: https://www.vut.cz/studenti/zav-prace/detail/151313. Master's thesis. Brno University of Technology. Faculty of electrical engineering and communication. Faculty of Electrical power engineering. Supervisor Jiří Drápela.

# Author's Declaration

| | |
|---|---|
| **Author:** | Tomáš Hudáč |
| **Author's ID:** | 214378 \| |
| **Paper type:** | Master's Thesis |
| **Academic year:** | 2022/23 |
| **Topic:** | Classification and modelling of LED light sources in terms of sensitivity to supply voltage fluctuations |

I declare that I have written this paper independently, under the guidance of the advisor and using exclusively the technical references and other sources of information cited in the project and listed in the comprehensive bibliography at the end of the project.

As the author, I furthermore declare that, with respect to the creation of this paper, I have not infringed any copyright or violated anyone's personal and/or ownership rights. In this context, I am fully aware of the consequences of breaking Regulation S 11 of the Copyright Act No. 121/2000 Coll. of the Czech Republic, as amended, and of any breach of rights related to intellectual property or introduced within amendments to relevant Acts such as the Intellectual Property Act or the Criminal Code, Act No. 40/2009 Coll., Section 2, Head VI, Part 4.

.

Brno, December 18, 2023 ----------

author's signature

# Acknowledgement

Foremost, I am sincerely grateful to my supervisor Prof. Ing. Jiři Drápela, Ph.D for the invaluable advice, intellectual support, guidance, and patience, which truly led me to enjoy all research and laboratory work. His shared knowledge and experience contributed to my own ideas, views and advancing in this field of study. Secondly I would like to thank Patrik Smihula for his relentless encouragement, effective revision and consistent support.


Brno, December 18, 2023 ----------

Author's signature

# Contents

# FIGURES

# TABLES

# INTRODUCTION

Artificial illumination has a very important role in human's lives. It ensures that every activity or work could be done with no regard to natural light conditions. Every technology develops and artificial illumination is no exception. Its first modern revolutions could be dated back to the invention of incandescent lamps and later to the invention of fluorescent light sources. Fifteen years ago, both technologies were on the TOP of the market [1]. Their dominance and highest market share started decreasing by introduction of new light sources on the public market based on high intensity white light emitting diodes (LED). In Europe LED light sources took over the vast majority of the LED lamps market [1]. This high paced change didn't come with no outcomes. As it was shown in [2], this situation for now ended up to the nowadays usage of at least 8 different driver circuit types. Generally, every type of LED lamp has different sensitivity to voltage fluctuations depending on the used topology of the driver circuit. Diversity among LED driver circuits is even higher than among compact fluorescent lamps, which after years of development matured to much more similar ballasts circuits [2]. Moreover, parameters like flicker index and percent flicker, which may have negative health effects, depend on their chosen driver topology too, and according to [3] their magnitudes vary greatly among available LED lamps. It can be concluded that in the current situation on the market neither the same topology and consequently nor the same parameters (flicker sensitivity, flicker index, percent flicker, etc.) are granted even between two similar looking LED lamps, from the same brand and with similar nominal power.

The aim of this thesis is to describe main causes of voltage fluctuations and to evaluate flicker performance of LED lamps available on market, together with describing their driver topology. Results found out by thesis should serve as a detailed overview across all varieties of parameters which describes flicker performance, frequency spectra of luminous flux, frequency spectra of drawn current and spectral parameters of radiant flux. Flicker performance will be evaluated by measuring sensitivity, immunity and in steady-state under ideal supply conditions by SVM and $P_{st,LM}$. By current waveforms and in some cases by disassembling will be identified all topologies of drivers. Every topology found among obtained LED lamps will be described by its flicker performance from measured results. Further on the end of the thesis will be a proposed model of LED lamp which can simulate gain factor curves of LED lamps with certain topology.

# 1. LIGHT FLICKER, CAUSES AND CLASSIFICATION

Flicker is defined as perception of visual unsteadiness induced by temporal and even spatial fluctuation of luminance or spectral distribution for a static observer in a static environment. Fluctuation is caused by power supply, light source itself or by other influencing factors. Fluctuation could be periodic or non-periodic [4].

## 1.1 Voltage fluctuations, AM modulation

Main cause of voltage fluctuations in the power grid can be described by using a simple circuit in Figure 1.

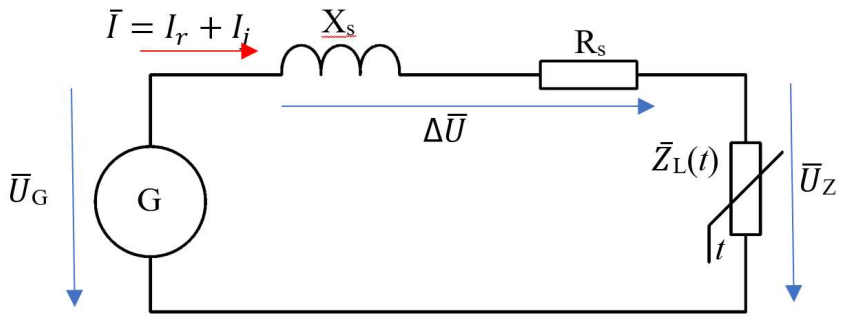


Figure 1 Equivalent schematic of power grid.

Placing $\bar{U}_G$ on the real axis as reference and considering the inductive character of impedance $\bar{Z}_L(t)$. Current and voltages from Figure 1 could be viewed in the complex plane as it is pictured in Figure 2. Using this representation is easier to understand relationships between load which in this case determines fluctuations of overall current $\bar{I}$ in time and voltage drop $\Delta\bar{U}$ which in complex summation with $\bar{U}_G$ forms voltage on the load $\bar{U}_Z$.

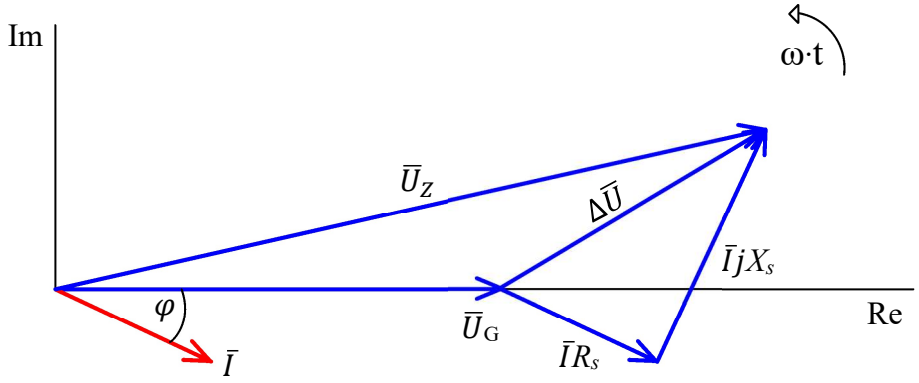


Figure 2 Current and voltages from Figure 1 described in complex plane.

To find mathematical representation how current $\bar{I}$ and its components affect voltage drop across the power line is needed to describe absolute value resp. length of the phasor $\Delta\bar{U}$ which could be for the sake of simplicity and further explanation approximated as:

$$\Delta U \cong R_s \cdot I_r + X_s \cdot I_j \tag{1.1}$$

- $I_j$ represents imaginary part of current $\bar{I}$
- $I_r$ represents real part of current $\bar{I}$
- $X_s$ serial inductive reactance of power line
- $R_s$ serial resistance of power line

Absolute voltage on load or on consumers side $U_Z$ is equal to:

$$U_Z = U_G - \Delta U \tag{1.2}$$

Origin of voltage fluctuations could be described as follows. Change in load impedance $\bar{Z}_{\mathrm{L}}(t)$ will generate fluctuations of currents $I_r$ and $I_j$. Fluctuations in currents according to (1.1) will lead to fluctuations in voltage drop. Finally, according to (1.2) fluctuations in voltage drop will cause fluctuations of voltage $U_Z$ on the load. From (1.1) is visible that value of $\Delta U$ is dependable on both components of current $\bar{I}$. Generally, voltage fluctuations and therefore flicker mainly depends on supply system short-circuit impedance in the place of a load connection.

As it was shown variations of load in time have direct effect on absolute value of voltage $U_Z$. Such a behaviour manifests as amplitude modulation of supply voltage waveform. Magnitude or modulation depth of waveform will be most pronounced in the place of load connection. Supply voltage waveform which was AM modulated by periodic load of frequency 5 Hz is shown in Figure 3. Its Frequency spectrum is right below. Spectrum contains one carrier tone on system frequency 50 Hz and two tones which are 5 Hz apart from 50 Hz. This shows how variable load and consequently its AM modulation effects, affects the supply voltage in time and in frequency spectrum. It is very important to know those interactions, because products of modulation may end up on frequencies where they will cause flickering of LED bulbs.

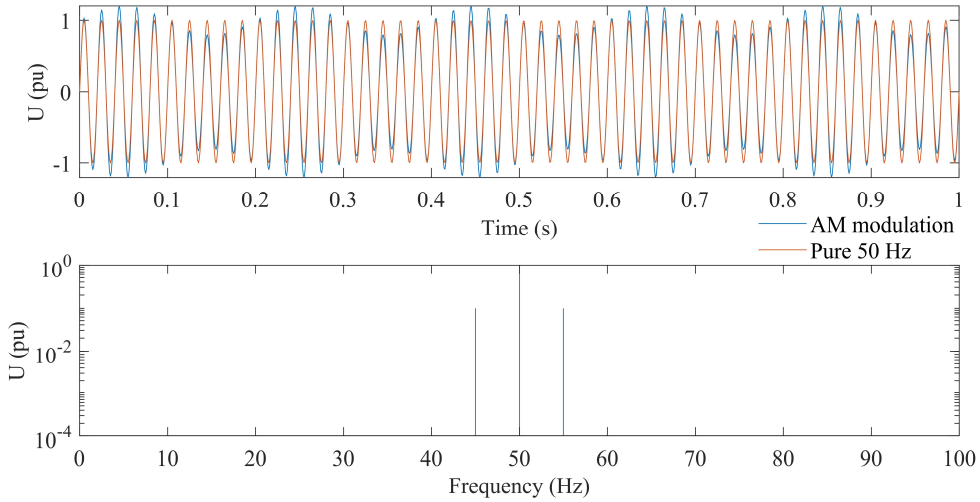


Figure 3 AM modulation in time and frequency domain.

## 1.2 Voltage fluctuations – PM modulation

Besides analysing consequences of variable load on absolute values of supply voltage it is also necessary to look if those fluctuations affect the value of voltage phase angle. In the previous chapter, load was considered as variable in time. However, in grids are also present manipulations within grid configuration and aperiodic switching of loads or parts of grid due to the faults. Schematics of grids representing mentioned operating situations are shown in Figure 4 a) and b).

In a) is shown change in configuration of UHV/HV transmission lines. $X_s$ now represent connection of another parallel supply system or transmission power line. Inductive reactance of the LV system is neglected because in general it is reaching significantly lower values in comparison with UHV/HV lines. $R_s$ is considered unchanged by connecting another transmission line due to its negligible value in comparison with inductive reactance.

In b) the meaning of components is the same as in the previous chapter, however load in time $t_0$ is switched on and has constant value. Conceptually a) and b) are very close. In both cases instantaneous impedance changes occur in time $t_0$. Only main difference between each other is in the character of changed impedance. In a) is change purely inductive in b) principally resistive. Because of their electrical similarity further will be analysed only in case a).

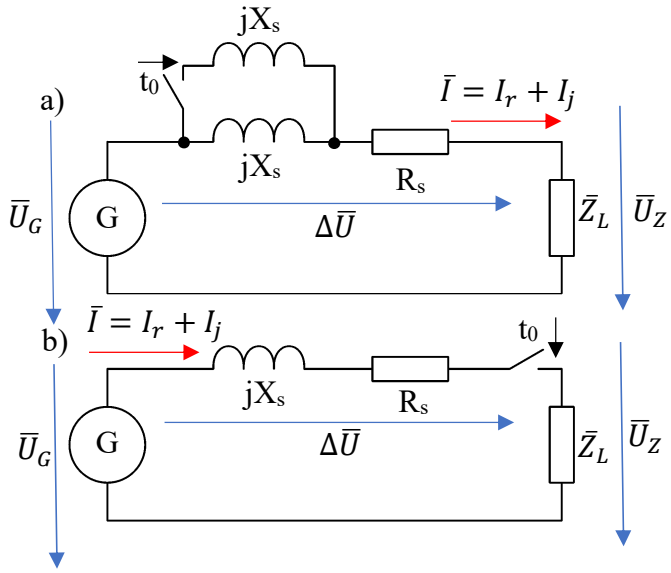


Figure 4 a) change in configuration of transmission lines, b) aperiodic load, fault

Voltage on load could be described as:

$$\bar{U}_Z = \bar{U}_G - \Delta\bar{U} = \bar{U}_G - \bar{I}\cdot\bar{Z}_s = \bar{U}_G\left(1 - \frac{\bar{Z}_s}{\bar{Z}_s + \bar{Z}_L}\right) \tag{1.3}$$

If formula for $\bar{U}_Z$ is finally known it is needed to find out the value of load voltage in both states, before switching ($t<t_0$) and after connection of parallel line ($t_0>t$).

Voltage $\bar{U}_Z(t < t_0)$ is therefore equal to:

$$\bar{U}_Z(t < t_0) = \bar{U}_G\left(1 - \frac{\bar{Z}_s(t < t_0)}{\bar{Z}_s(t < t_0) + \bar{Z}_L}\right) \tag{1.4}$$

And by the same principle $\bar{U}_Z(t > t_0)$:

$$\bar{U}_Z(t > t_0) = \bar{U}_G\left(1 - \frac{\bar{Z}_s(t > t_0)}{\bar{Z}_s(t > t_0) + \bar{Z}_L}\right) \tag{1.5}$$

RMS change in voltage is than equal to:

$$\delta U_Z = U_Z(t > t_0) - U_Z(t < t_0) \tag{1.6}$$

And finally difference in phase angle:

$$\Delta\varphi = \varphi_{U_L(t>t_0)} - \varphi_{U_L(t<t_0)} \tag{1.7}$$

To evaluate $\delta U_Z$ and $\Delta\varphi$ is needed to know electrical parameters of the circuit. Values selected below do not track any real measured values. They have been selected only for explanatory purposes. Individual values of circuit parameters are thus equal to:

$$\bar{U}_G = U_G = 230\ \text{V};\ \bar{Z}_s(t < t_0) = (0.5 + j1)\ \Omega\ \rightarrow \bar{Z}_s(t > t_0) = (0.5 + j0.5);$$

$$\bar{Z}_L = R_L = 10\ \Omega$$

By simple substitution of those values to (1.3) and (1.4) it has been calculated that difference in phase angle is equal to:

$$\Delta\varphi = 2.71°$$

and subsequently difference in RMS voltage:

$$\delta U_Z = 0.738\ \text{V}$$

By comparison of $\Delta\varphi$ against value of $\delta U_Z$ it could be clearly seen that phase change and therefore phase modulation is in this event much more pronounced. During the switching event shown in Figure 4 b) the situation would be only slightly different. Due to the much higher switched impedance the difference of RMS voltage would prevail. However as can be seen from the definitions of voltages $\overline{U}_Z(t < t_0)$ and $\overline{U}_Z(t > t_0)$ phase difference $\Delta\varphi$ will be still present. These phase differences are called phase jumps [5].

PM modulation of supply voltage with system frequency 50 Hz is shown in Figure 5. Modulation has phase deviation 0.3 rad and carrier tone with frequency 5 Hz. As it could be seen from the frequency spectrum, PM modulation is described by a sum of superimposed tones spaced by 5 Hz from 50 Hz. Generally, their frequencies and their amplitudes are not so straightforward to calculate as in case of AM modulation, especially in presence of more complex modulating signals. Main difference between each other is that PM modulation naturally creates more interharmonic products placed on broad bandwidth in comparison with single sine tone AM modulated signals. This from the standpoint of flicker creates increased requirements for immunity of devices against interharmonic components.

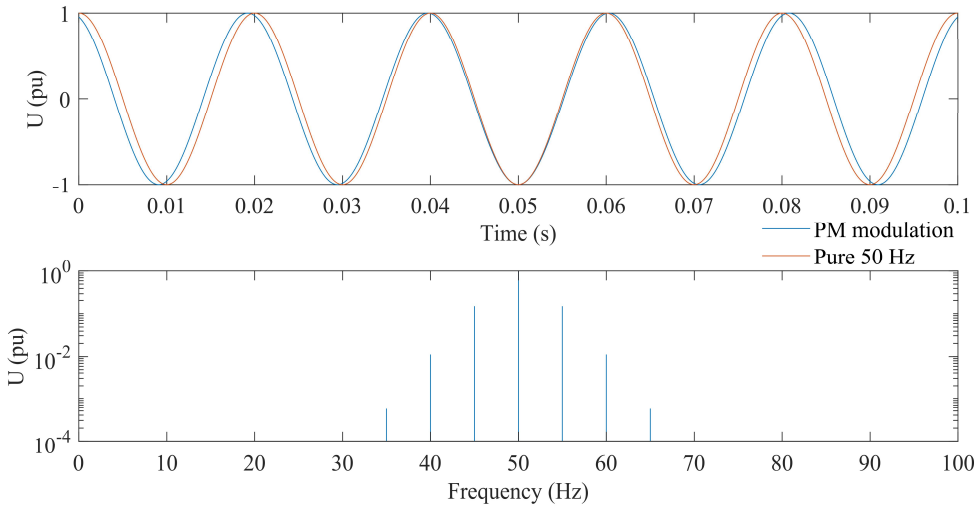


Figure 5 PM modulation in time and frequency domain

From the results described in this and in the previous chapter it can be concluded that it is hard to divide sources of voltage fluctuations to one group with pure AM modulation and to second with pure PM modulation. Because in most situations both modulations occur at the same time. It is only a matter of impedance change and its components during a specific event in which one modulation would prevail. However, it is evident from results that AM modulation will be the most common, due to fluctuations inducted by variable loads. Which is a very common behaviour in the majority of industrial machines or household appliances due to their various duty cycles or the very principle of operation. As an example, how radically current draw can fluctuate in industrial machinery in Figure 6 is shown current drawn by 80 MVA arc furnace during first minutes of melting process.

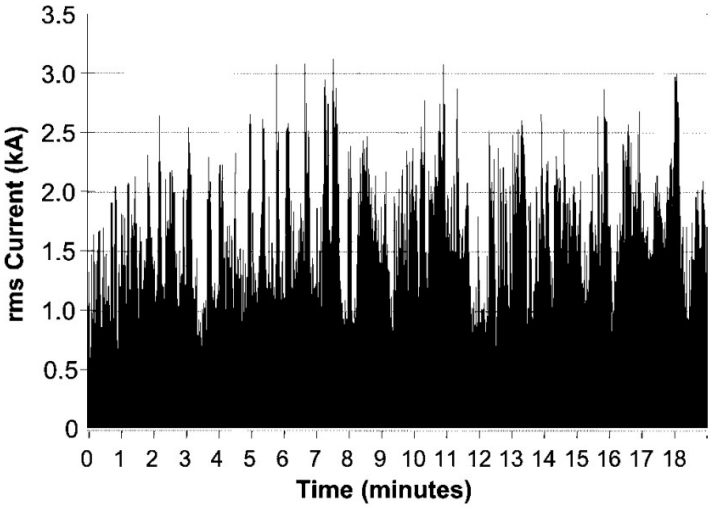


Figure 6 Current drawn by arc furnace [6]

Sources of voltage fluctuations are therefore more often classified by their periodicity as:

Periodic, mainly industrial and heavy-duty machines with long and sustain operation time as: band saw mills, stone crushers [6]

Quasi-periodic: electric stove, iron, microwave oven, WATTROUTER, resistance furnace [6]

Aperiodic: faults in power grids, start-ups of large machines (synchronous, asynchronous motors with high moment of inertia) [6]

## 1.3 Voltage fluctuations, interharmonic distortion (IHD)

Nonlinear devices, switched loads, and sources connected to power lines generate a vast number of harmonics and interharmonic frequencies. Summation of interharmonic components has a modulating effect on fundamental tone. Occurrence of interharmonic components therefore cause waveform fluctuations in RMS and in peak value of fluctuations [5].

The most common nonlinear power devices causing voltage fluctuations are:

- Induction motors supplied by Adjustable speed drives,
- HVAC systems (Inverter air conditioning)
- Home appliances (Washing machine)
- Arc furnaces
- PV system inverters

In contrast to previous categories which included only varying loads as sources of fluctuations. This category additionally includes devices as PV system inverters which primarily serve as power sources. However, most of them because of their nonlinear and switching-mode principle directly inject interharmonic frequencies to the grid. Major difference between both is in the mitigation of their negative effects on power quality. In theory by taking short circuit impedance at the point of load connection to 0 Ω would mitigate all consequences caused by load fluctuation and there will be no more problems with flicker. On the other hand, interharmonic and harmonic frequencies caused by sources as PV inverters are much harder to suppress. Lowering the short circuit impedance is in this case from the principle of cause not a reasonable option. Their output has a rich frequency spectrum starting with first interharmonics in range of 1-5 Hz with continuous propagation to nearly kHz range with frequency components that are unpredictable in amplitude as it is shown in Figure 7. The inverter present, during the 100 % sun irradiance, has produced much lower levels of interharmonics than in the case of 5 % irradiance. It is needed to be aware of this behaviour and by overall quality of

delivered power from such inventors connected to the grid. Popularity of PV installation in households in the Czech Republic is rising at a fast pace. Only last year ČEZ (Czech distribution company) got 70 212 requests to connect PV installations to the grid. 80 % from all requests were shared by installations with installed power under 10 kW [7]. It is in place to do rigorous control and monitoring of delivered inverters on the market because with such a high penetration of sources. Possible use of not sufficiently pure inventers from the standpoint of output frequency spectrum would have severe outcomes on overall power quality in the grid.

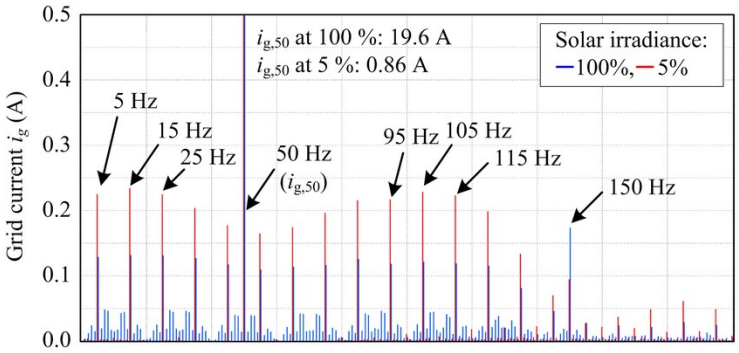


Figure 7 Frequency spectrum of the PV inverter in steady-state MPPT operation [9]

Another often used device in industry which produces a very unpredictable and dynamically changing frequency spectrum of drawn current dependable on current operating state respectively the set parameters is a PWM drive. In the bottom graph of Figure 8 are drawn zig-zag lines which precisely tracks how individual interharmonics are travelling through the spectrum with dependence on set output frequency. In the upper picture is the output frequency spectrum with the currently set 40 Hz drive frequency. The values of shown frequency components are in reference to current $I_{base}$ which is equal to 423 A. As it is visible, during the rising up of the output frequency from 0 to 50 Hz interharmonic and harmonic frequencies travel through nearly the whole spectrum from 0 to 1000 Hz. This behaviour only indicates need for the immunity of appliances against interharmonic components and especially because of this thesis, immunity of LED bulbs in the whole spectrum of frequencies starting down from 1 Hz up to kHz range.

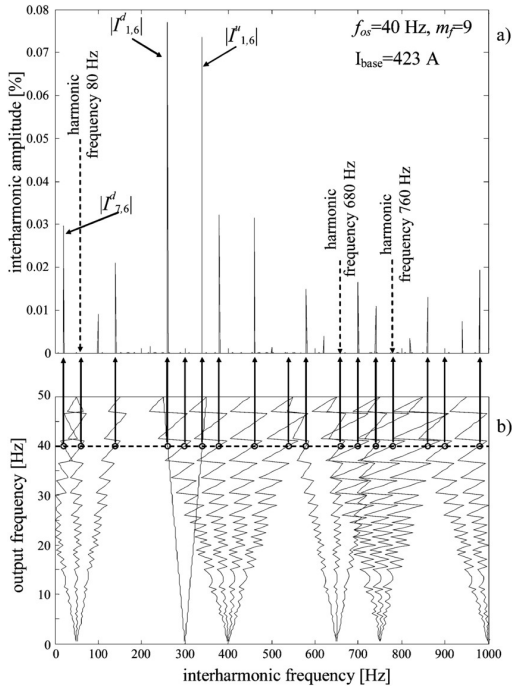


Figure 8 PWM drive output current frequency spectrum [10]

Now it is in the place to ask why are here discussed frequency components of voltage fluctuations with such high frequencies, when even instruments for flicker measurement in their blocks where measured signals represent luminous flux do not evaluate them. UIC/IEC flickermeter for 50 HZ power system has in its chain Butterworth low-pass filter of sixth order with cut-off frequency 35 Hz [11]. So, frequencies of luminous flux around higher harmonics do not play any role in evaluation of flicker. However, due to nonlinear response and thus intermodulation processes in LED bulbs even higher frequency components of supply voltage fluctuations up to 1000 Hz can propagate to visible luminous flux with frequencies under 50 Hz. To understand how it is possible, as first it is needed to look on mathematical description of instantaneous power which is equal to:

$$p(t) = u_1(t) \cdot i(t) = \frac{u(t)^2}{R} \tag{1.8}$$

For now, all variables are just considered as general voltages, currents etc. It is clearly visible that conversion from $u(t)$ to $p(t)$ is from the mathematical standpoint nonlinear process because of square of $u(t)$. What translates to possible creation of intermodulation products when more than one tone will occur in $u(t)$. To confirm this statement $u(t)$ will be considered as:

$$u(t) = u_1(t) = \sin(\omega \cdot t) \tag{1.9}$$

By substitution of $u(t)$ with $\sin(\omega \cdot t)$ in (1.8) and after using product-to-sum trigonometric identity $p(t)$ is equal to:

$$p(t) = \frac{\sin(\omega \cdot t)^2}{R} = \frac{1}{2R} - \frac{\cos(2 \cdot \omega \cdot t)}{R} \tag{1.10}$$

If $\omega = 2 \cdot \pi \cdot f$ and $f$ is equal to system frequency 50 Hz. Then by analysis of the (1.10) can be concluded that if voltage $u(t)$ is described by pure sinewave with one specific frequency the frequency spectrum will contain one DC component with value equal to $\frac{1}{2R}$ and one another frequency component on second harmonic frequency of $u(t)$ in this case 100 Hz.

To show what happens when $u(t) = u_1(t) + u_{IH}(t)$ so voltage $u(t)$ now contain 2 frequency components. First on system frequency 50 Hz and second on interharmonic frequency $f_{IH}$ = 170 Hz. Voltage $u_{IH}(t)$ is defined as:

$$u_{IH}(t) = \sin(\omega_{IH} \cdot t) \tag{1.11}$$

Where $\omega_{IH} = 2\pi \cdot f_{IH}$

Overall voltage $u(t)$ squared is equal to:

$$u(t)^2 = (u_1(t) + u_{IH}(t))^2 = u_1(t)^2 + 2 \cdot u_1(t) \cdot u_{IH}(t) + u_{IH}(t)^2 \tag{1.12}$$

Frequency products of $u_1(t)^2$ and $u_{IH}(t)^2$ are obtained by the same principle as it was in (1.10). Both contribute to the DC component and produce a second harmonic of its fundamental. Therefore, frequency component of $u_1(t)^2$ and $u_{IH}(t)^2$ have frequency equal to 100 Hz and 340 Hz, respectively.

The last term $2 \cdot u_1(t) \cdot u_{IH}(t)$ after substitution:

$$2 \cdot u_1(t) \cdot u_{IH}(t) = 2 \cdot \sin(2\pi \cdot f_{IH} \cdot t) \cdot \sin(2\pi \cdot f \cdot t) \tag{1.13}$$

And after a few manipulations:

$$2 \cdot u_1(t) \cdot u_{IH}(t) = \cos(\omega \cdot t - \omega_{IH} \cdot t) - \cos(\omega \cdot t + \omega_{IH} \cdot t) \tag{1.14}$$

(1.14) tells that two additional frequency components will be present in $p(t)$. First on frequency 120 Hz calculated from $f - f_{IH}$ and second on frequency 220 Hz from $f + f_{IH}$. In the end $p(t)$ will contain DC components and 100 Hz, 340 Hz, 120 Hz, 220 Hz sinewaves.

If $p(t)$ would be considered as an input power to the light source, it could be taken as approximation of its output luminous flux $\theta(t)$ because of its dependency on supply voltage $u(t)$ [7]:

$$p(t) \approx \theta(t) \tag{1.15}$$

Moreover, if R would be considered as a constant inner resistance of a light source, the whole analysis shown above is an accurate approximation of behaviour of an incandescent bulb in frequency spectrum. For better comprehension of mentioned facts Figure 9 shows how individual frequency components travel through the output frequency spectrum of luminous flux due to the presence of interharmonic. Grey lines indicate path of individual frequency components through frequency spectrum of output luminous flux in dependence to injected interharmonic with its frequency displayed on y-axis. Horizontal orange lines mark frequency spectrum of interharmonics (0-100 Hz), which from the supply voltage translates to output visible spectrum of luminous flux. By direct comparison of the immunity response of the incandescent bulb shown in Figure 13 with Figure 9. Is clearly visible that the range of interharmonic frequencies which affect the visible spectrum of luminous flux is the same.

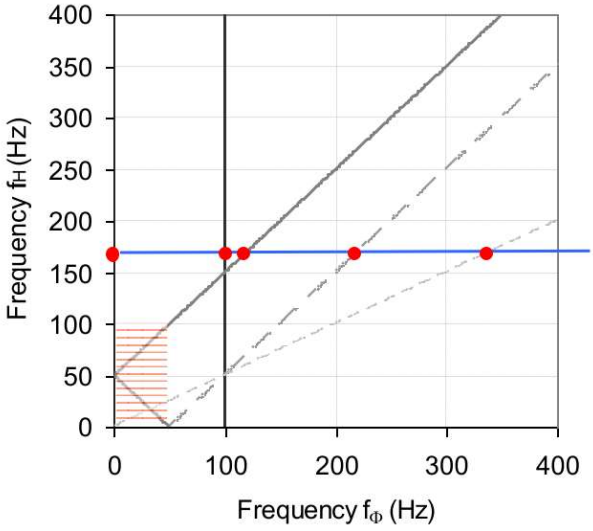


Figure 9 Response of output luminous flux spectrum to interharmonic component of supply voltage in linear light sources [5]

However, this was valid when incandescent lamps were the most popular. Today as the subsequent parts of the thesis will show, LED based lamps occur much more often. To simulate their behaviour of output luminous flux in presence of interharmonic in supply voltage. R must be considered as the function of supply voltage [6].

So (1.8) will be changed to:

$$p(t) = u_1(t) \cdot i(t) = \frac{u_1(t)^2}{R(u_1(t))} \tag{1.16}$$

Now frequency spectrum of $p(t)$ is not so straightforward to analyse. The equivalent of Figure 9 but for nonlinear sources of light is pictured in Figure 10.

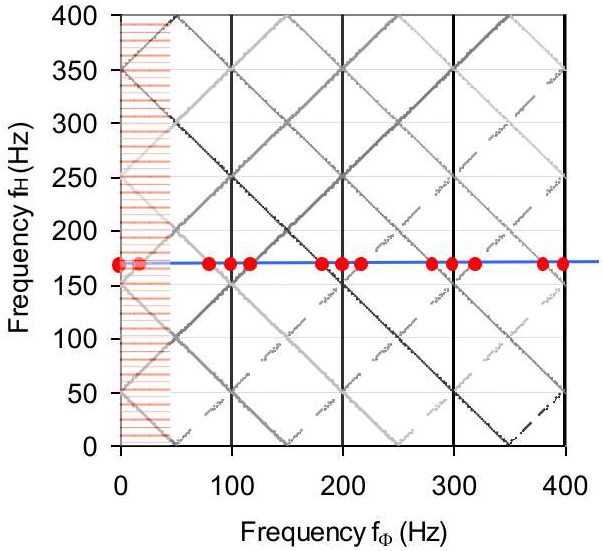


Figure 10 Response of output luminous flux spectrum to interharmonic component of supply voltage in nonlinear light sources [5].

As it is clearly visible each interharmonic from the frequency spectrum of 0 Hz to 400 Hz could propagate to the visible part of the output luminance flux spectrum and may cause flickering of a given light source. It is only a matter of its individual design how exactly it will perform. Shown spectrum of interharmonics (0-400 Hz) which affect visible output luminous flux are only indicative and their frequency limit depends, also as a whole performance on the specific parameters of bulb design.

In summary this chapter should provide more insights to behaviour and frequency of interharmonic components as a product of nonlinear devices connected to the power grid. Plus, brief introduction to how LED, and incandescent bulbs behave in presence of interharmonics in its supply voltage.

## 1.4 Classification of voltage fluctuations

All above mentioned sources of voltage fluctuations are a natural part of a functioning power grid. Because machinery or generally loads connected to the grid for their proper function must be able to draw current from the grid by their variable need. Moreover, consumers want to switch-on appliances when they want to and operational manipulations such as changes in configuration of transmission lines are common and essential events.

To be able to recognize and evaluate severity of occurring voltage fluctuations. Standard EN 50160:2021 classify two groups of voltage fluctuations which are mainly responsible for negative effects on flicker performance [12]:

- Supply voltage variations.
- Rapid voltage changes.

### 1.4.1 Supply voltage variations

In the low voltage systems, general supply voltage variations should not exceed 10 % of nominal voltage $U_{n.}$ Under normal operating conditions, testing runs for a period of one week. During each week, 95 % of all rms measured values, each measured by a period of 10 minutes should be within a given range of ±10 % $U_{n.}$ However, all rms values measured with a period of 10 min should be within the range of -15 % / +10 % $U_n$ [12].

### 1.4.2 Rapid voltage changes

Rapid voltage changes are further divided to single rapid changes which if during the change, voltage crosses the threshold value for dip or swell then are classified as dip or swell [12]. Rapid voltage changes are evaluated directly by flicker severity. Under normal operating condition, measurements of long-term flicker severity $P_{lt}$ run for a period of one week. During each week the $P_{lt}$ should be less than or equal to 1 for 95 % of testing time [12].

$P_{lt}$ is calculated from 12 consecutive measurements of $P_{st}$ as [11]:

$$P_{lt} = \sqrt[3]{\frac{1}{12}\sum_{i=1}^{12} P_{st}^3} \tag{1.17}$$

Specific duration of $P_{st}$ evaluation is 10 minutes. Duration of $P_{lt}$ evaluation is then clearly equal to 12 x 10 min so overall 2 hours.

Measurement of flicker severity is provided by a measuring instrument called flickermeter which is described in IEC 61000-4-15. It provides correct flicker perception

for all voltage fluctuation waveforms [6]. It is important to realise that flickermeter do not evaluate negative consequences of fluctuations on some technical infrastructure of power grid and especially it do not evaluate relative changes of fluctuations. But what flickermeter evaluates is the direct impact of voltage fluctuations on their perception by human in output luminous flux of incandescent lamps [11]. This function is provided by the lamp-brain-eye model which is included in the UIE/IEC flickermeter. For the measurement of light flicker has been developed new objective method which is described in standard IEC TR 61547:2020. The principle of this flicker is in omitting incandescent lamp blocks or parts of blocks from IEC voltage flickermeter presented in IEC 61000-4-15. Objective flickermeter was primarily developed for correct measurement of non-incandescent bulbs.

# 2. FLICKER PERFORMANCE OF LED LAMPS

Being able to describe flicker performance of lamps is very important because of mitigation of its possible health risks. Flickering of lamps has been linked as the cause of seizures, headaches, reduced visual performance and other negative effects [3].

## 2.1 Flicker performance metrics

For evaluation of flicker performance parameters, many methods have been developed. They mostly differ in their own very principles. The most important ones are described below.

### 2.1.1 Gain factor

It serves as a parameter which evaluates how well voltage fluctuation in supply voltage of a lamp propagates to its output luminous flux. In general standards describe gain factor or GF as ratio of percent change of output luminous flux to the percent change in input voltage [13]. However, in this thesis GF has been evaluated based on [14]. Following it GF could be described as [15]:

$$GF(f_{\mathrm{ih}}) = \frac{\frac{\phi(f_{\mathrm{vis}})}{\bar{\phi}}}{\frac{V(f_{\mathrm{ih}})}{\bar{V}}} \tag{2.1}$$

Where $\phi$ is value of the luminous flux with frequency $f_{\mathrm{vis}}$, $\bar{\phi}$ is the mean value of luminous flux, $V$ is level of interharmonic component, $\bar{V}$ is the supply voltage on fundamental frequency, $f_{\mathrm{ih}}$ is frequency of current tested interharmonic component and $f_{\mathrm{vis}}$ is a visible intermodulation product in output luminous flux from range of (0,50) Hz [14].

$f_{\mathrm{vis}}$ is equal to:

$$f_{\mathrm{vis}} = |h \cdot f_1 - f_{\mathrm{ih}}| \tag{2.2}$$

Where $f_1$ is fundamental frequency of supply voltage and h is always odd harmonic order closest to $f_{\mathrm{ih}}$ [15].

The GF does not perfectly estimate flicker produced by lamp because it describes only the transfer function to visible flicker components without considering average observer flicker sensitivity. However, GF excellently reflects the fundamental driver properties

[15]. The best understanding how GF varies among different lamp types could be obtained by comparing Figure 11 with Figure 12. In Both figures are shown various fluorescent lamps from different manufacturers, however when they have the same type of ballast circuit they manifest in GF by the same manner. Very similar behaviour is administered even in LED drivers. In Figure 19 are shown 8 GF curves. Each is specific in some tolerances to the topology of the driver circuit.

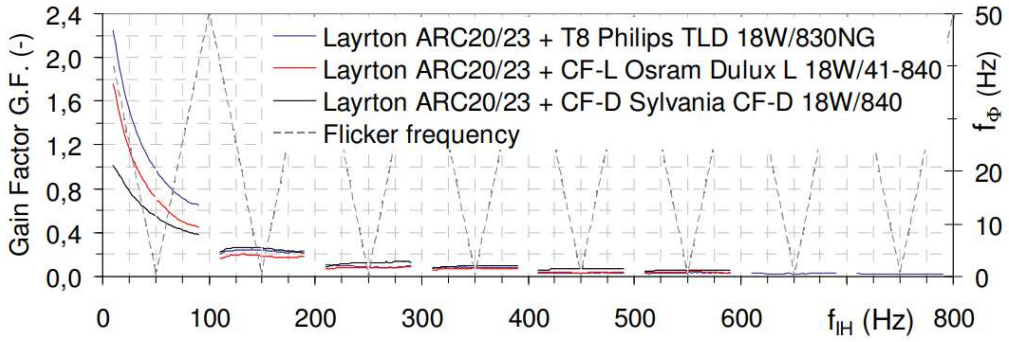


Figure 11 Gain factor curves of various types of fluorescent lamps with induction ballast [16]

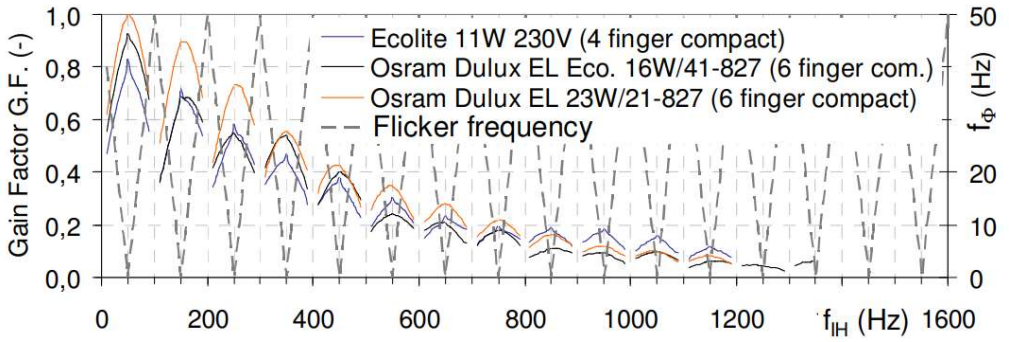


Figure 12 Gain factor curves of various CFLs with electronic ballast [16]

### 2.1.2 Flicker immunity

Exactly as GF, immunity is mostly not used as a single parameter by itself, but it is measured in range of desired frequencies for testing a flicker performance of bulbs. Parameters of testing method using objective light flickermeter are described in IEC TR 61547:2020. Generally, the principle of the method is to find maximal magnitude of an applied interharmonic to supply voltage of a lamp at specified interharmonic frequency for which lamp does not produce disturbing flicker by an average observer under reference conditions, thus $P_{st}$ = 1 [5]. This test exactly shows how particular lamps perform in presence of specified voltage fluctuations.

As an example, in Figure 13 are shown immunity curves for:

I1 – incandescent bulb, 60 W/230 V
I3 – halogen lamp 42 W/230 V
FL4 – CFL with built-in EB, w/o PFC, 23W/240V
FL8 – CFL with built in EB with passive capacitive PFC, 15W/240V
FL9 – FLs (4x18 W) with external EB with passive capacitive PFC
FL11 – CFL with built-in single-stage EB with active PFC, 20W/230V
LED2 – LED lamp, built-in non-isol. Step-down conv, output current regulation
LED3 – Power LEDs (22x) with external isol.step-down conv. w/o PFC and with output current regulation, 60W/100-240 V

As it follows from Figure 13 incandescent lamps and halogen lamps have very high immunity above 100 Hz in comparison with all other lamps. In the description of GF it was mentioned that GF is used for identification of individual driver topologies used in lamps. From Figure 13 it is seen that it would be very complicated to distinguish lamps by their individual topologies only using their immunity curves.

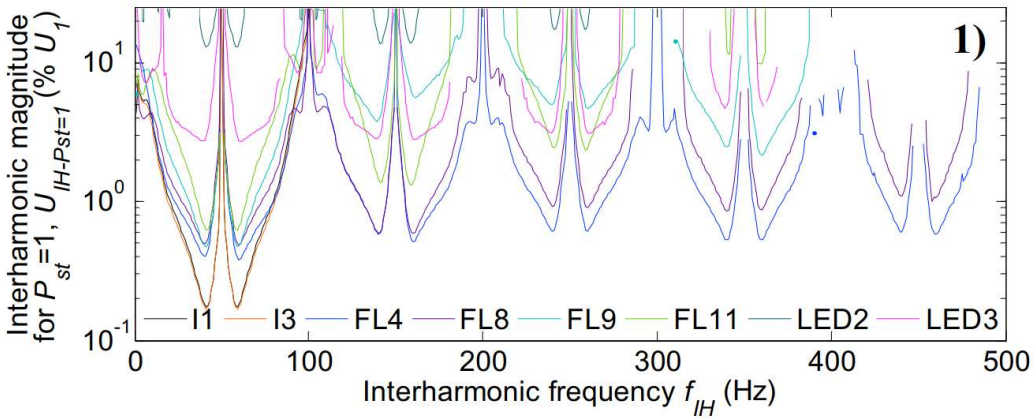


Figure 13 Immunity curves for various lamp types [20]

### 2.1.3 Flicker index, percent flicker

Other metrics which have been developed and used to quantify flickering of lamps are flicker index and percent flicker. Most often they are used only for steady-state evaluation.

Flicker index is defined referring to Figure 14 [3]:

$$\text{Flicker index} = \frac{\text{Area 1}}{\text{Area 1+Area 2}} \tag{2.3}$$

It is the ratio of area above average value of luminous flux in ratio with area above and below the average value for one cycle. Common flicker index for incandescent bulbs is 0.02.

Percent flicker is defined referring to Figure 14 [3]:

$$Mod\% = 100\frac{(\text{Max} - \text{Min})}{(\text{Max} + \text{Min})} = 100\frac{(\text{A} - \text{B})}{(\text{A} + \text{B})} \tag{2.4}$$

Essentially it is modulation depth which describes the relationship between difference and the sum of the maximum and minimum luminous flux amplitudes. Common percent flicker for incandescent bulbs is 6,6 % [3].

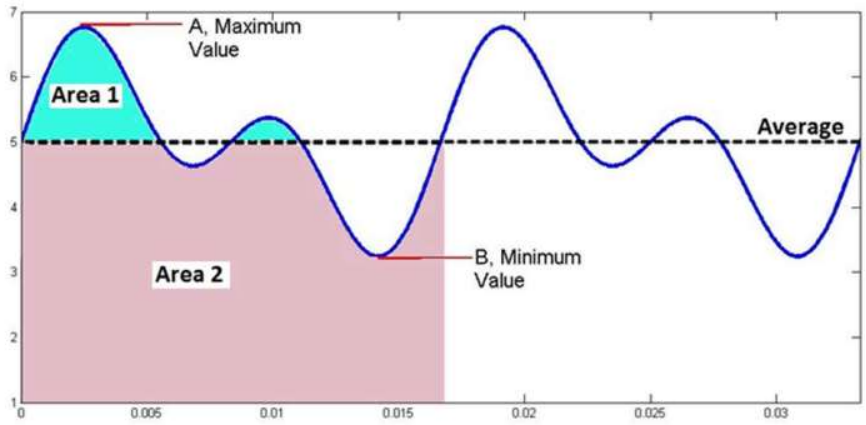


Figure 14 Definition of flicker index and percent flicker [3]

Percent flicker and flicker index are more commonly used for evaluation of invisible flicker above 50 Hz, below is used IEC flickermeter. In the presence of invisible flicker ,the human neurological system detects the modulation in light, but it is not consciously perceived. Or it manifests in terms of spatial effects like phantom array or stroboscopic effect [3]. The disadvantage of these metrics is that severity and occurrence of undesirable effects linked with light modulation depend on a certain frequency component and its modulation depth in output luminous flux but none of these parameters weight their results by modulation depth and frequency of certain components. This is the main reason why there is not one specified threshold or limit value for both. The limit values for percent flicker are represented by a graph in Figure 16. Where the green area represents no effect and yellow area low risk. Both areas are described on the basis of many studies shown in IEEE Std 1789-2015. Diamonds represent data for visible flicker, circles and squares represent limit values from various studies for stroboscopic effect.

### 2.1.4 Stroboscopic effect visibility measure

The disadvantage mentioned in the previous parameter is partially solved by SVM or stroboscopic effect visibility measure. This parameter is used to quantify the visibility of stroboscopic effects in the range of 80 to 2000 Hz [4]. Stroboscopic effect is defined for a static observer in a non-static environment as change in a motion of perception induced by light stimulus or spectral distribution which fluctuates in time [4].

SVM is calculated as [4]:

$$SVM = \left( \sum_{m=1}^{\infty} \left( \frac{C_m}{T_m} \right)^n \right)^{\frac{1}{n}} \tag{2.5}$$

Measured luminous flux in the time domain is transferred to a frequency domain by DFT. After the transformation, amplitudes of $m$-th fourier component are marked as $C_m$. The parameter $n$ is Minkowski norm parameter which in this case is equal to 3,7. $T_m$ is the visibility threshold which weights each sine wave at the frequency of the $m$-th fourier component. $T_m$ is equal to [4]:

$$T_m = \frac{1}{1 + e^{-a(f-b)}} + 20e^{-\frac{f}{10\,Hz}} \tag{2.6}$$

Where $f$ is frequency of $m$-th component, $a$ = 0,00518 s and b = 306,6 Hz [4]. $T_m(f)$ is a function which defines the sensitivity curve pictured in Figure 15. The main advantage of SVM is that there can be easily set one value as a limit for bulbs. If SVM = 1 then the stroboscopic effect is visible. It means that with 50 % probability the average observer will be able to detect a particular effect [4]. However, as a limit value is more used 0,4. The European regulation commission use 0,4 as a limit in their directive [17].

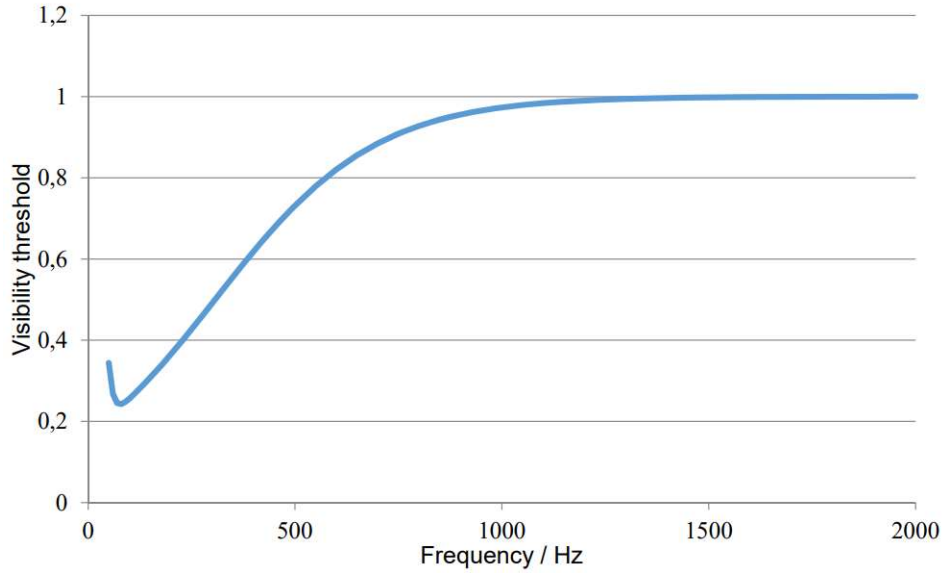


Figure 15 Sensitivity curve of SVM [4]

In Figure 16 are shown graphs when SVM is equal to 1 or 0,4. It is clearly visible that SVM equal 0,4 is closer to the upper limit of low-risk regions in the yellow area and therefore is more suitable to use in practice. Same as previous metrics, SVM is most often used for evaluation of steady-state performance of lamps.

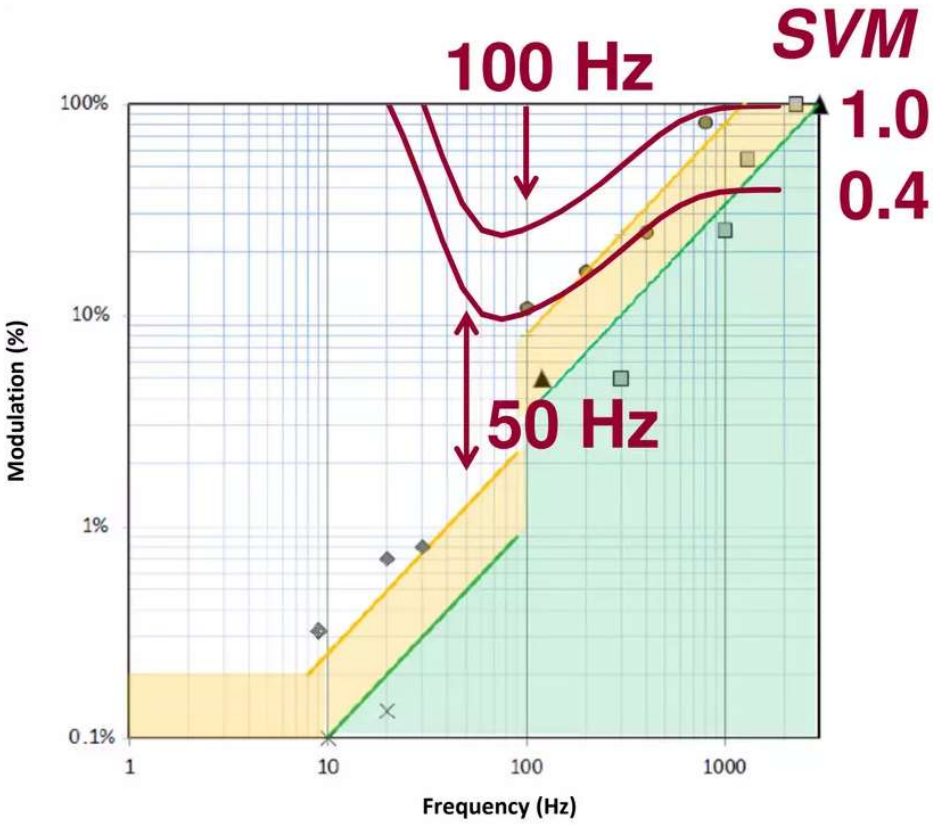


Figure 16 Comparison between both SVM limits [18]

## 2.2 LED lamps drivers flicker performance

Parameters as gain or immunity highly depend on used driver topology in LED lamps. Today, overall are classified eight main topologies marked from I to VIII [2]. Their principal schematics are shown in Figure 17.

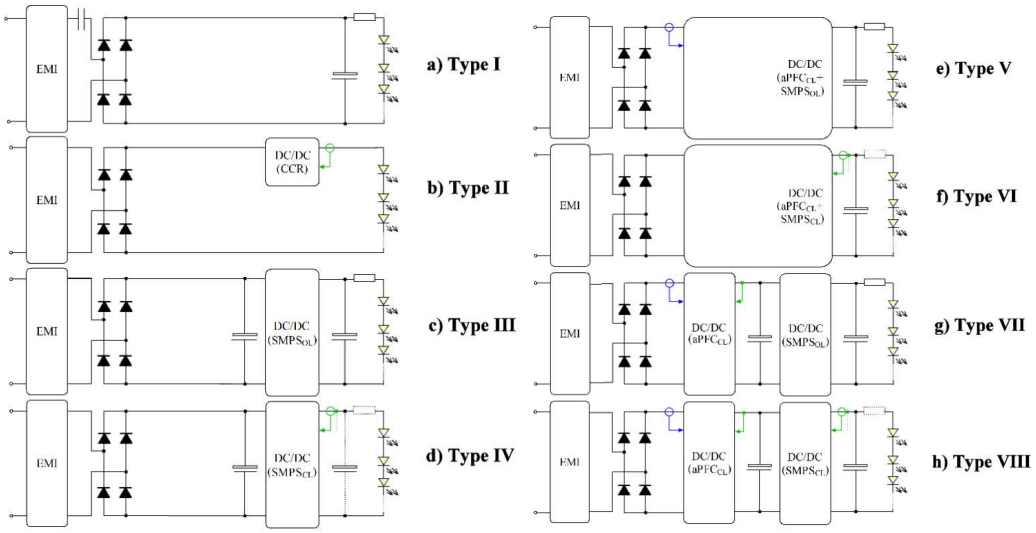


Figure 17 Main LED driver topologies and their classification [2]

Most of the shown topologies are very well studied and their specific flicker performance is known. In [2] authors proposed new Flicker index labels for LED bulbs very similar to already established energy labels. However, their intention is to mark sensitivity of lamps to voltage fluctuations from A to F (from best to worst). The mentioned study has been developed a new parameter named LFI which evaluates sensitivity of LED lamps to flicker. The higher the LFI is, the more sensitive the bulb is to voltage fluctuations. Ranking shown in Figure 18 creates a great picture about flicker performance across the various topologies.

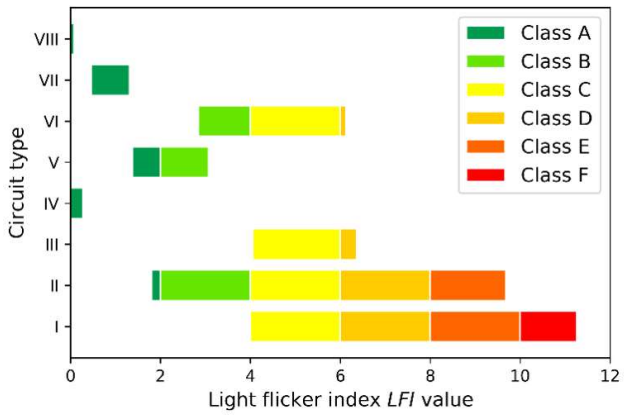


Figure 18 Flicker sensitivity of different topologies [2]

Type A(I), capacitive divider circuit – Consist only passive components, ac input voltage is through DBR converted to dc. EMI filter is included for suppression of high frequency emissions. Combination of two capacitors form voltage divider reduces the supply voltage. Resistor then only limits the current through the LED string. No present feedback makes this type of topology very sensitive [2].

Type B (II), constant current regulator circuit – Contain CCR circuit, which stabilize current through LED string across wide voltage range [2].

Type C (III, IV), offline switch-mode driver circuit – On input is rectifier with smoothing capacitor which feeds dc-dc converter. Converter then regulates current and voltage across the LED string. Type III is open-loop so its control is fixed or as a type IV it could be designed as closed-loop with feedback control. As it is seen from Figure 18 type IV has better flicker performance [2].

Type D (VII, VIII), double stage switch-mode driver circuit – Composed from two separate dc-dc converters. Role of the first converter from the ac side is serving as aPFC and pre-regulator. Second dc-dc converter provides load feeding according to requirements. The second converter could operate as open-loop in Type VII or closed-loop in Type VIII. As is seen from the Figure 18 flicker performance of such topology is great but disadvantage for manufacturers is higher cost of more components [2].

Type E (V, VI), single-stage switch-mode driver circuit – Basically merging both converters from the previous group together. However, it does not provide all double stage functionalities properly. As it is visible from Figure 18 Type E falls behind Type D. Besides disadvantages this topology could offer some advantage depending on exact Type of topology (V, VI). Better shaping of ac input current can be provided by PF control in Type V. Better output regulation of the LED string output is provided by Type VI [2].

Identification of particular types of drivers could be done by GF curves. As Figure 19 shows each class has its own distinct shape of GF curve.

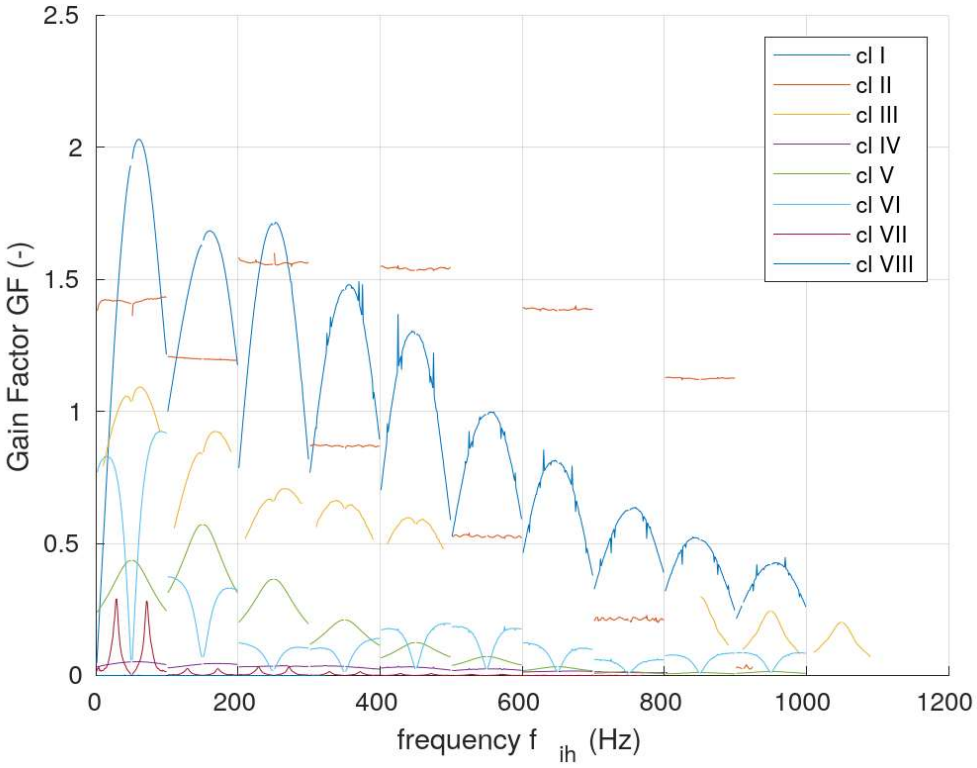


Figure 19 Gain factor curves of LED driver topologies from class I-VIII [15]

# 3. MARKET ANALYSIS WITH LED BASED LAMPS

For the subsequent evaluation of electric, light and flicker parameters of LED lamps it is needed to select samples which would ideally represent the most common ones on the consumer's side. In this thesis the focus was placed only on the retrofit LED bulbs which should serve as a replacement for CFLs and incandescent bulbs found mainly in households with socket types E27, E14, GU10, etc.

As the demand for LED lamps has been rising, their availability in a multitude of retail shops and warehouses was rising as well. Today they could be obtained even in grocery stores, small corner stores, furniture stores (i.e.: IKEA) and other primarily non-electrical hardware stores. Their massive availability was accelerated mainly because of customers' demand influenced by controlled phasing-out of an inefficient incandescent and halogen lamp according to EU Ecodesign lighting regulation, which has been in force since 2009 [1]. Regulation was later repealed and replaced with new updated versions aiming at stricter market rules for halogen lamps and banning inefficient halogen spotlights and halogen bulbs for household use by year 2016 and 2018 respectively [1].

The high pace of global transformation to the new artificial light sources based on LED technology could be seen in Figure 1. In the last 10 years, global market share increased tremendously to, almost about 50 %. In the year 2019, global market share with a value of 49 % represents over 10 billion LED lamps (bulbs, modules, tubes) and luminaries [4]. Most recent prediction for the year 2030 shows that market share for LED lamps will increase up to 99 % [1]. Data for market share growth in the European union and UK are even steeper. In 2009 LED lamps market share in the EU was around 9 % but in 2020 it reached substantially higher value approaching 72 % [19].

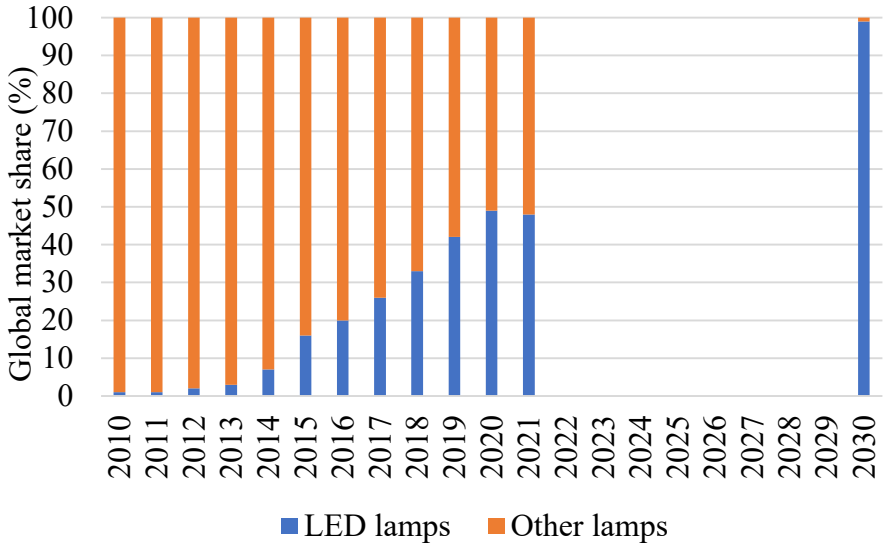


Figure 20 Global market share of LED Lamps [19]

It may be seen as staggering how relatively fast the whole supply chain reacted considering billions of LED lamps units needed. In a short time span many new R&D, manufacturing and distribution companies were founded to satisfy high demand. Whole chain from the beginning of development was, from the technological standpoint of the LED lamps, practically unregulated. It means that the transformation from incandescent and compact fluorescent lamps to LED ones with today's market share in the EU reaching about 72 % had been only in the hands of manufacturers. Technical regulation was developed gradually and with delays.

As it may seem from the mentioned facts, the most robust way to find out all possible topologies and their parameters would be measuring all LED lamps on the market. This idea as fantastic as it sounds can't be unfortunately accomplished in the real world. Therefore, instead of measuring all available LED lamps on the market, only the bestselling LED lamps are going to be selected. To find out the bestselling LED lamps on today's market, the market analysis must have been carried out.

As a market of concern, an online market in Slovakia has been selected. The main reason for this choice was the existing online free database called Finstat containing main financial stats and information (sales, profits, etc.) of almost all companies based in Slovakia. With the knowledge of those parameters, it is easier to conduct more meaningful market analysis.

## 3.1 Methodology and approach

In the first place, all e-shops have been categorised into three groups by sold products.

In group A) are warehouses focused on specialised products needed for electrical installations (cables, circuit breakers, sockets). Companies included in this group mostly operate only as B2B (business-to-business) partners or sell products only to persons who own trade certificates. As average consumers in this group are considered professionals or other retail companies across the country.

In group B) are placed e-shops focused only on retail of all kinds of light sources and luminaries. Average consumer here is mixed between professional and non-professional because companies don't have restrictions for consumers. Unlike in other categories here the whole value of annual sales is composed only by products related to lighting.

In group C) are companies which sell mainly consumer grade electronics (household appliances, PCs, etc.). They mostly operate as a site of brick-and-mortar stores, standing by itself or purely as an e-commerce site. Outcome from analysis of this kind of stores will show what types of LED lamps are bought by ordinary nonprofessional customers.

Companies from database Finstat had been sorted by annual sales for the year 2021 and placed in individual categories. Within sorting had been applied following rules:

- store or warehouse must have available e-shop
- e-shop must have built-in filtering by bestselling products
- e-shop must contain LED lamps with at least 3 different types of sockets
- preferred are companies, which business is foremost based on e-shops (more valid results out of bestselling filters)

Results sorted by annual sales for the first three companies in each group are shown below.

Table 1 Companies included in group A)

| Place | Company | Annual sales in 2021 (mil. €) |
|---|---|---|
| 1. | HAGARD: HAL s.r.o. | 94,1 |
| 2. | i – center s.r.o | 8,67 |
| 3. | CB elektro s.r.o | 4,59 |

Table 2 Companies included in group B)

| Place | Company | Annual sales in 2021 (mil. €) |
|---|---|---|
| 1. | Donoci s.r.o | 29,38 (read below) |
| 2. | LEDart s.r.o | 6,52 |
| 3. | FEIM-SK s.r.o | 4,61 |

Table 3 Companies included in group C)

| Place | Company | Annual sales in 2021 (mil. €) |
|---|---|---|
| 1. | NAY a.s | 380,3 |
| 2. | Alza.sk s.r.o | 78,55 |
| 3. | OKAY Slovakia s.r.o | 58,72 |

In Table 1 can be seen a large gap between annual sales of first and second place. Many companies between those places must have been filtered out, because they don't have available e-shop or filtering by bestselling products. To imagine how big are trading volumes of LED lamps in this group, the bestselling LED bulbs in CB elektro s.r.o are stocked in around 16000 pieces per model. In Table 2 company Donoci s.r.o is not listed in the Finstat database because it's based in the Czech Republic. Nevertheless, the company was included in Table 2 because it is probably as they on their website claim, the biggest online retailer of household lightning products in Slovak Republic. Annual sales were very roughly estimated only from the number of reviews written by customers on the most popular price comparison website www.Heureka.sk. With their 15 868 reviews they are 4,5 times more reviewed than LEDart s.r.o, if annual sales were

considered as a linear function of numbers of reviews, Donoci s.r.o annual sales would reach around 29,38 € mil. therefore, 4,5 times more than LEDart s.r.o.

To find out bestselling LED lamps across all e-shops were applied filters by bestselling products. Parameters of first 10 found lamps in each e-shop were gathered and by their overall share in e-shops, were created statistics representing share of LED lamps among 10 best-selling lamps in individual groups. Parameters presented in results are manufacturer, socket type, LED chip type, CCT, dimmability and RGB colour changing function. In Figure 21 are results for consumers in group A, in Figure 22 for consumers belonging to group B, in Figure 21 for group C and lastly in Figure 24 are shown overall results expressing the situation across the whole market.

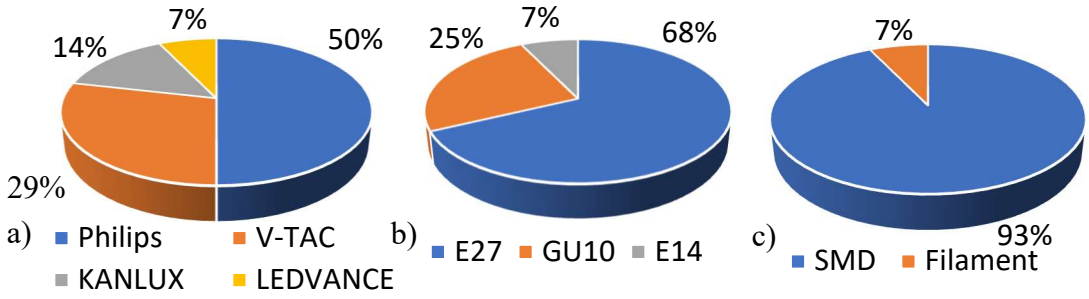


Figure 21 Share of LED lamps parameters among top 10 best-selling lamps in group A), each graph represents a) manufacturer, b) type of socket, c) LED chip type

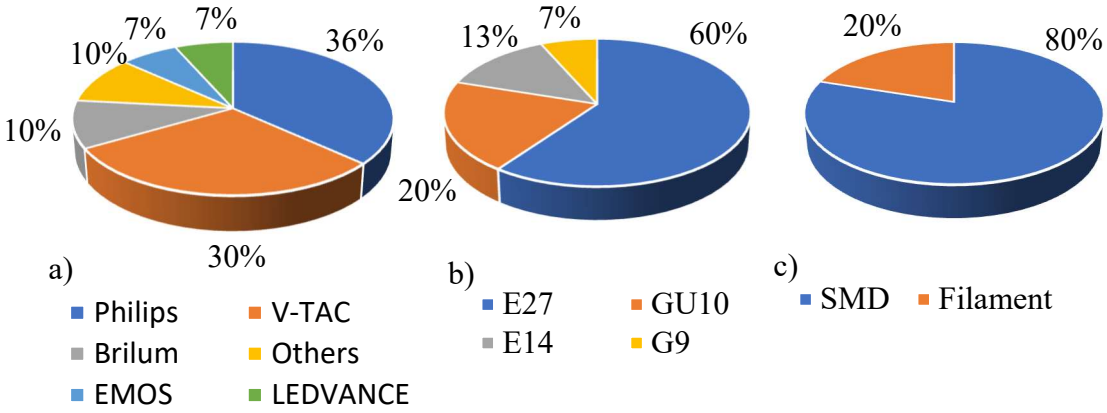


Figure 22 Share of LED lamps parameters among top 10 best-selling lamps in group B), each graph represents a) manufacturer, b) type of socket, c) LED chip type

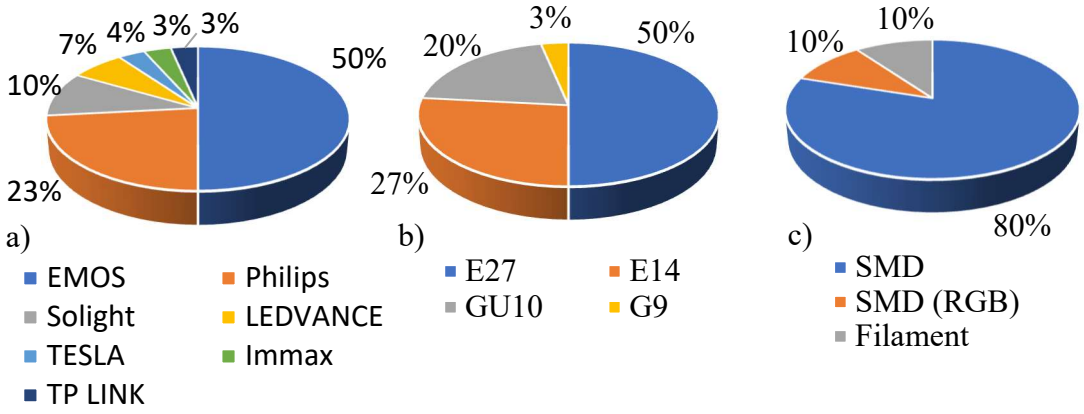


Figure 23 Share of LED lamps parameters among top 10 best-selling lamps C), each graph represents a) manufacturer, b) type of socket, c) LED chip type

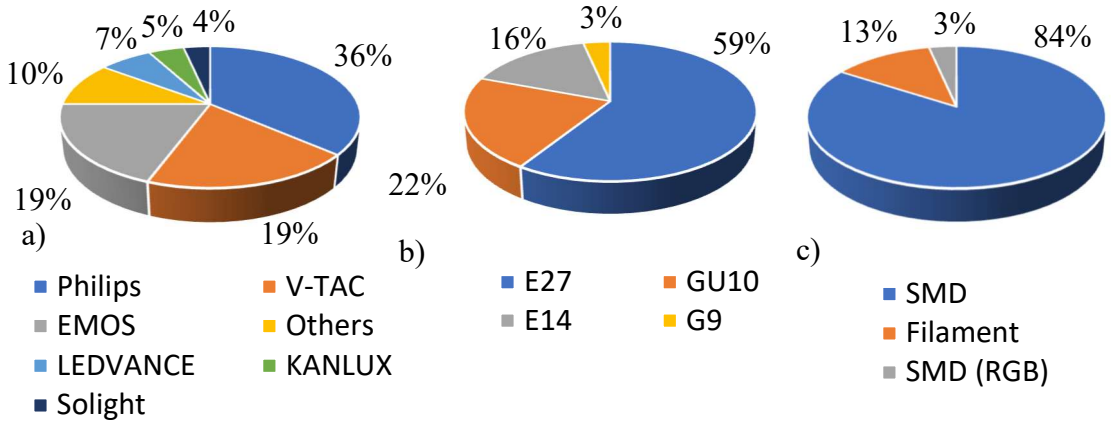


Figure 24 Share of LED lamps parameters among top 10 best-selling lamps in all three groups together, each graph represents a.) manufacturer, b.) type of socket, c) LED chip type

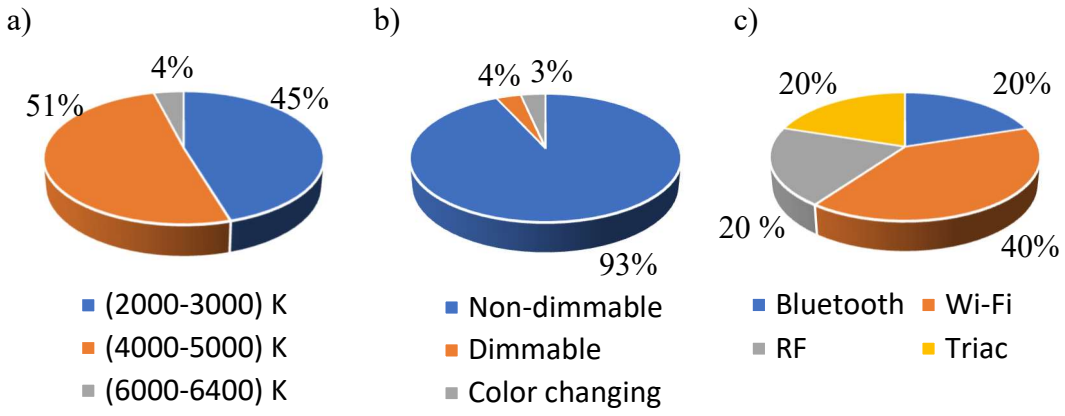


Figure 25 Share of LED lamps parameters among top 10 best-selling lamps in all three groups together, each graph represents a) CCT, b) Dimmability and colour changing function, c) Ways of controlling dimming.

It can be concluded, from the obtained results shown in Figure 21, that professional customers from group A), mostly buy LED lamps made by well-known manufactures such as Philips, V-TAC, LEDVANCE with market shares 50 %, 27 % and 7 % respectively. Results show that professionals are more conservative in choosing socket types and in used LED technology inside bulbs. The bestselling type of socket and LED technology in group A) is E27 with 68 % share and SMD chips with 93 % share. In other groups the market is a lot more diverse. Non-professional consumers in groups B) and C) are not so interested in selection of manufacturer. The analysed best-selling lamps from those groups are from up to 12 different manufacturers. Many of them are only budget oriented and not so profound in the lighting industry (TP-link, Immax, Brilagi, EMOS, Solight, etc.). However, despite the higher count of other manufacturers from Figure 22 for group B) and Figure 23 for group C) it is clearly visible that a substantial part of market share still belongs to well-known manufacturers such as Philips and V-TAC. Share of the E27 socket in other groups compared to group A) is lower in group B) by 8 % and in group C) is lower by 18 % so individual shares for groups B) and C) are 60 % and 50 % respectively.

Socket E27 is still bestselling among all groups with a lead up to 23 % in worst case against GU10 in group C). In comparison with group A) groups B) and C) additionally contain LED bulbs with socket type G9. However, individual shares are very low, reaching 7 % in group B) and 3 % in group C). From the standpoint of used LED chip technology in Figure 4, it could be seen that most recent wireless bulbs with RGB LEDs and bulbs with filament LEDs are getting more popular with an overall 20 % share among consumers in group C). In group B) RGB bulbs are not present but filament bulbs by itself cover 20 % of share. In comparison with group A) where the share of filaments bulb is 7 % it is nearly three times more.

Overall, as shown in Figure 24 across all groups, by wide margin, the best-selling LED bulbs are still basic ones with E27 socket, with 59 % share and with SMD LEDs inside, reaching 84 % share. Figure 25 shows, the distribution of CCT values in the market is fairly balanced. 45 % of all analysed lamps have a CCT in the range 2000 K – 3000 K and 51 % have a CCT in the range 4000 K – 5000 K. Only 4 % of bulbs are in a range between 6000 K – 6400 K. Furthermore, as Figure 25 b) shows, the most popular bulbs on market are non-dimmable with a 93 % share. The remaining 7 % is divided between dimmable (4 %) and colour changing bulbs (3 %), which of course also support dimming. Figure 25 c) shows the distribution of dimming control methods. Wi-Fi has been rated as the most popular method of bulbs controlling bulb dimming with 40 % share among dimmable bulbs. Bluetooth control was on par with RF with a 20 % share. As a RF were marked all bulbs controlled via handheld controller. Dimming control via triac regulation achieved 20 % share and it is also the only method on the list that requires wire to function.

## 3.2 Selected samples

The results pictured in Figure 24 shows the most common parameters of bestselling LED lamps on the market. Following those results, 31 different types of light bulbs were chosen for further testing. Brief overview of some acquired bulbs is shown in Figure 26. Their full list in attachment Nr.1. Focus was placed mainly on the most popular manufacturers V-TAC, Philips, EMOS and Solight. Judging by results LEDVANCE despite their higher popularity was not included for further measurements, instead of them was chosen Solight. As it is much more budget oriented and not as complex manufacturer as LEDVANCE, more problems with performance could be expected. Overall measurements including Solight are more balanced because now there are 2 well-known companies and 2 others which are not by any means specialised on lighting products.

Composition of socket types in acquired LEDs have been created according to results in Figure 24 b). From sockets E27, E14, GU10 and G9 were obtained 18, 6, 5 and 2 LED bulb pieces respectively. In percentage it represents 58 % for E27, 19 % for E14, 16 % percent for GU10 and 7 % for G9. Which very well corresponds with values in Figure 24 b). The highest percentage difference is in the number of bulbs with G9 sockets, which according to results should have only been 3 % of the share. However, one more LED bulb with filament inside was obtained for testing. It should provide a more comprehensive and up to date view on bulbs other than those with SMD chips inside.

Another factor used for selecting the LED bulbs has been the LED technology inside of them. Bulbs using SMD LED chip, SMD RGB LED chip and filament were obtained in 23, 1, and 7 pieces respectively. This distribution corresponds in percentage to 74 % for SMD chip, 23 % for filament and 3 % for SMD RGB chip. In comparison with results from Figure 25 c) is clearly visible that the percentage of SMD chips is lower by 10 % and percentage of filament ones is higher by 10 %. This distribution has been chosen because the number of filament lamps included in other earlier studies focused on measurement of flicker sensitivity is very low, which may have been due to their very low popularity and consequently low availability in earlier years. However, today in nonprofessional group B) is visible the notable popularity of filament bulbs reaching 20 % share. From the mentioned facts above it can be concluded that filament LED lights are becoming more popular, and it is on point to slightly increase their count.

Dimmable LED bulbs have been obtained in 7 pieces. Those 7 pieces are composed from 3 bulbs dimmable via Wi-Fi, 3 bulbs dimmable by triac and 1 bulb step dimmable. The colour changing bulb was obtained in 1 piece and it is already counted in those mentioned 3 pieces. In a percent, non-dimmable light bulbs account for 77 %, dimmable via Wi-Fi account for 10 %, dimmable via triac account for 10 % and step dimmable account for 3 % of the total number of bulbs. Distribution shown in Figure 25 b) and c) do not match with composition of obtained LED bulbs very well. Among obtained LED

bulbs are not bulbs dimmable via Bluetooth and RF. Instead, focus was placed mainly on one wireless and one wired category. LED bulbs from Wi-Fi and triac category are both obtained with LED SMDs and with filament. Filament bulbs in both categories were obtained in 1 piece per category. Chosen composition of bulbs enable better understanding of outcomes from measurement of different LED technologies with same dimming control. Which should help to filter out any possible phenomena dependable on the dimming controlling method. Earlier mentioned 1 piece of step dimmable led bulb was taken mainly because no other known studies evaluate parameters of such type of dimmable bulb. This type of bulbs is mainly visible in group B.) e-shops.


Figure 26 Overview of a few specific models from all selected samples.

Composition of manufacturers across acquired LED bulbs is shown in Figure 27. By comparing Figure 27 with Figure 24 a) it is clearly visible that distribution of selected manufacturers don't match very well with results from market analysis but the total number of obtained LED lamps from individual manufacturers correlates with manufacturer ranking from analysis. This difference is caused by the fact that in the beginning Philips and EMOS were chosen as the main manufacturers from whom the widest range of LED lamps with comparable parameters will be acquired. The results from such a composed distribution among manufacturers will offer a more complex and complete picture about how performance of LED lamps fluctuate across product lines of

manufacturers. In addition, as it was mentioned above, some bulbs as step dimming and filament G9 were acquired not because of market analysis results but for completeness of thesis and better understanding how other types of bulbs can behave.

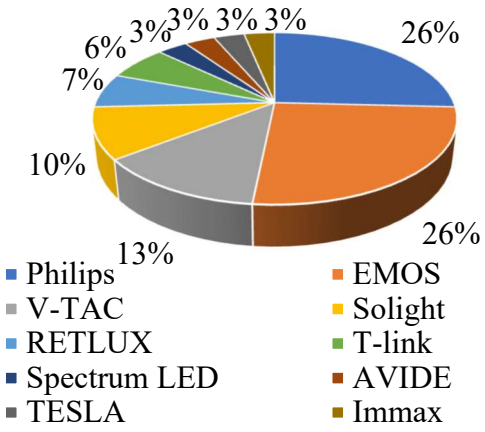


Figure 27 Manufacturers distribution of acquired LED bulbs.

All selected bulbs and their package were marked with their own unique ID code as it is pictured in Figure 28 . System of ID code creation is very practical and does not require looking at existing databases all over again. For example, in ID code PH/4D/-/1. First two characters represent the first two characters in the manufacturer's name. In this case it is PH which stands for PHILIPS. Second pair of characters is composed from the last two characters from the model number of the given LED bulb. The model number of this particular sample is 9290013124D. Third pair of characters express dimmability and type of dimmability. For this position have been used following markings: (-) non-dimmable, (T) dimmable by triac, (W) wireless, (S) step dimmable. This lamp, as non-dimmable, has therefore been marked with a dash. From every model were bought 3 in some models 4 pieces. To recognize those units between each. In the last place is the number which describes order in the pack. The highest value occurring in this position is 4 and lowest 1. This concrete ID distinctly belongs to the first lamp in the batch.


Figure 28 Example of marked bulb along with its package

# 4. PRELIMINARY CHARACTERIZATION

Packages of all selected LED bulbs or their official technical documentation contain no information about electrical parameters which would at least indicate their flicker performance or impact on power quality. Prevailing number of parameters listed by manufacturers are only rudimentary as nominal power, current draw, luminous flux and colour temperature. All mentioned parameters are insufficient and inadequate to describe such a diverse light source by driver circuit topology as a LED bulb. To better understand how LED bulbs perform within ideal supply conditions it was needed to conduct measurements with the aim to find frequent characteristic patterns in their behaviour. Following parts try to divide and characterise as many LED lamps as possible with common behaviour to groups.

## 4.1 Measuring parameters of LED lamps under nominal conditions

Measurements in this chapter were performed on all 31 models selected in the previous chapter. From each batch of three selected bulbs per model, one piece was chosen for testing. As first were measured instantaneous values of current, voltage and luminous flux. For measuring was used setup shown in Figure 29.

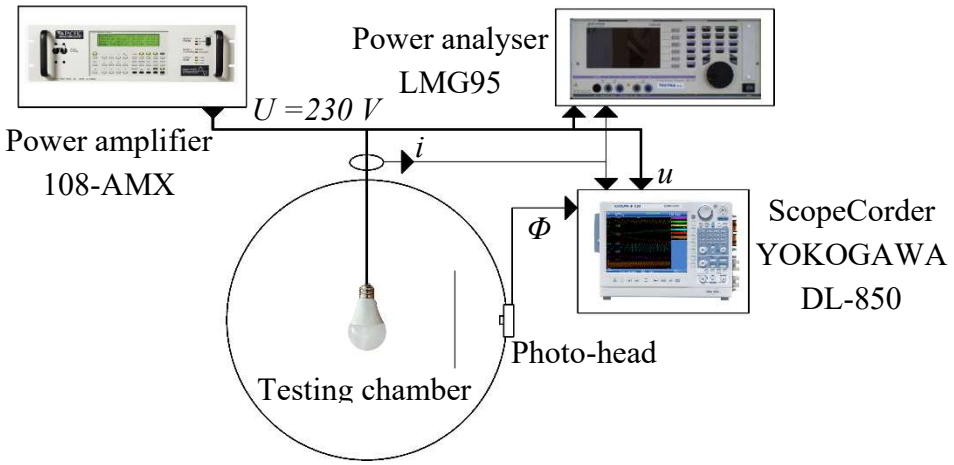


Figure 29 Schematic of test system for first series of measurements

Before execution of each measurement, the tested bulb sample was always left turned on for 15 minutes to stabilise its operation point. Samples were supplied from power source Pacific Power AMX-108 which helped to create an ideal power supply by isolating the test system from distortion and disturbances propagated from the public power grid. Power source was always set to nominal supply voltage (rms) 230 V and frequency 50 Hz. Analyzer LMG95 served only as reference for the set voltage and drawn current. The main instrument for analysis was ScopeCorder YOKOGAWA DL-850 with 16-bit resolution. Its sampling frequency on all channels was set to 500 kS/s and recording time

to 0,5 s. Current drawn by bulbs was measured via hall effect current probe. Supply voltage was measured via voltage probe 10:1 and output from photo-head which represents luminous flux as function of voltage was connected directly to the measuring channel. All recorded values from the ScopeCorder were later evaluated and processed by 10 cycle analysis. The tested LED lamp was placed in an Ulbricht-type test sphere with 2.5 m diameter. Additionally were measured 10-minut light flicker values $P_{st,LM.}$

### 4.1.1 Evaluation of fundamental parameters from measured values

After execution of measurement, all results from 31 samples were divided by their specific signs into four main groups (A, C, AC, D). Meaning behind division into the groups and their differences are described in the next chapter.

As follows from shown evaluated parameters in Table 4. The highest current total harmonic distortion was measured in sample TE/40/-/1 with value 176.4 %. On the other hand, the lowest $THD_I$ 29.4 % was registered in sample VT/84/T/1. All mentioned samples in paragraphs are for better orientation in the table highlighted by red colour.

In comparison between the difference of measured input active power and nominal input power consumption given by the manufacturer. Sample PH/7C/-/1 has among all the highest differences equals 4.2 % above the nominal value. On the other hand, sample EM/20/-/1 has the highest difference to the negative side, equals 16.8 % below the nominal input power.

Similarly, as in previous but with luminous flux. The highest differences between measured luminous flux and nominal luminous flux rated by manufacturer has sample VT/12/-/1 with measured output luminous flux higher by 17.8 % above nominal value and sample PH/69/-/1 with 11.3 % below the nominal output luminous flux.

The worst lamp efficacy 75 lm/W was found in sample EM/40/-/1 which well corresponds with grade G on its energy label. On the other hand the highest efficacy 198 lm/W was measured in sample PH/67/-/1 which meet grade A on its energy label.

The highest $P_{st,LM}$ equal to 0.351 was found in sample VT/84/T/1. Increased value of $P_{st,LM}$ in steady-state tells that output luminous flux contains frequency components below the 50 Hz. What corresponds to unstable operation, caused by improper driver design. Furthermore, the increased value of SVM to 0.344 expresses present frequency components in output luminous flux even above the 80 Hz. Overall percent flicker is equal to 9.5 % which is only about 3 % higher than in incandescent bulbs.

SVM higher than 0.4 was found in 3 samples. In the first sample RE/96/-/1 SVM is equal to 6.23, $P_{st,LM}$ is only slightly increased to 0.121, however percent flicker is equal to 100 %. High $P_{st,LM}$ percent flicker together with high SVM but low $P_{st,LM}$ indicate that

main frequency components causing the high modulation depth are on frequencies above the 80 Hz. Second sample VT/61/-/1 has SVM equal to 0.617. Symptoms are the same as in the previous sample, low $P_{st,LM}$ 0.013 and increased percent flicker to 23.7 %. Third sample SP/76/T/1 has SVM 0.413 together with increased percent flicker to 11.1 % and negligible $P_{st,LM.}$

The highest percent flicker was found in the already mentioned sample RE/96/-/1 with value equal to 100 %. The lowest percent flicker has a sample EM/80/-/1 with value reaching only 0.1 %. This is of course related to negligible values of $P_{st,LM}$ and SVM. Another sample worth mentioning is SO/07/-/1 which has percent flicker 13.4 %, Thus higher than mentioned SP/76/T/1 but it has negligible SVM and $P_{st,LM.}$ This behavior corresponds to presence of frequency components in output luminous flux above the $P_{st,LM}$ and SVM evaluating range 2000 Hz.

During all measurements total harmonic distortion of supply voltage was 0,08 %.

Table 4 Overview of results from testing

| Label | I (mA) | $THD_I$ (%) | P (W) | PF (-) | Φ (lm) | $K_p$ (lm/w) | $P_{st,LM}$ (-) | SVM (-) | *Mod%* (%) |
|---|---|---|---|---|---|---|---|---|---|
| PH/4D/-/1 | 88.5 | 105.7 | 12.2 | 0.60 | 1520 | 124 | 0.009 | 0.015 | 2.2 |
| PH/69/-/1 | 89.7 | 115.0 | 12 | 0.58 | 1366 | 114 | 0.013 | 0.002 | 3.5 |
| PH/62/-/1 | 57.0 | 110.6 | 7.9 | 0.60 | 782 | 99 | 0.005 | 0.017 | 2.3 |
| PH/67/-/1* | 36.8 | 154.3 | 4 | 0.47 | 782 | 198 | 0.019 | 0.015 | 1.8 |
| PH/89/-/1* | 53.0 | 110.7 | 6.9 | 0.56 | 768 | 112 | 0.004 | 0.012 | 0.5 |
| PH/7C/-/1 | 36.0 | 141.7 | 4.5 | 0.54 | 468 | 104 | 0.007 | 0.002 | 0.3 |
| PH/86/-/1* | 35.2 | 108.7 | 4.4 | 0.54 | 418 | 95 | 0.002 | 0.024 | 1.9 |
| PH/12/-/1* | 39.3 | 133.1 | 4.8 | 0.53 | 530 | 111 | 0.004 | 0.020 | 1.0 |
| EM/45/-/1 | 53.0 | 113.9 | 7.2 | 0.61 | 839 | 117 | 0.019 | 0.015 | 3.2 |
| EM/42/-/1 | 59.4 | 146.5 | 7.4 | 0.54 | 835 | 113 | 0.010 | 0.003 | 0.3 |
| EM/31/-/1 | 55.7 | 134.3 | 7.2 | 0.56 | 931 | 129 | 0.016 | 0.006 | 1.1 |
| EM/01/-/1 | 35.8 | 143.6 | 4.4 | 0.53 | 398 | 91 | 0.006 | 0.100 | 9.8 |
| EM/20/-/1 | 41.0 | 150.0 | 5 | 0.53 | 457 | 92 | 0.007 | 0.003 | 0.3 |
| EM/80/-/1 | 50.4 | 140.3 | 6.4 | 0.55 | 598 | 94 | 0.010 | 0.001 | 0.1 |
| EM/40/-/1 | 31.9 | 146.5 | 3.9 | 0.53 | 292 | 75 | 0.007 | 0.002 | 0.3 |
| VT/28/-/1* | 71.0 | 141.4 | 8.4 | 0.51 | 760 | 91 | 0.015 | 0.005 | 0.6 |
| VT/12/-/1* | 58.5 | 131.4 | 7.1 | 0.53 | 730 | 103 | 0.003 | 0.019 | 1.3 |
| SO/06/-/1 | 79.2 | 152.3 | 9.6 | 0.53 | 922 | 96 | 0.014 | 0.003 | 2.6 |
| SO/07/-/1 | 96.5 | 150.3 | 11.7 | 0.53 | 1006 | 86 | 0.024 | 0.003 | 13.4 |
| SO/09/-/1 | 48.1 | 144.1 | 6 | 0.54 | 477 | 80 | 0.023 | 0.005 | 2.2 |
| RE/10/S/1* | 48.6 | 132.4 | 5.8 | 0.52 | 466 | 80 | 0.011 | 0.010 | 0.6 |
| TE/40/-/1 | 32.6 | 176.4 | 3.5 | 0.47 | 379 | 107 | 0.009 | 0.001 | 0.2 |
| TP/10/W/1 | 69.9 | 159.2 | 8.4 | 0.52 | 818 | 97 | 0.031 | 0.004 | 0.3 |
| IM/3L/W/1* | 54.6 | 140.2 | 6.6 | 0.53 | 817 | 123 | 0.002 | 0.001 | 0.9 |
| RE/96/-/1 | 15.7 | 68.0 | 3 | 0.83 | 325 | 109 | 0.121 | 6.231 | 100 |
| EM/03/-/1 | 38.3 | 104.8 | 5.9 | 0.67 | 804 | 135 | 0.020 | 0.022 | 7.5 |
| VT/61/-/1 | 47.5 | 80.4 | 8.4 | 0.77 | 761 | 90 | 0.013 | 0.617 | 23.7 |
| AV/WW/T/1 | 42.8 | 89.1 | 7.3 | 0.74 | 676 | 93 | 0.096 | 0.178 | 10.5 |
| TP/30/W/1 | 51.1 | 81.6 | 8.6 | 0.73 | 698 | 81 | 0.005 | 0.011 | 1.8 |
| VT/84/T/1 | 53.2 | 29.4 | 10.8 | 0.88 | 1232 | 114 | 0.351 | 0.344 | 9.5 |
| SP/76/T/1 | 55.5 | 40.9 | 10.6 | 0.83 | 1058 | 100 | 0.009 | 0.413 | 11.1 |

Meaning of collored label columns : pale blue – class Aa/Ab (* asterisk marks class Ab), gray – class C, yellow – class Da, orange – class Db
Highligted values with red color are decribed in text above

Values in Table 5 were calculated as follows:

The lamp efficacy $K_P$:

$$K_p = \frac{\Phi}{P} \tag{4.1}$$

$\Phi$ – measured luminous flux
$P$ – measured input active power of LED bulb

The effective value of current $I_{RMS}$:

$$I_{RMS} = \sqrt{\frac{1}{N} \cdot \sum_{k=1}^{N} i_k^2} \tag{4.2}$$

$N$ – number of samples in 10 cycles of 50 Hz system sampled by DL850
$i_k$ – instantaneous value of current sample $k$ measured by DL850

The effective value of voltage $U_{RMS}$:

$$U_{RMS} = \sqrt{\frac{1}{N} \cdot \sum_{k=1}^{N} u_k^2} \tag{4.3}$$

$N$ – number of samples in 10 cycles of 50 Hz system sampled by DL850
$u_k$ – instantaneous value of voltage sample $k$ measured by DL850

Input active power $P$:

$$P = \frac{1}{N} \cdot \sum_{k=1}^{N} \frac{u_k \cdot i_k}{n} \tag{4.4}$$

$N$ – number of samples in 10 cycles of 50 Hz system sampled by DL850
$u_k$ – instantaneous value of voltage sample $k$ measured by DL850
$i_k$ – instantaneous value of current sample $k$ measured by DL850

Apparent power S:

$$S = I_{RMS} \cdot U_{RMS} \tag{4.5}$$

Reactive power Q:

$$Q = \sqrt{S^2 - P^2} \tag{4.6}$$

### 4.1.2 Analysing current and output luminous flux waveforms in time domain

To better distinguish LED lamps by their behaviour between each other. Current waveforms have been chosen as one of the main parameters for categorization of measured lamps. Four main groups A, C, AC and D have been created. Group A is divided to subgroups Aa and Ab. The following text will describe the main characteristic WFs for each group. The values of current and luminous flux in Figures are shown in reference to their rms values.

Characteristic current WFs for group Aa are pictured in Figure 30. In this group are placed more than half of all tested LED bulbs (16 from 31).

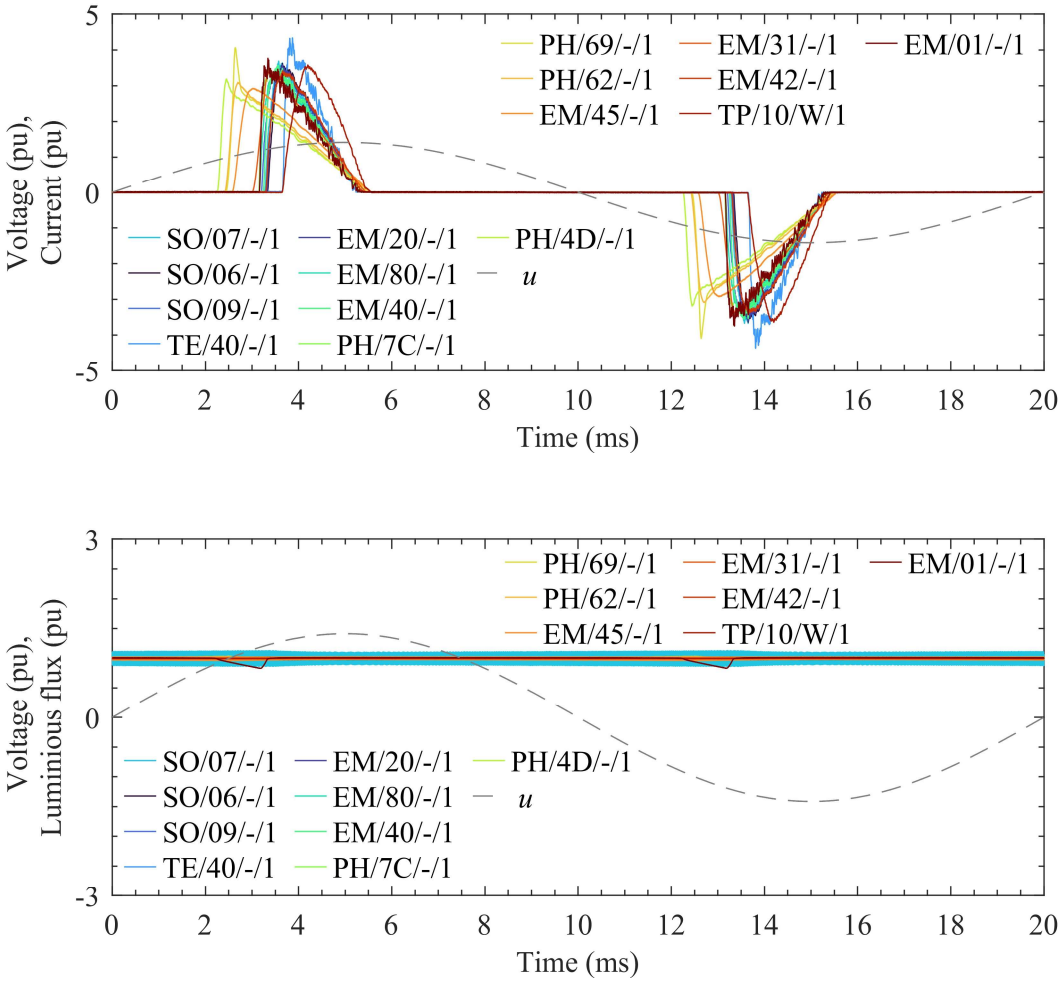


Figure 30 Normalized waveforms of current and luminous flux of each LED bulb in group Aa

To group A belong LED bulbs which topology have DBR at the input as ac/dc converter followed by bulk capacitor, after the capacitor is connected dc/dc switching converter. By current WFs, A group is divided to subgroups Aa an Ab. In current WFs of group Ab can be seen that current is drawn even in off-state. It is caused by parallel component (capacitor, etc.) most often in the EMI filter which is placed at the input of the driver (ac side).

As it is seen, sample TE/40/1 have the shortest pulse duration. It is the main reason for its highest total harmonic distortion of drawn current.

From WFs of luminous flux is visible that notable dips were found only in sample EM/01/-/1. Thick blue WF belongs to sample SO/07/-/1. Its thickness corresponds to its measured percent flicker 13.4 %. Moreover, the whole WF is clearly modulated by significantly higher frequencies than a few harmonics of 50 Hz.

WFs belonging to group Ab are shown in Figure 31.

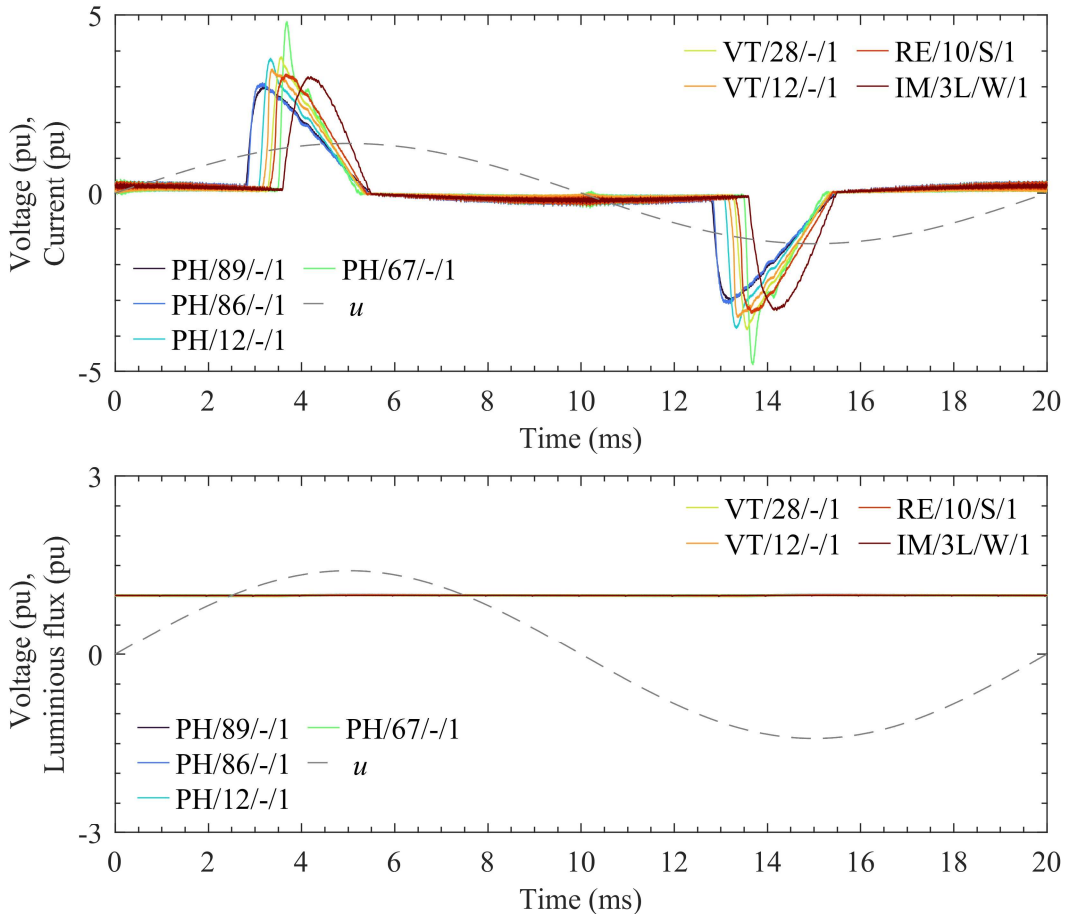


Figure 31 Normalized waveforms of current and luminous flux for each LED bulb in group A

To the next group C belongs only one bulb RE/96/-/1. Topology specific for group C has at the input ac/dc converter DBR followed by CCR. After DBR may followed capacitor or EMI filter, however it is not mandatory. CCR directly regulates current through the string so current is drawn only if input rectified voltage (its instantaneous value) reaches higher voltage than forward voltage of LED string. Characteristic current and luminous flux WFs for LED belonging to group C are drawn in Figure 32. As it is visible from luminous flux WF, modulated is the whole envelope which corresponds to the calculated percent flicker 100 % shown in Table 4. Because of high modulation on relatively low frequencies this bulb reaches SVM of 6.2 together with slightly higher $P_{st,LM}$ of 0.12.

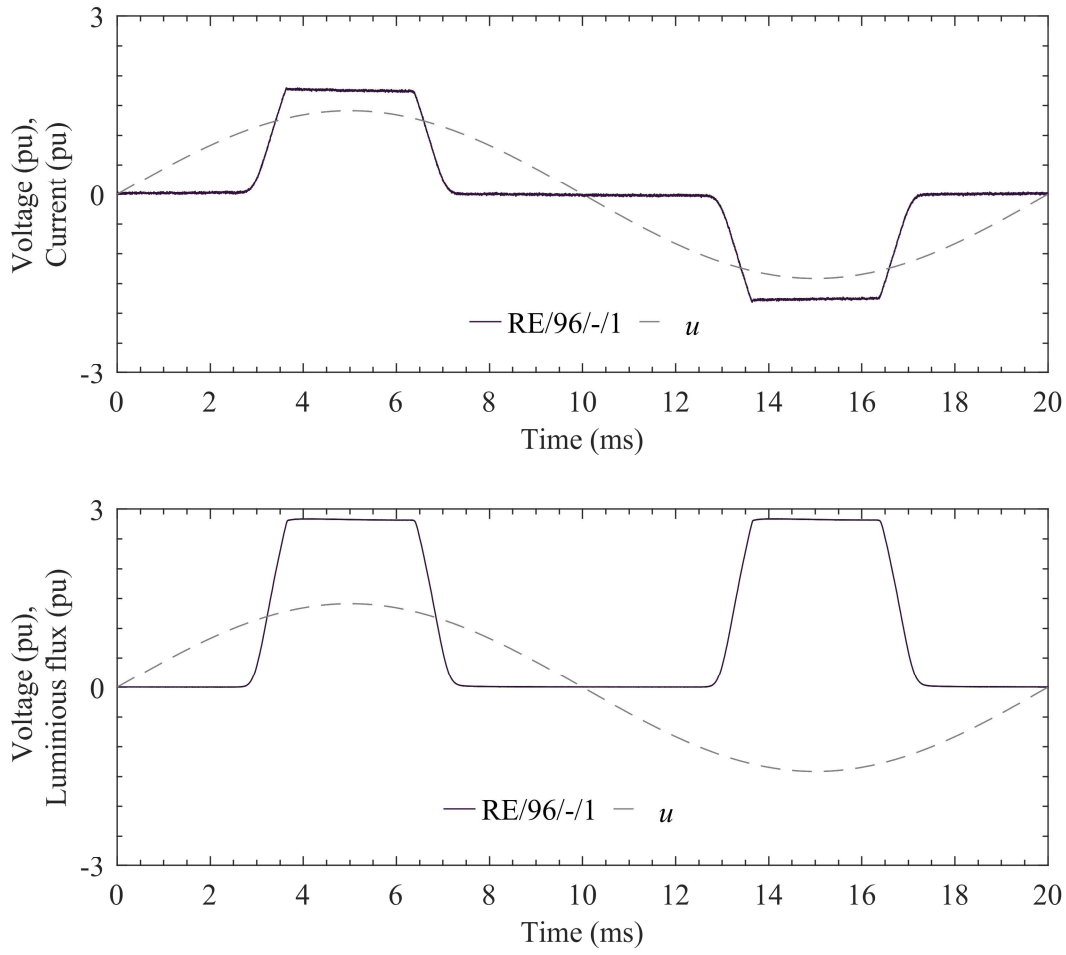


Figure 32 Normalized waveforms of current and luminous flux for LED bulb in C group

LED bulbs producing current WFs shown in Figure 33 are classified as group AC. Their current WFs have “double spike” shape. By disassembling it was figured out that characteristic topology of LED lamps belonging to AC group have at the input DBR as ac/dc converter followed by CCR limiting current though bulk capacitor and second CCR limiting current through LED string. As it is visible in sample TP/30/W/1 were administreted oscillations during on-state. In WFs of luminous flux are very prevalent

ripples. All LED lamps in this group beside TP/30/W/1 have percent flicker higher than 7.5 %. VT/61/-/1 belonging to this group have SVM higher than 0.4 and $P_{st,LM}$ is also bit higher than in group A.

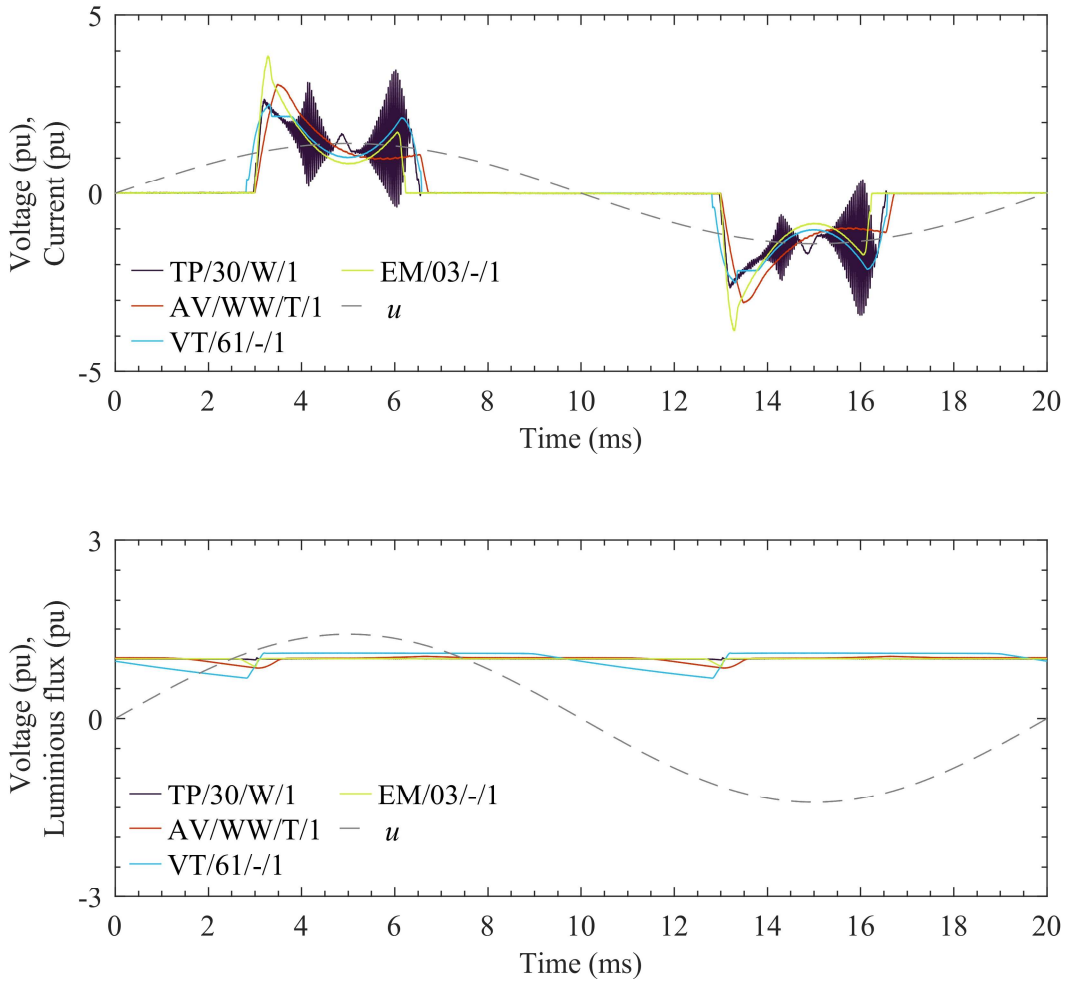


Figure 33 Normalized waveforms of current and luminous flux for LED bulbs in group AC

LED bulbs belonging to group D and their WFs are shown in Figure 34. Characteritic topology of LED lamps in this group have active PF correction with single-stage switching-mode dc/dc converter. Both LED lamps in this group are dimmable by triac. Currents drawn by by both bulbs have lowest total harmonic distortion among all tested bulbs their $THD_I$ is in the range 30 to 41 %. WF of output luminous flux in both cases have WF resembling sine shape. Both samples exhibit higher SVM, SP/76/T/1 even over 0.4.

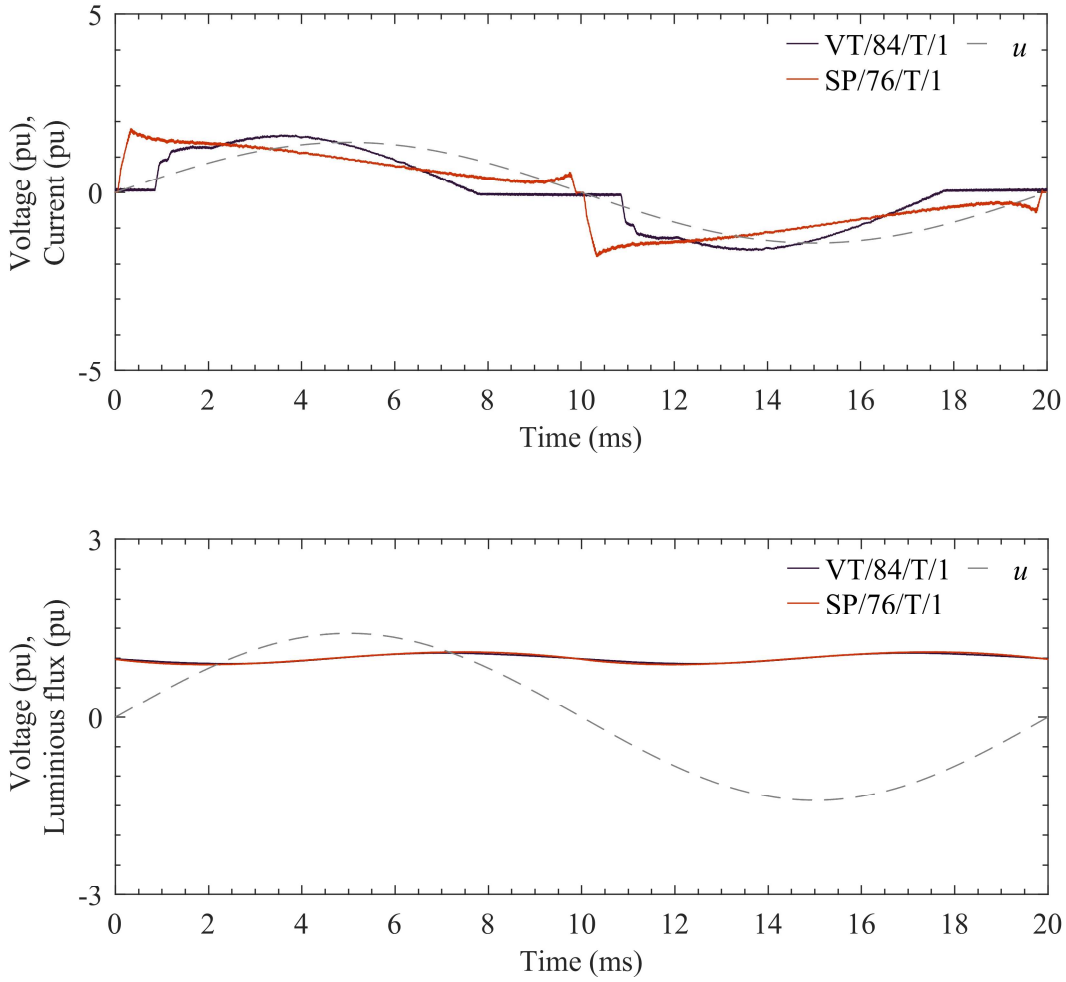


Figure 34 Normalized waveforms of current and luminous flux for LED bulbs in group Db

### 4.1.3 Analysing current and output luminous flux waveforms in frequency domain

Furthermore, were analysed current and luminous flux waveforms in frequency domain. From shown waveforms in the time domain it is hard to distinguish any major functional differences between LED lamps in the same group. And it is not possible to tell how categories differ between each other in regions where switching frequencies of drivers may occur, roughly 20-200 kHz. Knowledge of specific frequency spectrum patterns in luminous flux or in drawn current may serve as a “fingerprint” which will help with further investigation of individual topologies and differences between them. The aim during the analysis of each frequency spectrum was placed to describe common signs of LED bulbs in the same group and to verify their belonging to a specific group. For transformation from time domain to frequency domain, DFT was used with the FFT algorithm implemented in MATLAB. As data for FFT were used raw measured data without any further filtration or modification. For windowing of measured values a

rectangular function was used. Measured data were analysed on 10 cycles of system frequency 50 Hz. Since frequency resolution of DFT is finite, in this case 5 Hz and frequency components of measured signals naturally may not be synchronised, thus may not correspond with frequency of DFT bins. It can be predicted that later shown spectra of luminous flux and drawn current are affected by spectral leakage. However, as a power supply was used source with stable output frequency as it is pictured in Figure 29. Which should provide sufficient and much more stable frequency of output voltage than for example power grid. Moreover, the goal of this part is to find and show characteristic patterns in the whole frequency spectra and not a precise evaluation of frequency components magnitude.

Because of the high number of other close spaced frequency components, analysis of current frequency spectra was not very straightforward. It was hard to find any major and clear characteristic patterns which repeatedly occur in more cases and thus cover some wider portion of measured LED bulbs. From measured results was found that better characterization would be done by using frequency spectra of luminous flux which carries more distinct patterns with better signal to noise ratio. Spectra of drawn current will be displayed alongside with luminous flux spectra for better comprehension of how frequency components in current relate to frequency components in output luminous flux.

Because of the fact that between groups Aa and Ab were found no major differences in their patterns of luminous flux. Their characteristic patterns will be shown only in one figure for both groups. Characteristic frequency spectra of luminous flux on the right with frequency spectra of drawn current on the left are shown in Figure 35. Among the spectra of luminous flux were overall identified 3 different frequency spectrum patterns. In Figure 35 a.) is shown AM modulation like pattern. It was found in samples PH/62/-/1, PH/86/-/1 and PH/12/-/1. In this representation of AM modulation. Width of sidebands and carrier was registered among samples in range of 1 to 20 kHz. As could be seen from Figure 35 in the spectrum of drawn current is the same pattern as in the spectrum of luminous flux but it is more difficult to recognize, than from luminous flux. This is true among all samples in group A but in most cases the component with lowest frequency is not visible because other frequency products are covering it up.

In b.) is shown a specific pattern which contains a number of harmonics. In the shown example are visible 3 harmonic components. Their exact number among samples vary. In Aa group, this particular pattern was recognized in samples PH/4D/-1, PH/69/-/1, EM/45/-/1, EM/31/-/1, SO/06/-/1, SO/07/-/1, SO/09/-/1. Subsequently for group Ab this pattern was recognized in samples PH/67/-/1, PH/89/-/1, VT/28/-/1, VT/12/-/1, RE/10/S/1. The width of the occurring harmonic components among all samples from group Aa and Ab vary in range from 1 to 57 kHz.

In c.) is pictured pattern where in luminous flux are no clearly visible frequency components which could belong to driver switching processes. Frequency spectra of drawn currents are among the LED lamps in this group very similar, and it is difficult to find any distinct differences. It is also hard to assign specific frequency components to some switching or operating processes of the driver, which would tell more about driver behaviour. Around 10 - 100 kHz in drawn current are visible irregularities across all measured samples but it is not possible to give them specific meaning without more investigation. This pattern in frequency spectra of output luminous flux was registered in samples PH/7C/-/1, EM/42/-/1, EM/01/-/1, EM/20/-/1, EM/80/-/1, EM/40/-/1, TE/40/-/1, TP/10/W/1.

In most samples harmonics belonging to system frequency in luminous flux above 1000 Hz significantly decay or already have negligible value around background noise floor in range of $10^{-4}$ to $10^{-5}$ lm. Only in one sample EM/01/-/1 which has visible ripples in luminous flux shown in Figure 30 was registered spreading of harmonics from 50 Hz up to 15000 kHz.

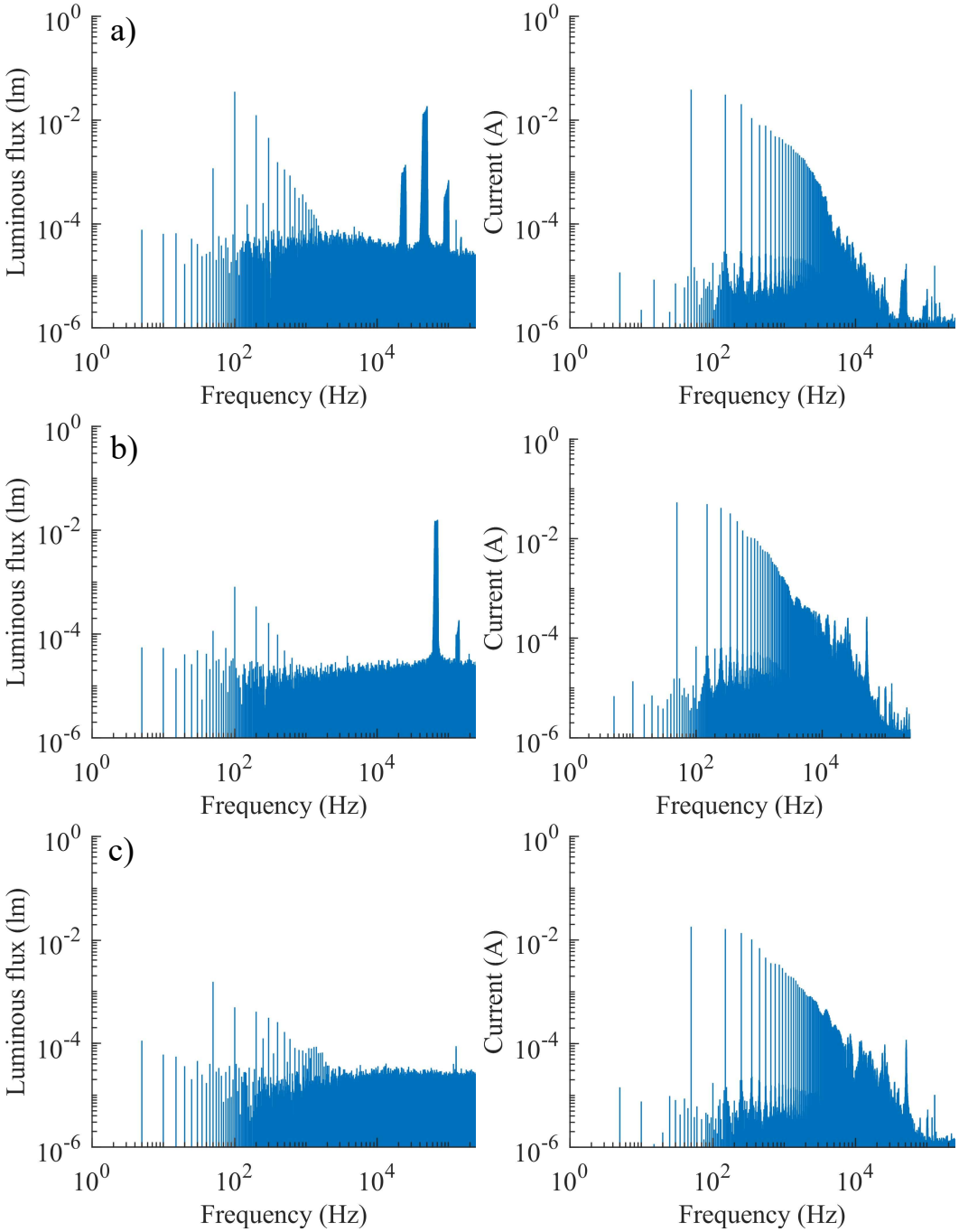


Figure 35 Characteristic frequency spectra of radiated luminous flux and drawn current for LED bulbs, a.) AM modulation (PH/62/-/1), b.) Harmonic components (SO/07/-/1), e.) no switching frequency components present (EM40/-/1)

Pattern found in group C is shown in Figure 36. Amplitudes of harmonics in luminous flux are significantly higher than in other groups which well corresponds to the highest measured *Mod%* among all tested LED bulbs as follows from Table 4. Harmonics components around 1000 Hz in luminous flux are 100 to 1000 higher than in most samples included in group A. In the frequency spectrum of output luminous flux and drawn current

were not found patterns of frequency components belonging to switching-mode operation of the driver.

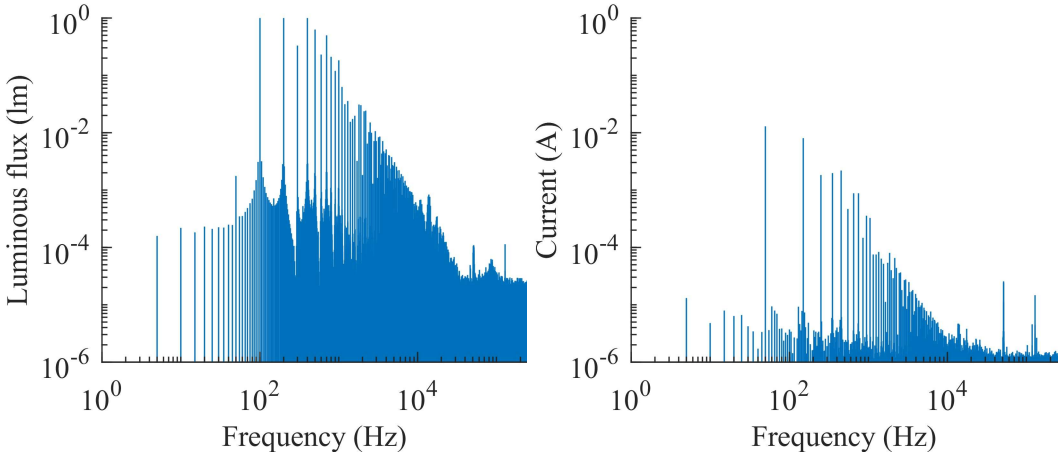


Figure 36 Characteristic frequency spectrum of luminous flux and current for group C (RE/96/-/1)

Specific pattern of luminous flux frequency spectrum found among LED bulbs belonging to group AC is shown in Figure 37 a). Characteristic for luminous flux frequency spectra of LED lamps in AC group is slow decay and still relatively high amplitudes of harmonics to 1-3 kHz. Beyond 1-3 kHz their amplitude gradually attenuates up to 10-50 kHz. In addition, dense presence of frequency components around and beyond 10 kHz is visible in all current and luminous flux spectra across the whole AC group. In Figure 37 b) are shown spectra of sample TP/30/W/1. This sample is shown as an example how spectra across the group may differ. TP/30/W/1 current WF shown in Figure 33 contain oscillations which manifest in frequency domain as harmonic products starting at 25 kHz with propagation over 100 kHz. Their presence may originate from unstable and improper design of the driver. Amplitude of the first frequency product from oscillations at 25 kHz reaches a magnitude close to current drawn on the 3rd and 5th harmonic of the system's frequency. To this group belong only 4 samples so it is hard to say how statistically prevalent are WFs of current with such oscillations among all LED bulbs available on market. The AC group is enough characterised with only one pattern in Figure 37 a) which clearly describes the main characteristic signs occurring in other spectra of bulbs belonging to this group. This is the main reason why no other pattern classifications were made.

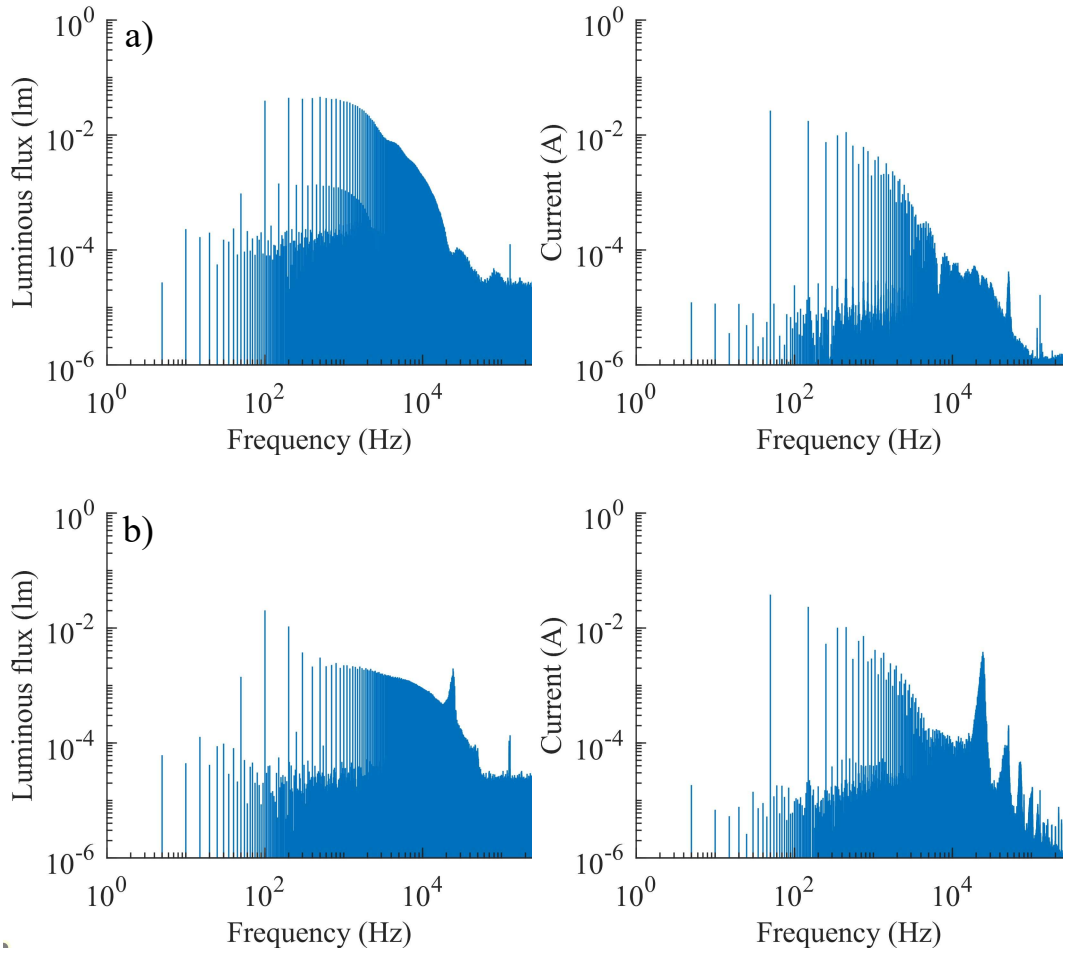


Figure 37 a) Characteristic frequency spectrum of luminous flux and current for group AC (EM/03/-/1), b) Frequency spectra of LED lamp belonging to the same group (TP/30/W/1)

To group D belong overall only 2 samples. Because of their lower count, spectra of luminous flux and drawn current are shown for both samples in Figure 38 a.) and b). In a) are pictured spectra of sample VT/84/T/-/1. On a first sight in the spectrum of luminous flux are visible significant frequency components under 50 Hz with maximum amplitude only at 5 Hz. These frequency components are the main reason why VT/84/T/-/1 reach the highest measured $P_{st,LM}$, among the all tested LED bulbs. In the second sample SP/76/T/1 shown in b), frequency components under 50 Hz in luminous flux are very well attenuated. Above the 100 Hz spectra of luminous flux in both samples are quite similar and harmonics do not propagate well beyond 1-2 kHz. Further whole spectra up to 250 kHz is composed only with background noise. No frequency components related to switch-mode driver are registered in this frequency range.

Spectra of current are roughly to 10 kHz very similar, however around 100 kHz in sample SP/76/T/1 is registered modulation which belongs to some active switching parts of its driver topology.

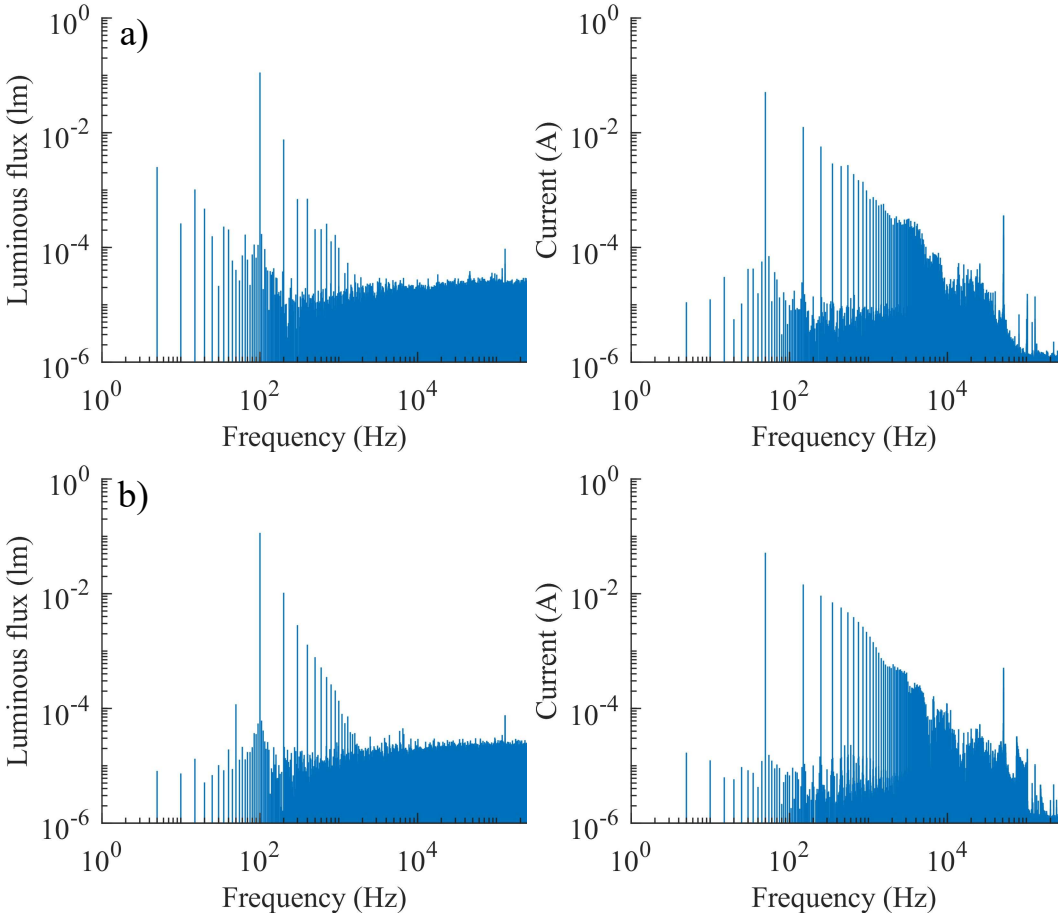


Figure 38 Frequency spectra of luminous flux and current in group D, a) VT/84/T/-/1, b) SP/76/T/1

### 4.1.4 Analysing frequency spectrum of current and output luminous flux in time domain

The previous section described the analysis and characterisation of frequency spectra transformed by DFT from the measured values of luminous flux and current, sampled during the 10 periods of 50 Hz system frequency. However, such a method of analysis has certain shortcomings in evaluation of LED bulbs driver behaviour. Shown spectra provide a very good representation of what is happening in luminous flux and current frequency domain during the 10 periods of 50 Hz. But it is needed to be aware that magnitude of shown frequency components depends on their duration in the analysed signal, thus on their averaged value per whole analysed time interval. Following that, frequency components present in signal with high magnitude but with low periodicity and short duration, may end up in showed frequency spectrum with apparently low magnitude. On the other hand, frequency components which are present in signal during the whole time of measurement, having low magnitude. May end up being displayed in frequency spectrum with higher magnitude, than frequency components present in signal

with higher magnitude but low periodicity and duration. Furthermore, as it was shown in group A. Frequency spectra of luminous flux contain patterns of frequency components linked to driver function, but from shown frequency spectra it is not possible to tell their duration and overall behaviour in time. Same principles are applicable even for group AC. In this group are not characteristic distinct frequency components as in group A. Therefore, it is more difficult to characterise function of their driver exactly. To overcome mentioned disadvantages and to create a more complete picture about the function of drivers. Measured data were analysed by STFT.

STFT provides a suitable tool to reveal behaviour of LED drivers in time. Principle of this method lies in performing DFT on shorter time intervals of the analysed signal. As a result, it will determine the Fourier spectrum on each shorter time segment. Measured values of luminous flux and current were before performing STFT filtered to attenuate fundamental component and its strong harmonics. For filtration of input data was used elliptic high-pass filter of third order. Parameters of filter were set to 0.1 dB passband ripple, 10 kHz passband edge and to 60 dB stop band attenuation. Its exact magnitude response is plotted in Figure 39.

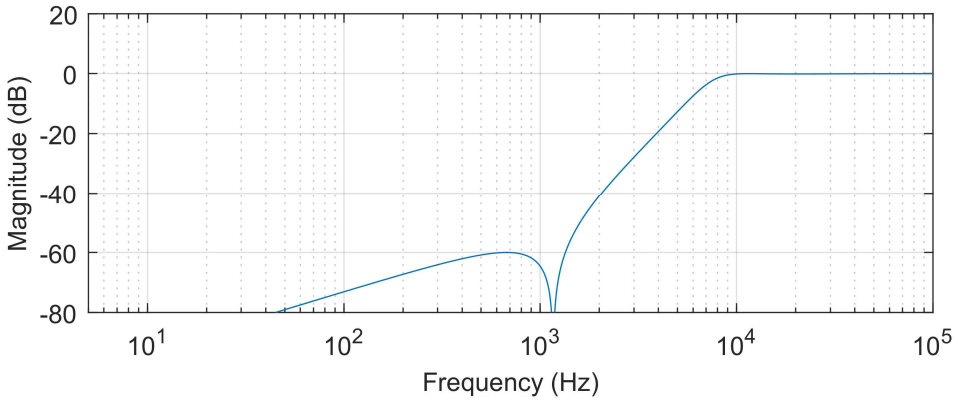


Figure 39 Frequency response of used elliptic filter.

Subsequently after the filtration was performed STFT with FFT window length set to 500 samples, reaching 1 kHz of frequency resolution. Type of window used was Hanning with 50 % overlap. Obtained spectrograms from STFT were further analysed and classified by the same principles as frequency spectra in the previous section. For better comprehension of how frequency spectra showed earlier, relates to spectrograms obtained by STFT all following spectrograms are shown on the same bulb samples. Frequency spectrograms of all tested LED bulbs are in attachment Nr.3.

Analysed spectrograms from STFT in group A shows no major differences between group Aa and Ab in patterns and behaviour of frequency components in the analysed frequency range. The only main registered difference was much higher background noise

in the current of Ab group due to its present parallel component in the EMI filter before DBR (ac side). Because of no other significant differences, groups Aa and Ab are described as one group. In Figure 40 are shown spectrograms of current and luminous flux of AM modulation like pattern, registered in sample PH/62/-/1. In spectrograms of luminous flux, across all samples manifesting with this pattern, are present 3 FM modulated frequency components. With the strongest one in the middle. The same but obviously shorter FM modulated components are visible even in the current spectrogram during the on-state of the driver. The lowest one with frequency around 25 kHz is very faint, but it is present too. Frequency of these FM modulated components from the beginning till the end of the on-state of driver is rising then as it is seen from luminous flux their frequency decline. This behaviour is directly linked to the driver topology, which by the change of switching frequency or duty cycle, regulates the output voltage to the LED chain.

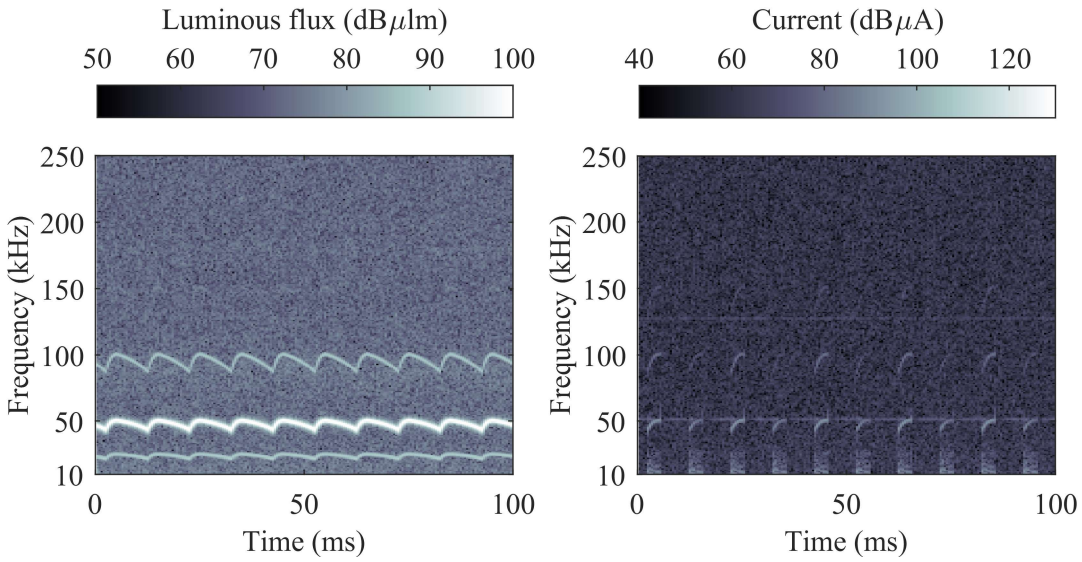


Figure 40 Spectrograms of luminous flux and current registered in groups with AM modulation pattern (PH/62/-/1).

As a second, were analysed samples belonging to group A, which exhibit characteristic harmonic pattern in their frequency spectrum of luminous flux. Within analysis of their current spectrograms were found 2 different types of patterns. Together with luminous flux their characteristic spectrograms are showed in Figure 41 a) and b). Luminous flux spectrograms of all samples exhibiting this pattern, are very similar and contain 1 to 3 visible FM modulated harmonic components. Their width respectively their frequency drift corresponds with values listed before in the description of their frequency spectra. On the other hand, their spectrograms of current distinctly differ. In a) current spectrogram do not have visible FM modulated frequency components related to its output luminous flux spectrum. During the on-state, driver draws current with wideband frequency components from 10 to 150 kHz. This type was registered in samples SO/06/-

/1, SO/07/-/1, SO/09/-/1. In second group, b) are shown spectrograms of sample PH/67/-/1 which belong to Ab group. As it visible the background noise in spectrogram of current is much more pronounced as in comparison with SO/07/-/1 shown in a), which belongs to Aa group. Characteristic signs of current spectrograms belonging to b) are FM modulated components which change frequency during the on-state of driver. And their presence in current is then directly translated to output luminous flux. Similar spectrograms as are shown in b) were found in samples PH/67/-/1, PH/4D/-/1, PH/69/-/1, PH/89/-/1, PH/86/-/1, PH/12/-/1, EM/45/-/1, EM/31/-/1, VT/12/-/1, VT/28/-/1, RE/10/S/1.

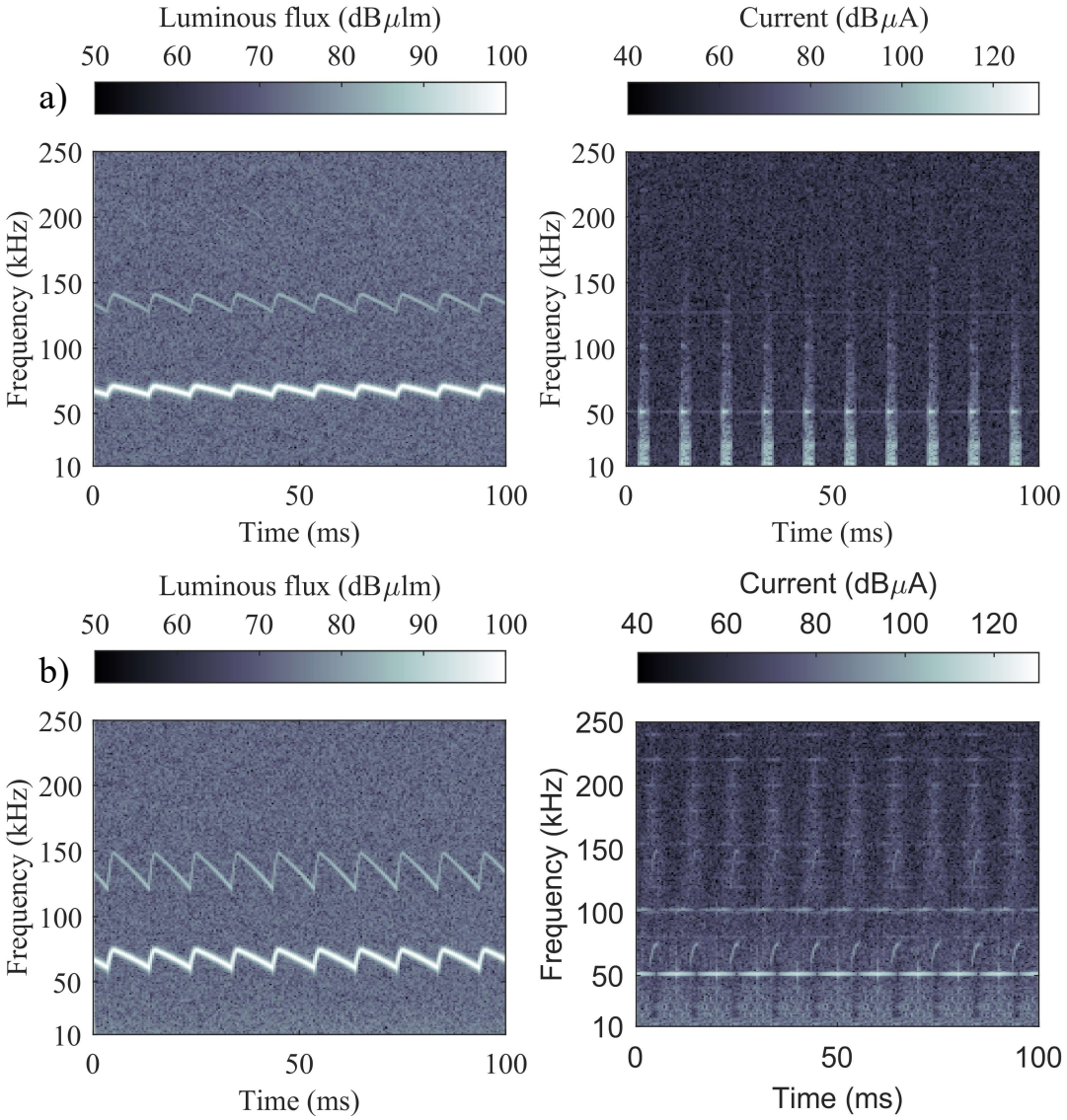


Figure 41 Characteristic spectrograms of luminous flux and current registered in group exhibiting harmonic pattern in frequency spectrum of luminous flux, a.) SO/07/-/1, b) PH/67/-/1

The next analysed type of lamps is one where no frequencies related to the operation of the driver in switching mode were found in the luminous flux spectrum. Their

characteristic spectrograms of current and luminous flux are shown in Figure 42. From spectrograms of luminous flux, it has been proven that all samples listed in this group from previous analysis of their frequency spectra really do not exhibit any signs of modulation in the shown frequency range of their luminous flux spectrum. By comparison of current spectrograms between each other. It was found that drivers included in this group do not vary very much. Therefore, this group have only one characteristic current spectrogram. As it follows from Figure 42 the spectrogram of current in this group is the same as was found in previous group shown in Figure 41 a). This perfectly captures the similarity of at least input stage of a drivers. Indeed, it is possible that drivers shown and belonging to currently described group are same as those described in Figure 41 a). Because they may work on much higher switching frequencies outside of shown range. So, their spectrum of luminous flux appears as blank. To further prove or disprove if drivers belong to the same group, it will be needed to disassemble LED lamps and exactly find and describe differences between these groups. Despite this, finding identical spectrograms of currents between described group and group shown in Figure 41. Helps to shrink 23 samples from 7 different brands belonging to group A only to 3 specific types with same behaviour in current spectrograms. If it will be further proved that this group have frequency components in luminous flux above analysed range. Then all 23 samples could be divided overall, only to three specific groups with same characteristic behaviour in current and luminous flux frequency spectra.

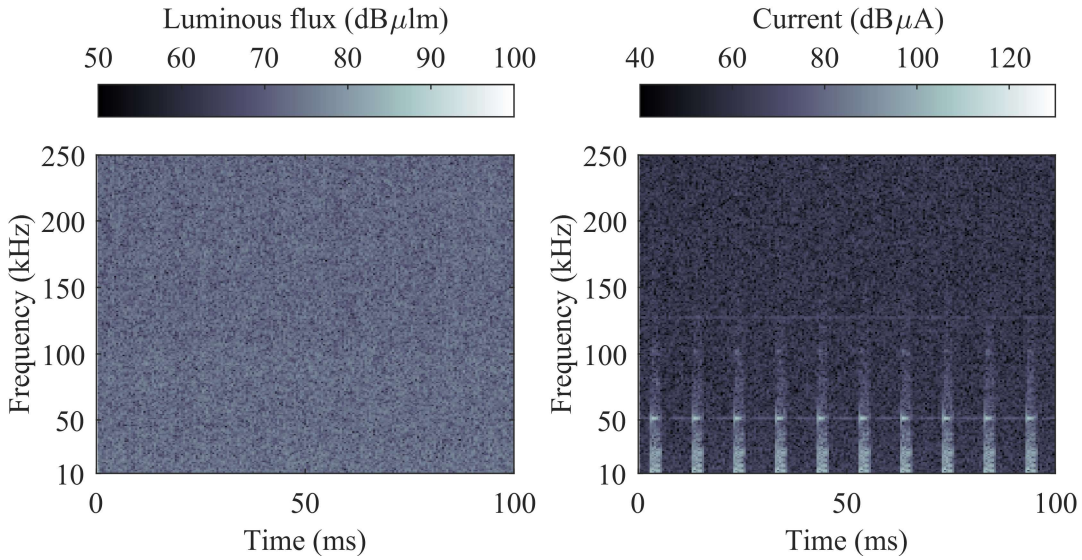


Figure 42 Characteristic spectrograms of luminous flux and current registered in group A among LEDs with no switching frequency components present in frequency spectrum of luminous flux (PH/7C/-/1)

Whole group A has been already described, now it is time to look on spectrograms of LED bulb RE/96/-/1 belonging to group C shown in Figure 43. In luminous flux are visible peaks which are linked to frequency components caused by slew rate of rising and

falling edge of luminous flux WF. The same behaviour as in luminous flux is also visible in spectrogram of current. Frequency components caused by slew rate in WF of current. propagate only to about 15 kHz which is a lot less then in showed spectrograms of LED bulbs in group A and overall whole spectrum is much cleaner. In time interval when CCR is working, thus between falling and rising edge (shorter distance between shown pulses) no modulation or other frequency components related to switch-mode operation were observed. So, driver used in this LED bulb seems to be working as linear.

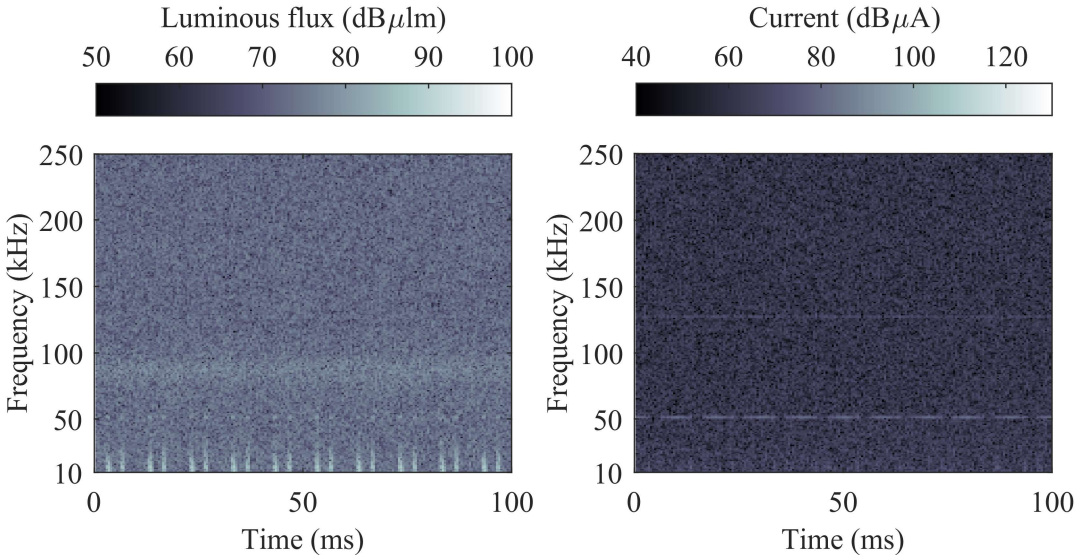


Figure 43 Characteristic spectrograms of luminous flux and current registered in group C (RE/96/-/1)

Next, Figure 44 a) shows the characteristic spectrograms for LEDs belonging to the AC group. Found spectrograms within this group are with some differences very similar to the characteristic one in group C. The same spectrograms as are shown in a) were recorded even in sample EM/03/-/1. In sample AW/WW/T/1 the only difference is that the driver visibly draws current during the on-state. With decaying wideband spectrum range from 10 kHz to only 20 kHz. However, this frequency components are not translated to its output luminous flux. Their occurrence is probably related only to some additional components which, provides ability of triac regulation. Luminous flux spectrogram of AW/WW/T/1 thus look line as one depicted in Figure 44 a). Among all samples besides the TP/30/W/1 shown in Figure 44, luminous flux and current spectrograms do not show any signs of modulating frequencies linked to switching-mode drivers. In this group the highest visible frequency components in current were registered in sample TP/30/W/1. Harmonics of its oscillations propagate up to 250 kHz and as it is visible form Figure 44 b) they apparently propagate even further. The highest visible frequency components in current, within other more standard samples were observed in

shown sample VT/61/-/1 in Figure 44 with frequency about 100 kHz. In the output luminous flux reaches highest frequencies sample EM/03/-/1 with peaks up to 55 kHz.

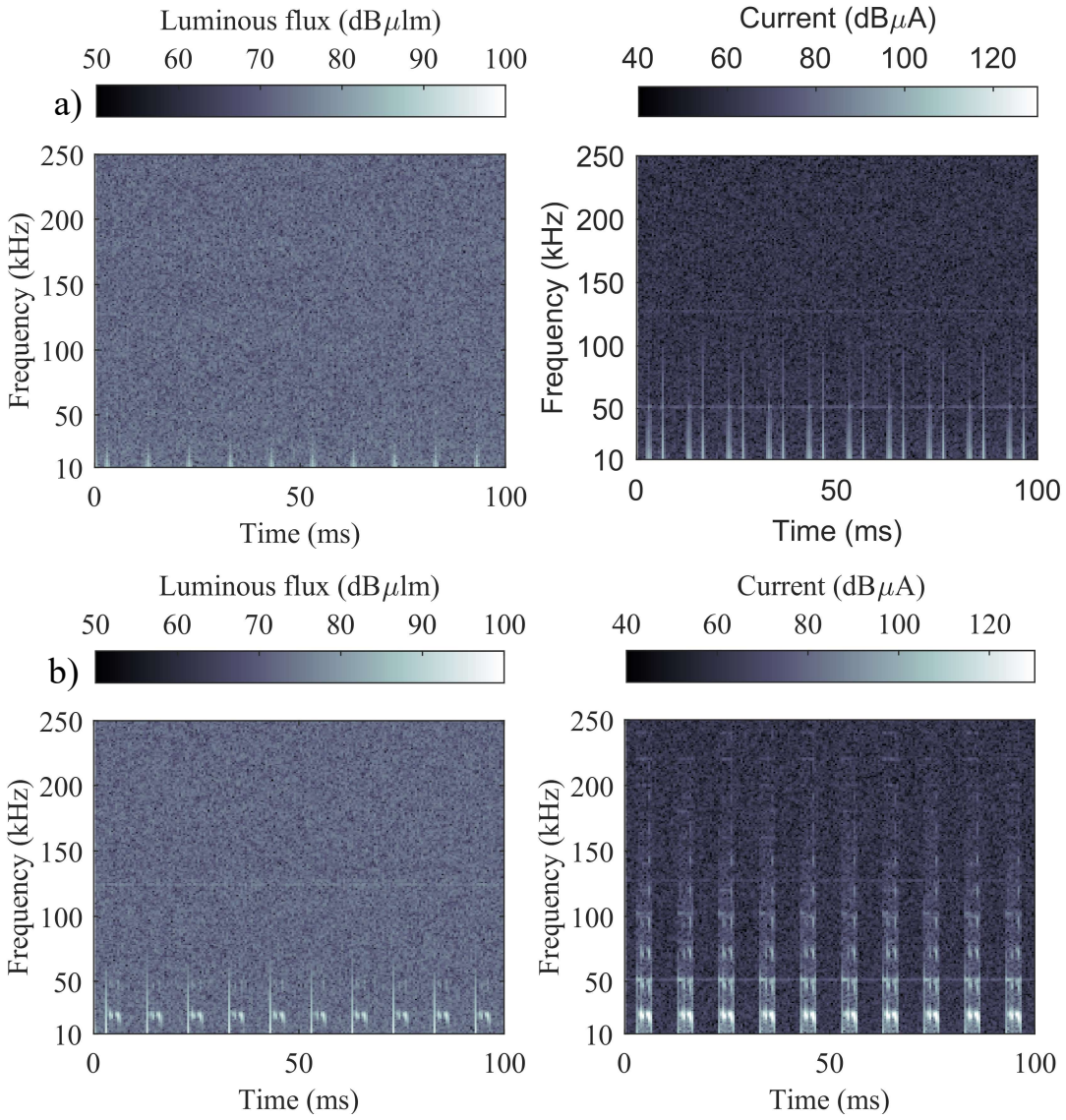


Figure 44 a) characteristic spectrogram of luminous flux and current registered in group AC, b) spectrogram of luminous flux and current of LED lamp with observed oscillations in its current WF

Among the bulbs SP/76/T/1 and VT/84/T/1 belonging to the last group D, were found characteristic spectrograms shown in Figure 45. Both spectrograms belong to sample SP/76/T/1. In this sample were observed most distinct FM modulated components visible in current with highest magnitude. The same modulated components with similar shape are even present in sample VT/84/T/1 however, they are barely recognizable. Current WFs of SP/76/T/1 and VT/84/T/1 showed in Figure 34 have clearly different shape. And belonging of samples to the same group may seemes as questionable. However, spectrograms obtained by STFT clearly showed that these samples belong to same group and share common blocks in their drivers.

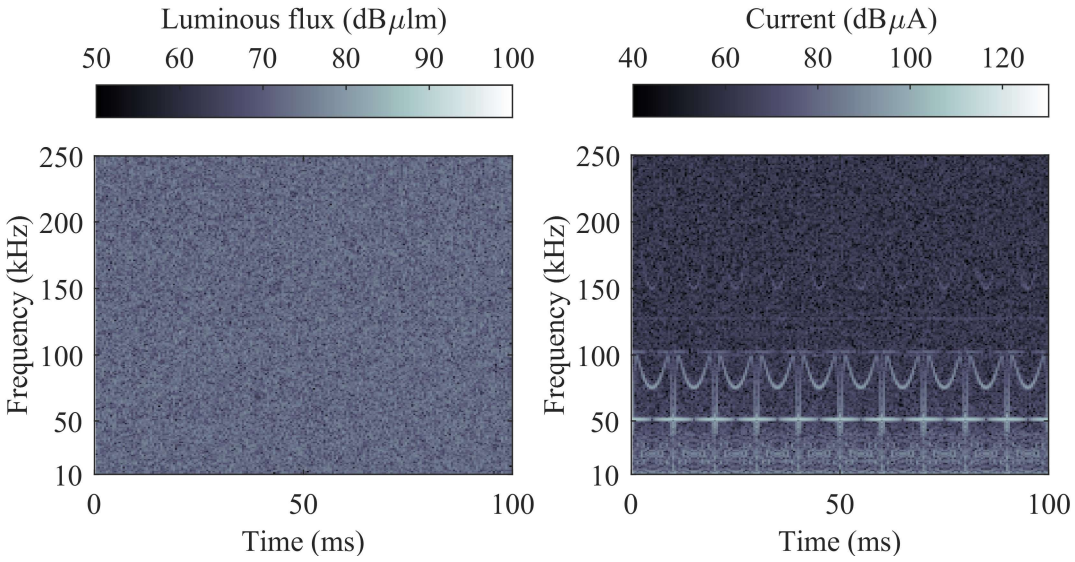


Figure 45 Characteristic spectrograms of luminous flux and current registered in group D (SP/76/T/1)

### 4.1.5 Measurement of spectral parameters

Correct composition of radiated light spectrum by LED lamps is by no means less important for good eye comfort as their sufficient flicker performance. On packages of LED bulbs are listed only two parameters related to spectral parameters. First one is *CCT* or correlated colour temperature which in general describes the apparent coolness or warmth of radiated light. Second parameter is the *CRI* or colour rendering index which describes the ability of a light source to accurately reproduce colours. Aim of this section is to measure and verificate mentioned catalogue parameters. Together with finding spectra of radiated flux. Measurements were done by using the setup shown in Figure 46.

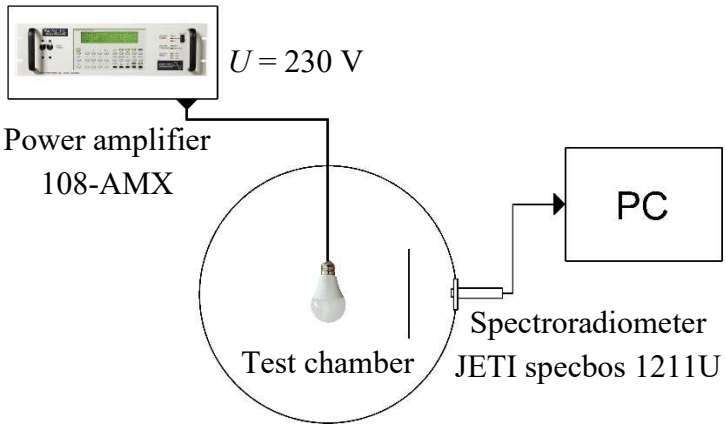


Figure 46 Test system used for measuring spectral parameters of LED lamps

Power amplifier 108-AMX was turned on and set to output voltage 230 V with nominal frequency 50 Hz. Tested sample was then placed inside the chamber (with same

parameters as in previous test). Then measurement was immediately executed without waiting for a settling of the operation point, because the heating up of the LED bulb have minimal impact on its radiated light spectrum. Radiant flux from measured lamp was gathered by spectroradiometer JETI specbos 1211U. From measured spectrum were by JETI software evaluated parameters *CCT*, and *CRI*. Same measuring routine was performed on 29 tested samples. Test was not performed on 2 samples marked in Table 5 with dashes, because of their RGB or *CCT* changing features. A summary of the evaluated results could be seen in Table 5. All further mentioned values in text are in table highlighted in red. $CCT_N$ and $CRI_N$ represent the nominal values of LED lamps given by manufacturers. On the other hand, $CCT_M$ and $CRI_M$ represent the measured values. For comparison of differences between nominal $CCT_N$ , $CRI_N$ and their measured values $CCT_M$ ,$CRI_M$ are in Table 5 shown calculated percentual differences marked as $\delta_{CCT}$ for *CCT* and $\delta_{CRI}$ for *CRI* . The highest positive difference between $CCT_N$ and $CCT_M$ was recorded in sample VT/61/-/1 with a value of 5.64 %. The highest negative difference was recorded in sample TE/40/-/1 with a value of -4.24 %. On average, the nominal value*s* of LEDs *CCT* differ from their measured *CCT* by 1,54 %. Across all samples, measured *CRI* was higher than their minimal limit $CRI_N$. The largest difference between $CRI_M$ and $CCT_N$ was recorded in sample EM/42/-/1 with $\delta_{CRI}$ equal to 6,84 %. Overall, the $CRI_M$ across all tested LED bulbs is on average higher by 4.84 % than the $CCT_N$.

From the analysis of the radiometric spectra obtained with specbos 1211U, it was find out that output light spectra of LED bulbs do not differ very much within same nominal values of *CCT* and *CRI.* Specific spectra of LED lamp with CCT equal to 4000 K is shown in Figure 47 c). The peak in blue region of spectrum at 450 nm reaches largest value across all light wavelengths. Second specific spectrum found in LED lamps with nominal CCT around 2700 K is depicted in Figure 47 d.). In this case peak located at 450 nm do not reach such a high magnitude than in previous case. As it is visible, its magnitude reach value comparable with wavelengths of green light. The most obvious difference observed between LED bulbs with different CCTs is mostly only in their relative magnitude at 450 nm compared to other wavelengths of emitted light.

The most distinct differences in output light spectra were observed in LED lamps with CRI higher than 90. In Figure 47 a) is shown spectra of EM/45/-/1 which has the highest nominal CRI from all tested lamps. Manufacturer of this LED lamp moved specific peak in blue color from mentioned 450 nm to 468 nm. It produces a more balanced light spectrum composition, and it does not longer exhibit dips in cyan color around 480 nm as majority of LED bulbs. The second sample PH/89/-/1 also have CRI value over 90 but its shape of light spectrum is totally different. As can be seen in Figure 47 b) the manufacturer compensates the lack of red color in it the output spectrum by special

treatment of its phosphor layer. Which produce distinct and split peaks in its output light spectrum. All measured radiometric spectra are placed in attachment Nr.4.

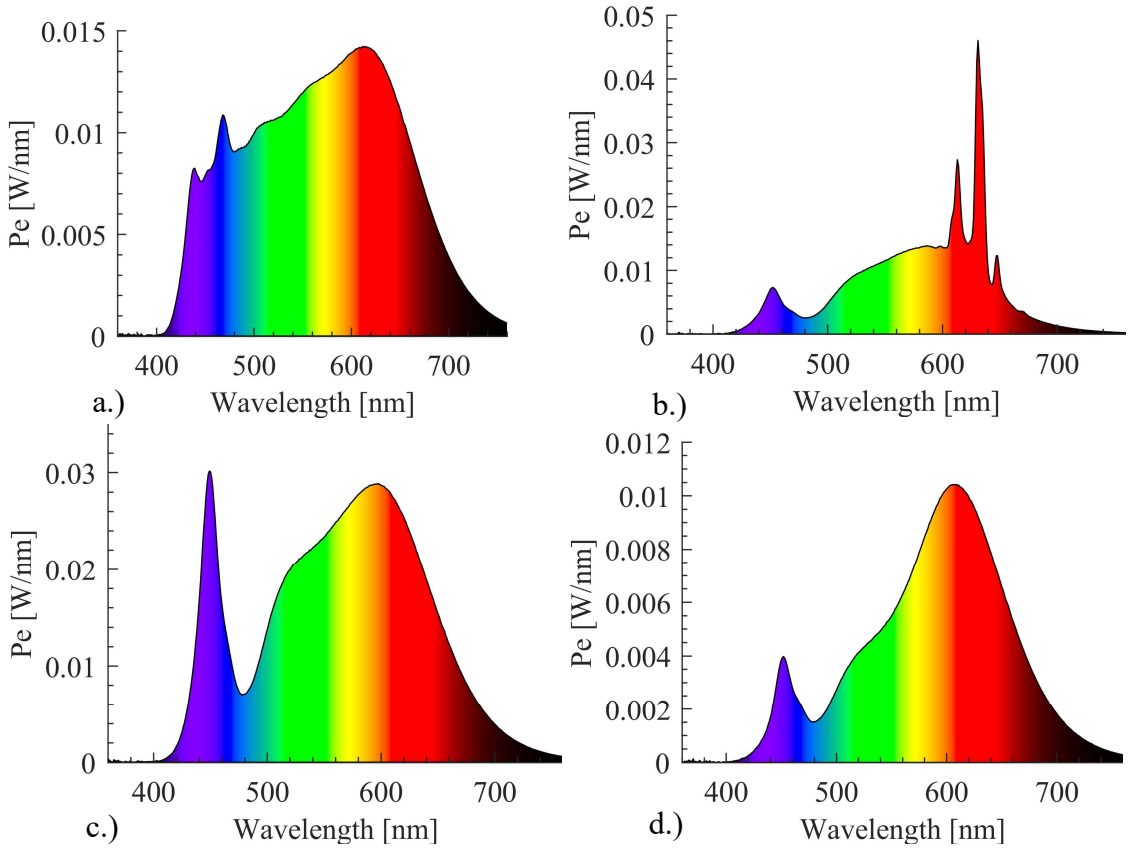


Figure 47 Radiometric spectra of LED bulbs, a.) EM/45/-/1, b.) PH/89/-/1, c.) PH/4D/-/1, d.) PH/86/-/1

Table 5 Measured spectral parameters of all tested LED lamps.

| Label | $CCT_N$ (K) | $CRI_N$ (-) | $CCT_M$ (K) | $CRI_M$ (-) | $\delta_{CCT}$ (%) | $\delta_{CRI}$ (%) |
|---|---|---|---|---|---|---|
| PH/4D/-/1 | 4000 | 80.0 | 3960 | 83.0 | -1.00 | 3.79 |
| PH/69/-/1 | 4000 | 80.0 | 3999 | 82.9 | -0.04 | 3.64 |
| PH/62/-/1 | 2700 | 80.0 | 2778 | 82.6 | 2.88 | 3.30 |
| PH/67/-/1* | 3000 | 80.0 | 2978 | 80.9 | -0.74 | 1.10 |
| PH/89/-/1* | 2700 | 90.0 | 2798 | 92.4 | 3.62 | 2.68 |
| PH/7C/-/1 | 2700 | 80.0 | 2669 | 84.1 | -1.13 | 5.12 |
| PH/86/-/1* | 2700 | 80.0 | 2690 | 83.1 | -0.37 | 3.87 |
| PH/12/-/1* | 3000 | 80.0 | 3040 | 84.7 | 1.32 | 5.90 |
| EM/45/-/1 | 4000 | 94.0 | 4099 | 94.7 | 2.48 | 0.73 |
| EM/42/-/1 | 6500 | 80.0 | 6505 | 85.5 | 0.08 | 6.84 |
| EM/31/-/1 | 4000 | 80.0 | 3877 | 83.9 | -3.07 | 4.93 |
| EM/01/-/1 | 2200 | 80.0 | 2242 | 84.1 | 1.89 | 5.14 |
| EM/20/-/1 | 2700 | 80.0 | 2705 | 83.7 | 0.19 | 4.59 |
| EM/80/-/1 | 4000 | 80.0 | 3984 | 85.0 | -0.39 | 6.26 |
| EM/40/-/1 | 3000 | 80.0 | 3013 | 84.7 | 0.43 | 5.88 |
| VT/28/-/1* | 3000 | 80.0 | 2928 | 83.0 | -2.40 | 3.76 |
| VT/12/-/1* | 4000 | 80.0 | 4049 | 85.3 | 1.22 | 6.62 |
| SO/06/-/1 | 4000 | 80.0 | 4036 | 82.0 | 0.90 | 2.49 |
| SO/07/-/1 | 3000 | 80.0 | 3014 | 83.7 | 0.48 | 4.61 |
| SO/09/-/1 | 3000 | 80.0 | 3018 | 83.3 | 0.60 | 4.10 |
| RE/10/S/1* | 3000 | 80.0 | 3022 | 83.6 | 0.73 | 4.55 |
| TE/40/-/1 | 4000 | 80.0 | 3830 | 84.8 | -4.24 | 6.00 |
| TP/10/W/1 | 2700 | 80.0 | 2754 | 83.9 | 2.00 | 4.86 |
| IM/3L/W/1* | - | - | - | - | - | - |
| RE/96/-/1 | 3000 | 80.0 | 3028 | 83.6 | 0.92 | 4.52 |
| EM/03/-/1 | 2700 | 80.0 | 2686 | 83.7 | -0.51 | 4.62 |
| VT/61/-/1 | 4000 | 80.0 | 4226 | 83.6 | 5.64 | 4.54 |
| AV/WW/T/1 | 2500 | 80.0 | 2431 | 82.5 | -2.74 | 3.10 |
| TP/30/W/1 | - | - | - | - | - | - |
| VT/84/T/1 | 4000 | 80.0 | 4087 | 85.1 | 2.18 | 6.34 |
| SP/76/T/1 | 4000 | 80.0 | 4022 | 82.6 | 0.55 | 3.22 |

# 5. FLICKER PERFORMANCE OF LED LAMPS

All tests so far have been done to evaluate or characterise LED bulbs parameters under the ideal supply conditions. However, as it was mentioned in the first chapter of the thesis. Occurrence of voltage fluctuations is a natural part of a functioning power grid. So, LED bulbs or other appliances are naturally exposed to various types of modulations. Which may then manifest in the frequency spectrum of the supply voltage by multiple harmonic and interharmonic components. Frequencies of interharmonic components do not have to be static. They can dynamically change according to the set operating parameters of a specific device. An example of such a device has been shown PWM drive with its frequency spectrum in Figure 8. In the picture is depicted how interharmonics by changing output frequency of drive can cover nearly entire spectrum from 0 to 1000 Hz. By principles described in chapter 1.3 it was shown that the output luminous flux of an incandescent bulb is not affected by frequency components in its supply voltage with frequency higher than 100 Hz. On the other hand, the output luminous flux of LED lamps can be affected over a very wide frequency range up to units of kHz. Therefore, the aim of this chapter is to describe and evaluate the flicker performance (GF curves, response of $P_{st}$ on injected interharmonic, and immunity curves with various modulation types) of LED bulbs over a wide range of frequencies with different types of modulation. It will provide a complete picture of flicker performance among the best-selling LED bulbs on the current market.

## 5.1 Flicker sensitivity of LED lamps

This section deals with measuring gain factor curves and responses of $P_{st}$ on injected interharmonic components. Both measurements were evaluated simultaneously in NI PXI under the one measuring setup. Schematic of used testing setup is shown in Figure 48

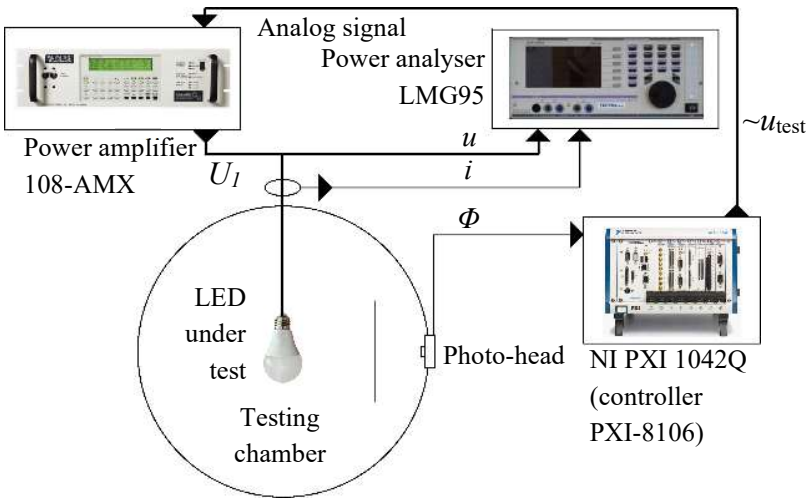


Figure 48 Test setup for measurement GF curves of LED lamps

NI PXI serves as the main controlling unit for measuring generating testing signals and evaluating measured data. The test signal is generated by a PXI-5421 arbitrary waveform generator card using NI PXI with LabView SW. In 108-AMX is test signal amplified to a preset level. In this case the test signal on the output of the amplifier was composed of a fundamental waveform $U_1$ = 230 Vrms with frequency 50 Hz and one superimposed component with magnitude equals to 2 % of $U_1$. The used frequency range of superimposed components may vary by group of tested lamp. The widest one was from 1 to 1000 Hz. Within all used ranges of superimposed components frequencies, the frequency step of measurement was always 1 Hz. The output luminous flux is sensed by the photo-head. The output signal from photo-head goes directly to input terminals of dynamic data acquisition card PXI-4472. At each measuring point in this case at each increment of IH by 1 Hz. GF and $P_{st}$ are evaluated simultaneously. Measure was performed on all 31 samples. Bulbs were set to their nominal output power without using their built-in dimming function or external dimmers.

Obtained IH GF curves and responses of $P_{st}$ will be described and shown for each group together because of their mutual correlation. Results for LED bulbs belonging to group Aa are depicted in Figure 49 and Figure 50. From IH GF curves shown in Figure 49 it was figured out that all 15 out of 16 samples are very immune to flicker and do not translate IH components from supply voltage to the visible luminous flux very significantly. All these 15 samples have their largest part of the GF curve in the range of $10^{-3}$ to $10^{-1}$. As can be seen from IG GF curves only sample EM/01/-/1 has notably high GF peaking around 1. This lack of performance is due to the inability of its driver to regulate constant output. Which manifest during the steady-state in its luminous flux WF shown in Figure 30 by large dips. In most bulbs, GF across the shown frequency declines very slowly. Thus, their GF in range 500 Hz to 600 Hz is not even 10 times lower than in range 1 Hz to 100 Hz. The similar situation is captured even in Figure 50. The 15 out of 16 bulbs responded to injected IH with $P_{st}$ in range from $6 \cdot 10^{-3}$ to 0.3. The EM/01/-/1 reaches in a peak 4.8 which is outstandingly higher than others. As it follows from Figure 49 and Figure 50 the relative positions of curves between graphs are very similar. Thus, GF is very suitable parameter for prediction of flicker performance.

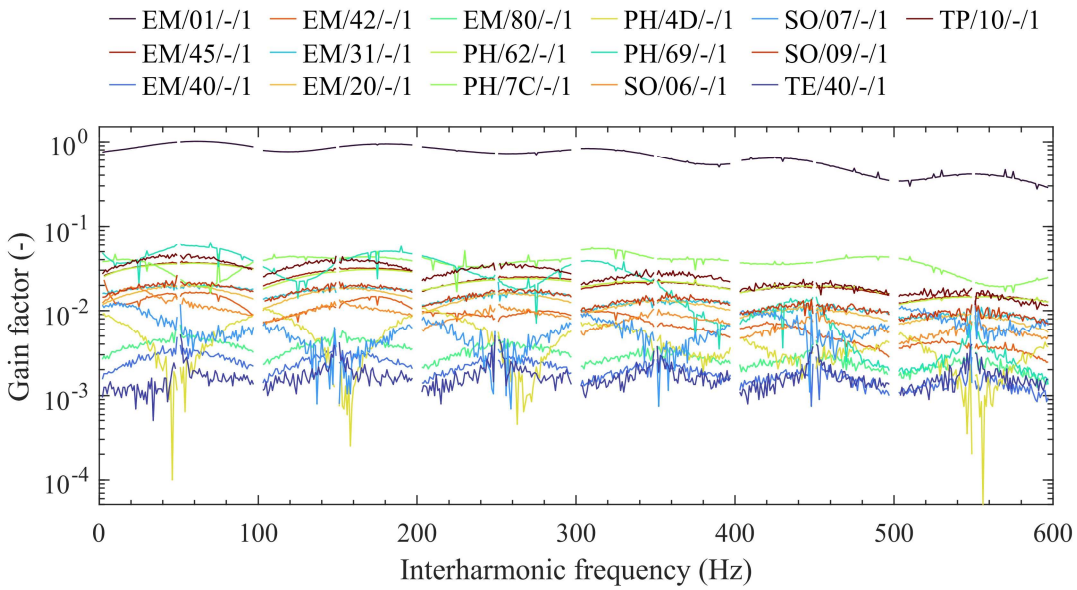


Figure 49 IH GF curves of LED bulbs belonging to class Aa

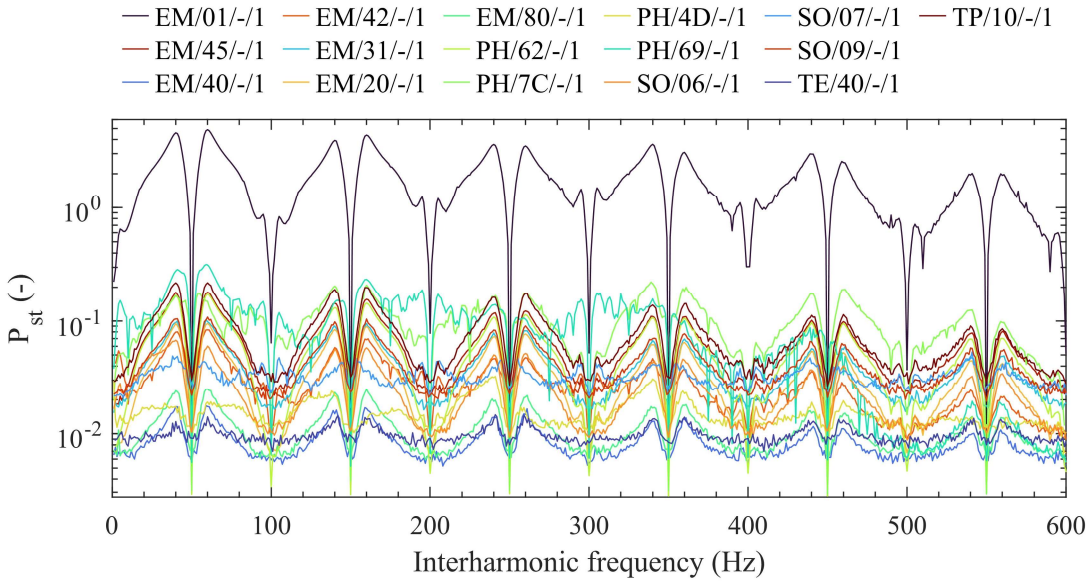


Figure 50 Response of $P_{st}$ to superimposed IH of LED bulbs belonging to class Aa

Results for group Ab do not differ very much from shown and described figures in group Aa. From GF curves depicted in Figure 51 it is visible that most curves are placed in a very same range as curves in group Aa. The same applies to Figure 52. Thus, flicker performance is not affected by described differences between both groups. In Figure 51 are very good visible, specific for group A, bell-like shape curves with center around odd harmonics (samples with GF around $10^{-1}$). As it is described in [14] their presence is characteristic for DBR with bulk capacitor. Its value then affects the shape of the bell curve. The higher the capacitance the ends of bell curve will be more gradually attenuated, so curves will be steeper.

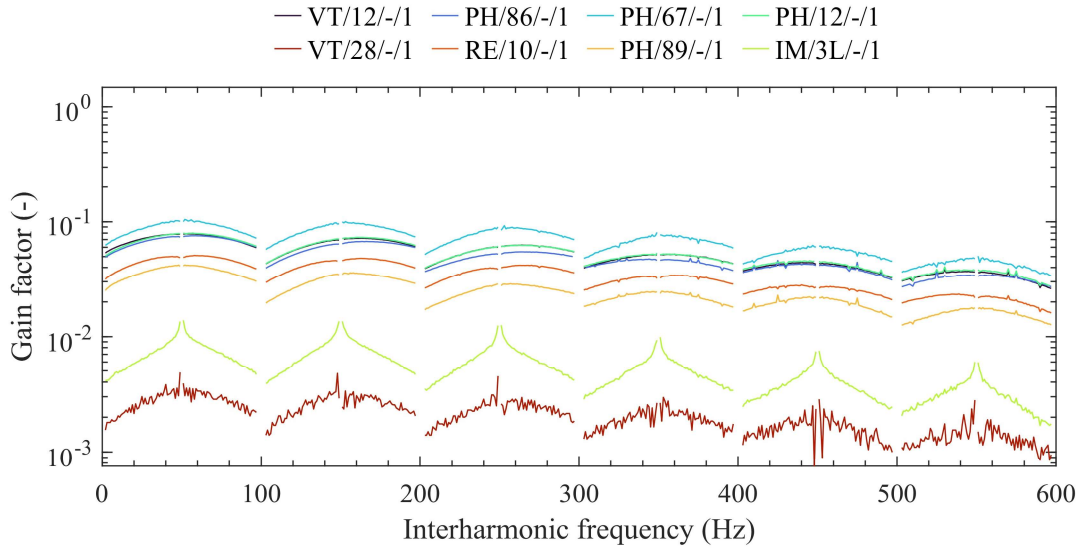


Figure 51 IH GF curves of LED bulbs belonging to class Ab

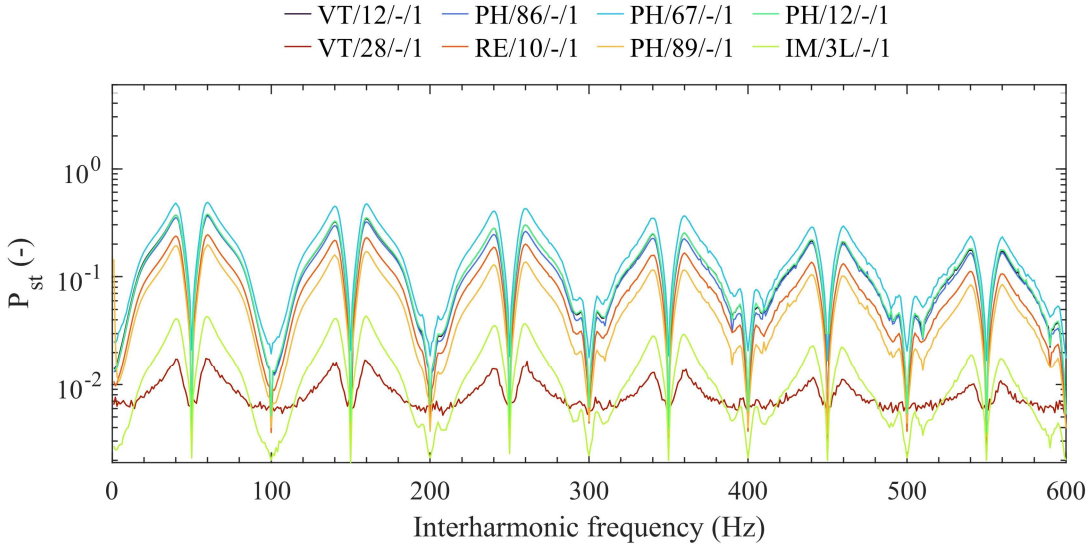


Figure 52 Response of $P_{st}$ to superimposed IH of LED bulbs belonging to class Ab

Curves obtained for LED lamps belonging to group C are shown in Figure 53 and Figure 54. In Figure 53 is shown the IH GF curve of sample RE/96/-/1 in comparison to IH GF curve of incandescent lamp. As Figure 53 shows, lamps belonging to group C are very sensitive to flicker. The most distinct difference in comparison to the previous category is that lamps in C class are most sensitive in region above 200 Hz. Where they are reaching gain factor over 3. The same typical pattern of GF curve is visible even in Figure 19 for Type II driver topology. Which is the CCR topology same as class C. It just shows how greatly GF captures the topology of drivers and creates their "fingerprint". From the response of $P_{st}$ shown in Figure 54 is clearly visible that C topology may suffer from severe levels of $P_{st}$ if IH is present in supply voltage. In this test, $P_{st}$ in peaks reached

values up to 14.4. Severe values of $P_{st}$ (over 10) are occuring in peaks in whole frequency range up to 600 Hz.

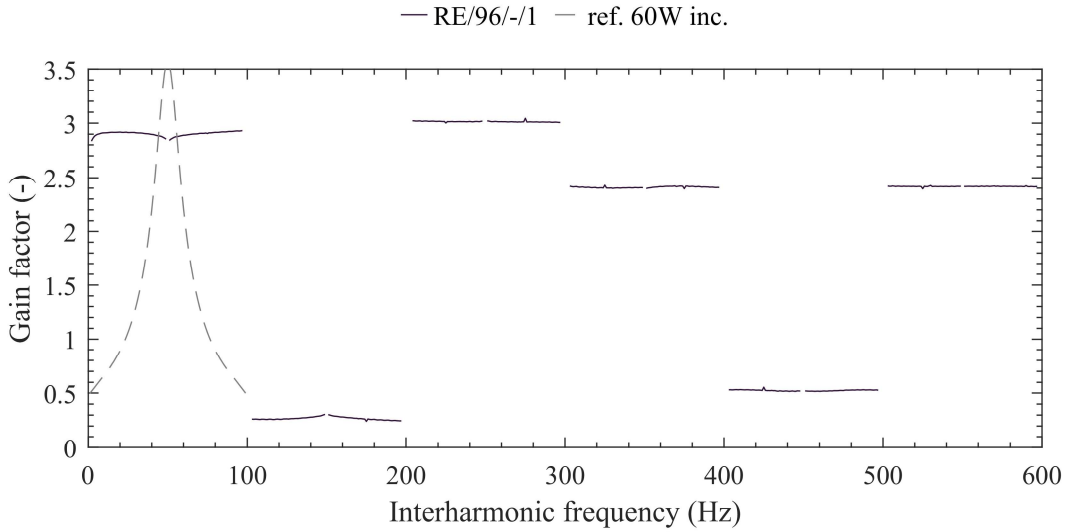


Figure 53 IH GF curves of LED bulbs belonging to class C

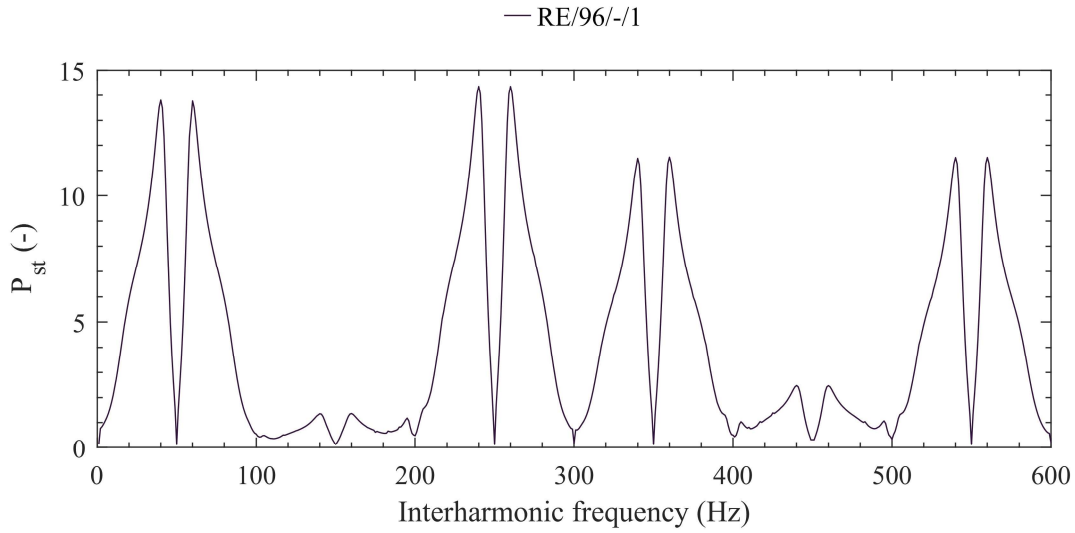


Figure 54 Response of $P_{st}$ to superimposed IH of LED bulbs belonging to class C

Results for the mix of the A and C topology marked as AC are pictured in Figure 55 and Figure 56. From obtained GF curves in Figure 55 it can be seen that the *GF*, as in class C reaches the highest value in the frequency range 200 - 300 Hz. On the other hand, *GF* values around fundamental so in range 1 - 100 Hz are in comparison with *GF* values reached across the whole tested range substantially lower. GF curves have shape of earlier decribed bell curves. So, after the DBR is connected bulk capacitor. However, CCRs are clearly not designed properly to regulate present voltage variations. Therefore, the highest measured *GF* was in sample VT/61/-/1 reaching value over 3. Same as class C the class AC is also very sensitive in whole measured range up to 600 Hz. In measured responses

of $P_{st}$ to superimposed IH shown in Figure 56, all samples in some frequency range of IH reached $P_{st}$ over 1. The highest measured $P_{st}$ was recorded in sample VT/61/-/1 with value of 13.9.

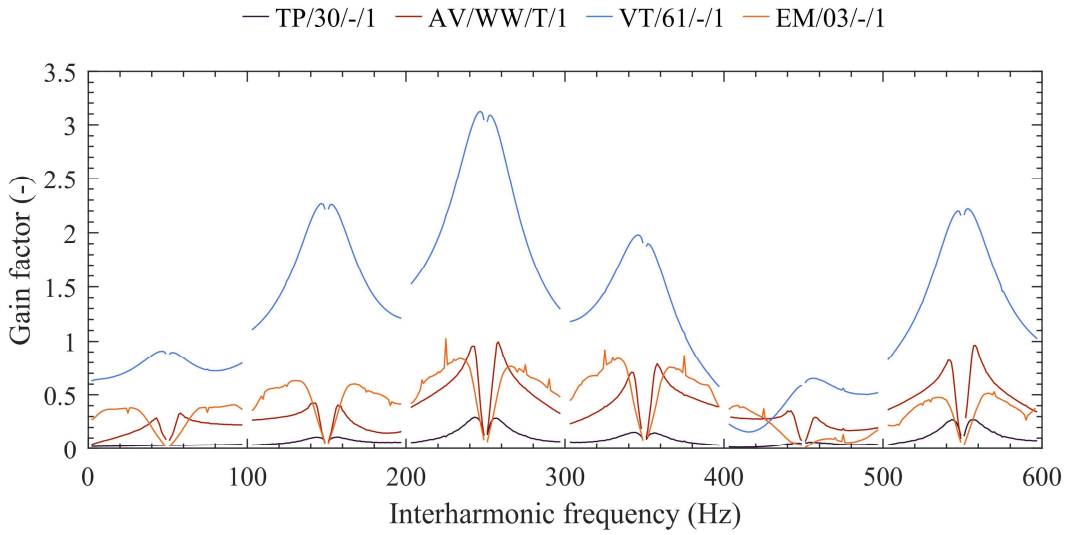


Figure 55 IH GF curves of LED bulbs belonging to class AC

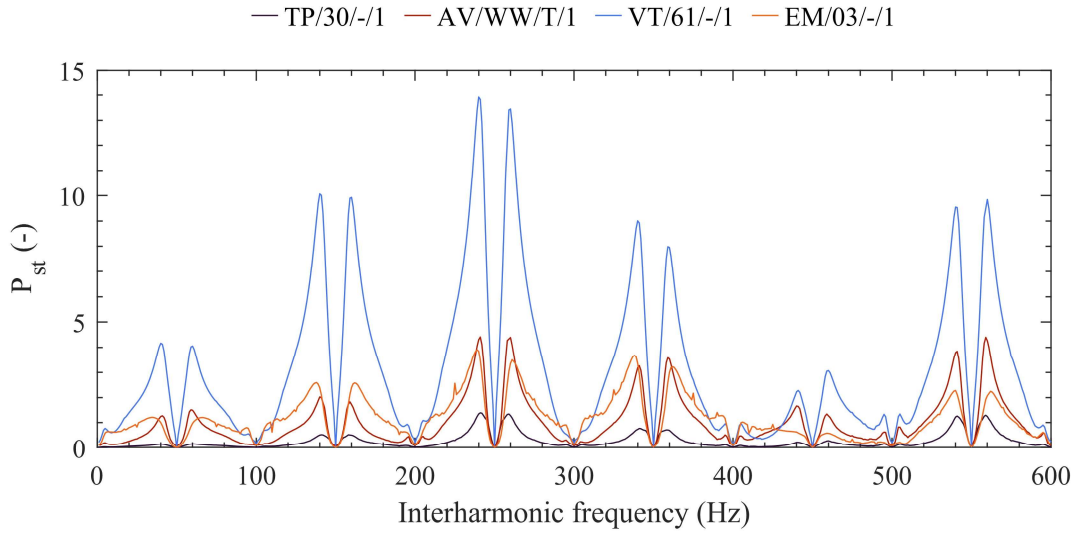


Figure 56 Response of *Pst* to superimposed IH of LED bulbs belonging to class AC

The results for the LED bulbs assigned to the last class D are shown in Figure 57 and Figure 58. IH GF curves showed in Figure 57 have significant decline of GF with rising IH frequency. However, in frequency range of IH 1 - 100 Hz they exhibit increased flicker sensitivity with GF over 1. Distinct differences between both samples can be seen in the shape of GF curves around odd harmonics. By approaching to odd harmonics, sample VT/84/-/1 tries to regulate output signal and reach GF = 0. Which are signs of closed-loop feedback driver topology with output current/voltage regulation. However, sample SP/76/-/1 do not exhibit signs of regulation with approaching odd harmonics.

Therefore, its driver uses input current regulation with already preset parameters to reach desired output values.

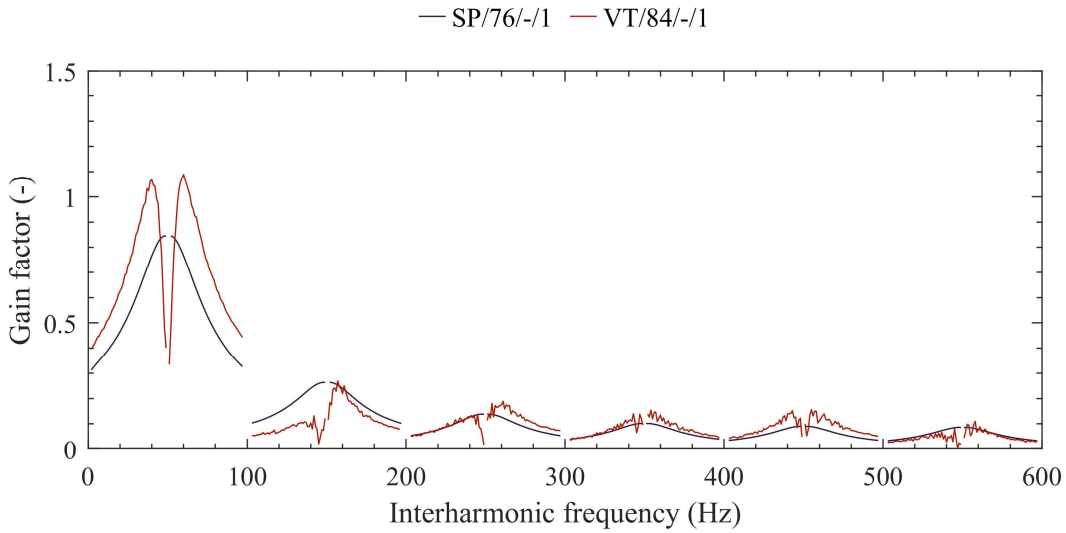


Figure 57 IH GF curves of LED bulbs belonging to class D

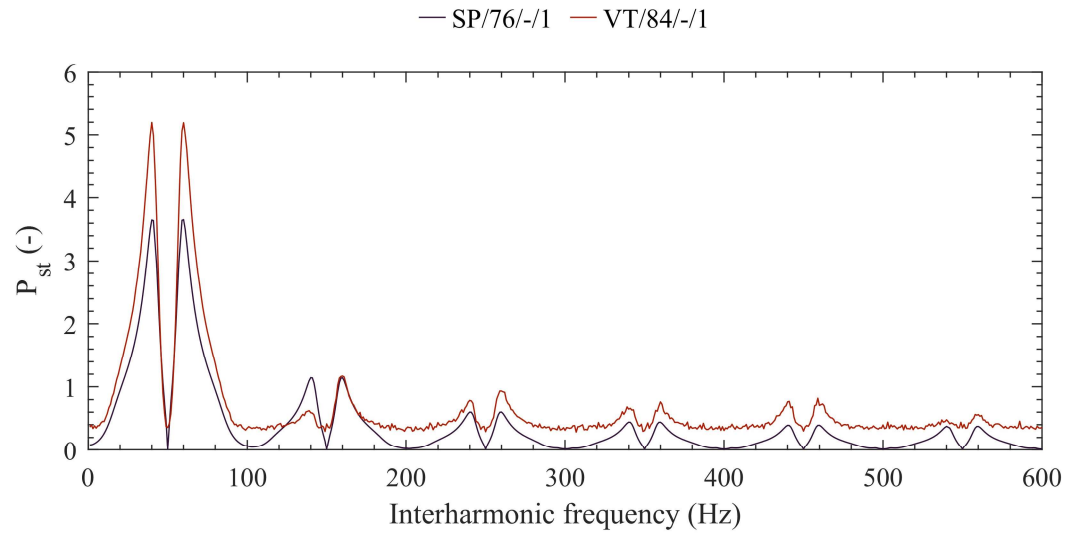


Figure 58 Response of Pst to superimposed IH of LED bulbs belonging to class D

## 5.1 Flicker immunity of LED lamps

The aim of this section is to find out immunity of LED lamps to superimposed IH in its supply voltage across a wide range of frequencies. Setup used in this test is the same as in the previous flicker sensitivity test shown in Figure 48. The LabView SW is obviously different and designed to perform immunity tests. However, the basic principles of measuring setup remained the same. The test signal at the output of the amplifier is composed of fundamental waveform $U_1$ = 230 Vrms with frequency 50 Hz and one superimposed component with magnitude up to 25 % of $U_1$. Its magnitude is changing by the needs of test setup. At each measuring point, are done 10 iterations to find the magnitude of IH component which will translate to $P_{st}$ = 1 in output luminous flux with accuracy ± 2%. Test is performed by using 2 different testing signals. First series of test are performed with sine WF of IH and second with rectangular AM modulation with 50 % duty cycle. With aim to find out the flicker immunity of LED bulbs if multiply IH frequency components are present in its supply voltage. The used frequency range of superimposed component or modulation frequency may vary by group of tested lamps. The widest one is from 1 to 1000 Hz for IH and 1 to 300 Hz for rectangular AM modulation. Within all used ranges, the frequency step of measurement is always 1 Hz. Because immunity tests are very time demanding up to 20 hours per sample. Tested were only selected samples from every class. Overall were tested 7 LED bulbs. From group A were tested 2 samples one from class Aa and other from class Ab, from class AC were tested 2 samples and from C and D were tested all samples belonging to them.

During the measurement, the test equipment was not always able to converge within 10 iterations to $P_{st}$ = 1 at each tested frequency. It was caused by 2 reasons. First the maximum magnitude of applied IH 25% of $U_1$ was not enough to produce $P_{st}$ = 1. These events are shown in following curves with value outside of range. Second reason why test setup was not able to converge was very unstable output of luminous flux. Magnitude of superimposed IH or modulation was sufficient to reach values around $P_{st}$ = 1 and even over, however output luminous flux fluctuates to such extends that it was hard to find desired value of $P_{st}$ within accuracy ± 2%. Because of that results of immunity test in these measuring points were not evaluated and in following curves are on certain frequencies blank parts with no value.

Due to the low number of tested LED bulbs in groups Aa and Ab. Both samples are showed in same figures. In Figure 59 are showed immunity curves for injected sine IH component. Sample EM/01/-/1 belong to group Aa. It was chosen because of its insufficient flicker performance in previous tests to find out what is the lowest find immunity of lamps occurring in group Aa resp. A. As it can be seen its immunity is very low. Around 450 Hz it has similar immunity as around fundamental 50 Hz. $P_{st}$ = 1 is caused only by IH component with magnitude 0.2 % of $U_1$. On the other hand sample

PH/67/-/1 have much higher immunity across all ranges of tested frequencies compared to sample EM/01/-/1. PH/67/-/1 following its IH GF curve in Figure 51 represent the average sample by flicker sensitivity. Despite this, its immunity curves shows good immunity to flicker with gradually rising $U_{IH}$ with rising frequency of IH. With applied rectangular AM modulation shown in Figure 60 their performance do not dramatically change PH/67/-/1 still performs sufficiently across whole frequency range. In comparison with incandescent 60 W bulb. Sample PH/67/-/1 significantly outperforms incandescent lamp to 150 Hz.

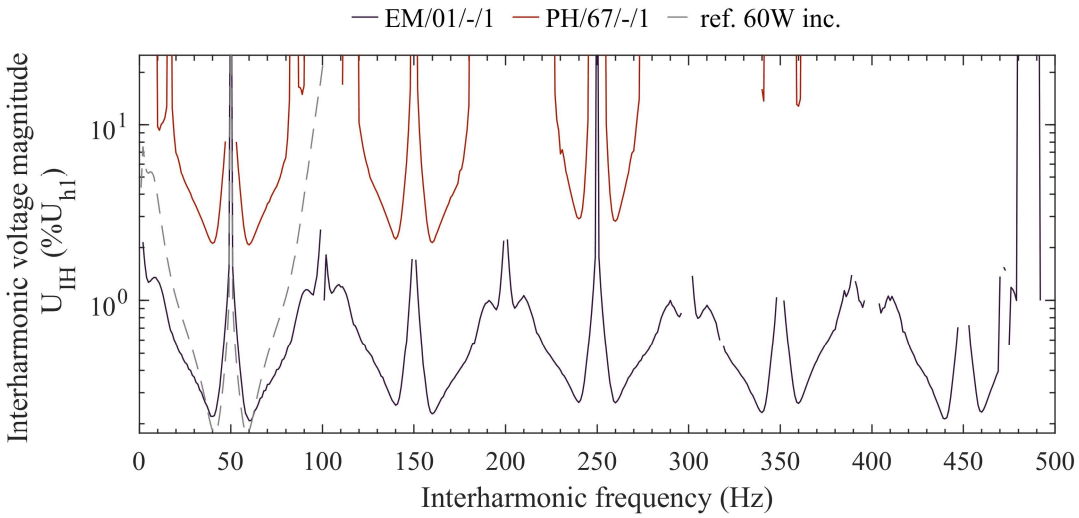


Figure 59 Immunity curves of LED lamps belonging to class Aa and Ab with applied sine IH

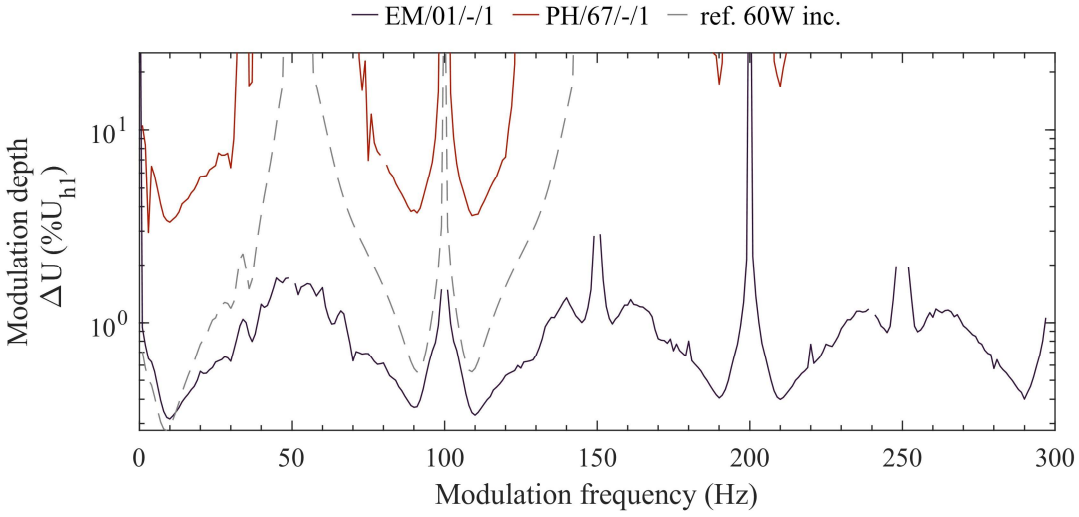


Figure 60 Immunity curves of LED lamps belonging to class Aa and Ab with applied rectangular AM modulation.

Obtained immunity curve with injected sine IH for sample RE/96/-/1 belonging to class C is shown in Figure 61. Sample exhibit very low immunity to flicker in lowest regions around 50 Hz, it reaches only 0,07 % of $U_{l.}$ In this frequency region it has even much lower immunity than the shown incandescent bulb. With increasing frequency of IH, immunity does not significantly rise. This LED bulb has in frequency range 900 Hz-1000 Hz measured $U_{IH}$ which causes $P_{st}$ = 1 only 0.23 % of $U_{l.}$ Immunity curves with applied rectangular AM modulation are shown in Figure 62. RE/96/-/1 within rectangular AM modulation reach much low performance than in comparison incandescent lamp. Overall performance with applied rectangular modulation do not significantly change in comparison with Figure 61

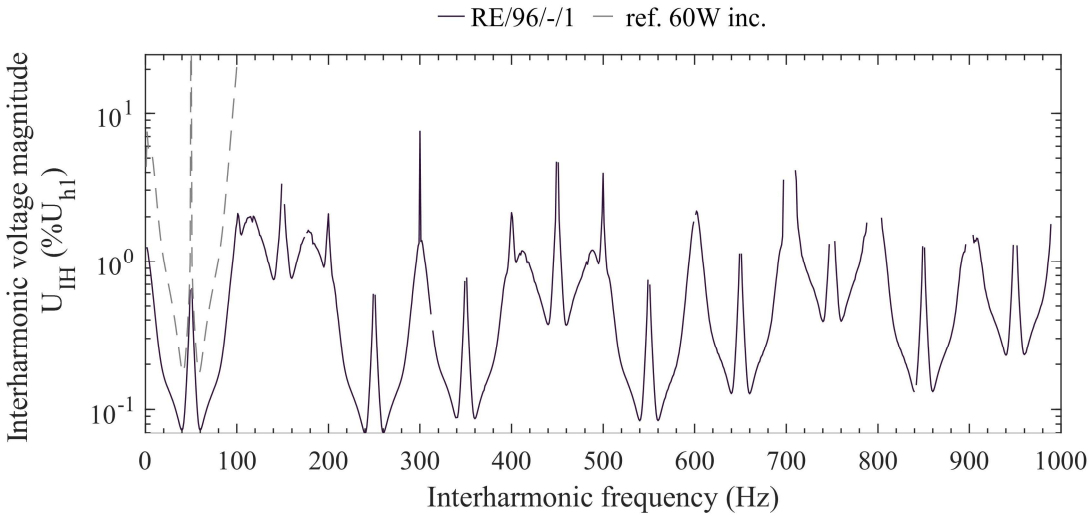


Figure 61 Immunity curves of LED lamp belonging to class C with applied sine IH.

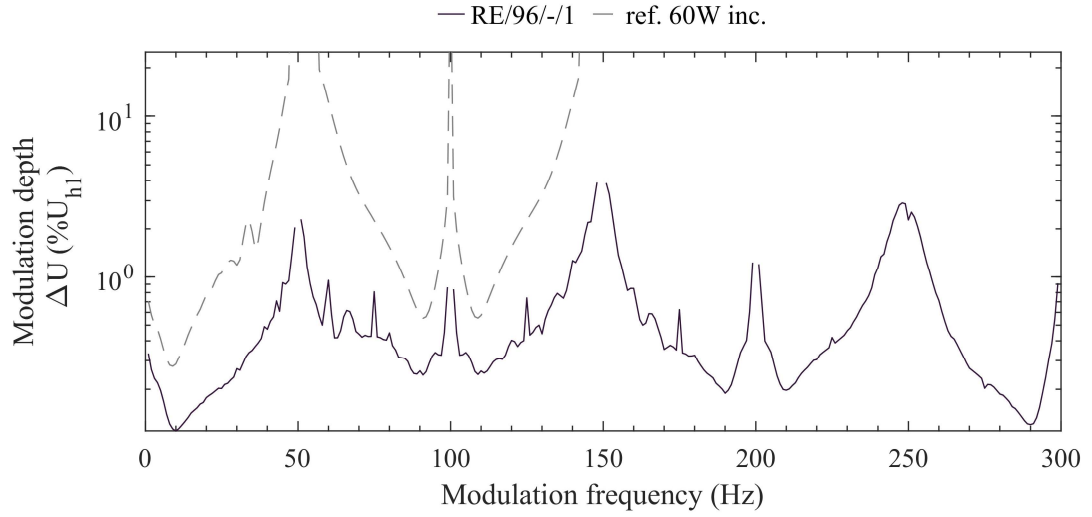


Figure 62 Immunity curves of LED lamp belonging to class C with applied rectangular AM modulation.

Immunity curves for bulbs belonging to group AC with injected sine IH component are shown Figure 63. For both samples it is characteristic that their immunity is lower on the higher frequencies especially in range 200 – 300 Hz and then is some regions above, than around fundamental 50 Hz. In both samples immunity do not rise very much with rising frequency of IH. Same as it was in group C. The lowest measured value of $U_{IH}$ wich cause $P_{st} = 1$ has sample VT/61/-/1 with value only 0,08 % of $U_1$. From Figure 64 its visible that in the presence of more frequency components their lowest immunity is also located at higher frequencies around 200 – 300 Hz with $\Delta U$ 0.13 % of $U_1$.

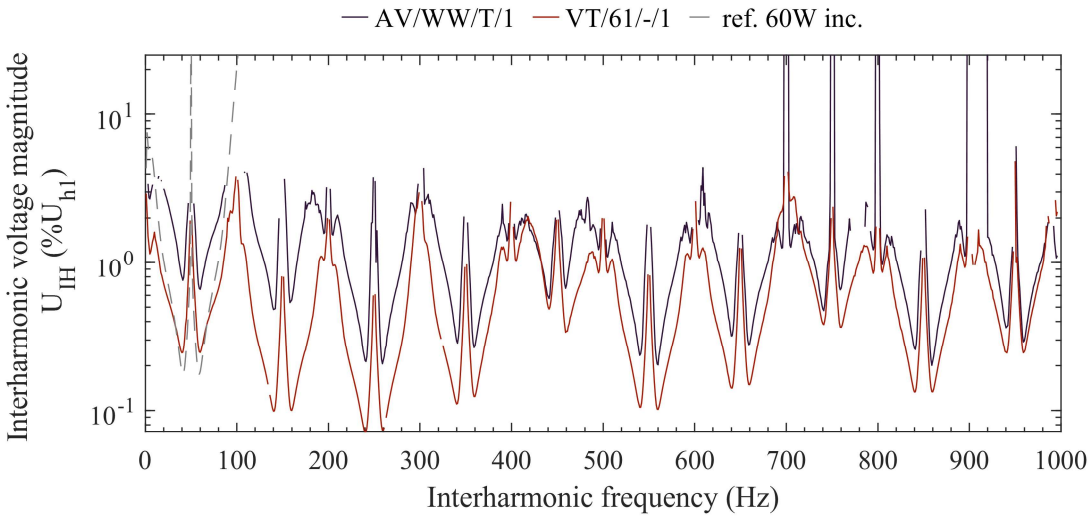


Figure 63 Immunity curves of LED lamp belonging to class AC with applied sine IH.

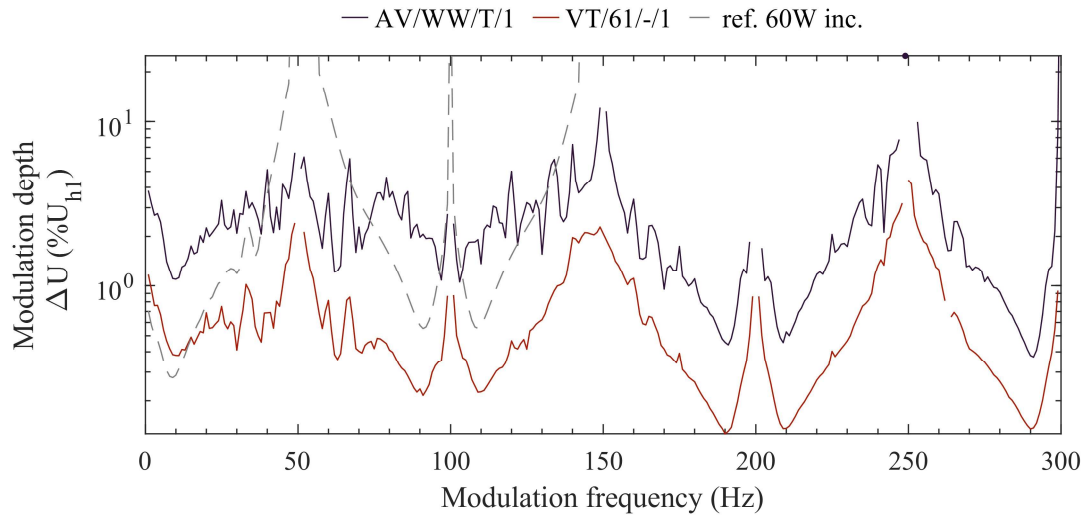


Figure 64 Immunity curves of LED lamp belonging to class AC with applied rectangular AM modulation.

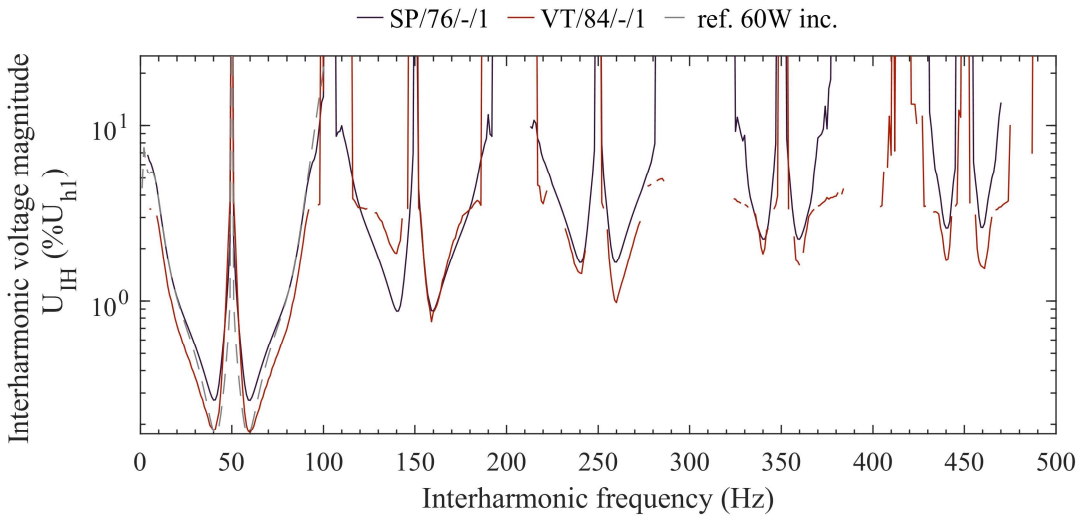


Figure 65 Immunity curves of LED lamp belonging to class D with applied sine IH.

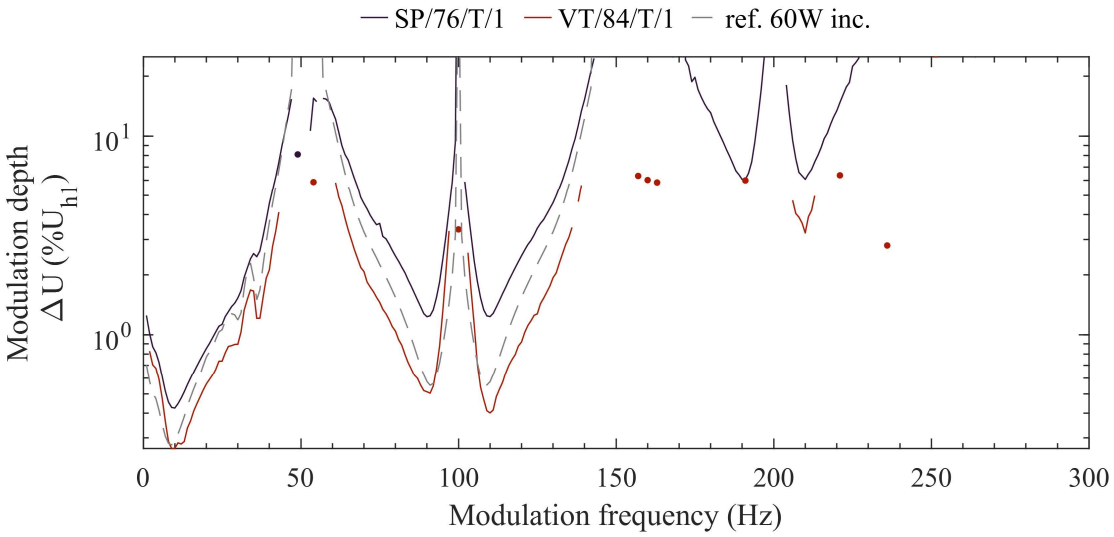


Figure 66 Immunity curves of LED lamp belonging to class D with applied rectangular AM modulation.

Figure 65 depicts immunity curves of LED lamps belonging to class D. As it can be seen in range 1-50 Hz, they very well track the immunity curve of incandescent lamp. With rising frequency of IH their immunity has trend to rise and is higher than around fundamental 50 Hz. Immunity curves of both samples have wide parts with immunity better than 25% of $U_I$. However, as it can be seen from immunity curve for sample VT/84/-/1. Above 250 Hz in wide portions of curve are visible blank parts. It tells about high instability of luminous flux thus immunity in these parts is not guaranteed. From immunity curves with applied rectangular AM modulation shown in Figure 66 it can be seen that also, samples track the shape of immunity curve for incandescent lamp. With points are marked measured values which from both sides do not have valid results so

they can't make a line. They can bring more information about possible direction of immunity curve. In sample SP/76/T/1 immunity above 150 Hz significantly rise.

## 5.2 Flicker performance summary

This section should serve as a brief overview and evaluation of overall flicker performance of LED lamp classes based on the results obtained from the previous tests in this chapter.

Class A – The best performing class. In tests were not found notable differences between class Aa and Ab. The least sensitive bulb to flicker by *GF* across the whole tested frequency range was found in this category. It is a sample TE/40/-/1 reaching *GF* around $10^{-3}$. However, at the same time because of its shortest conduction time this sample has highest $THD_I$ from all tested lamps with value 179.2 %. From 24 samples included in this class only one sample EM/01/-/1 have relatively high *GF*, in peaks around 1. Its maximum measured $P_{st}$ reached 4.8 with superimposed IH with magnitude 2 % of $U_1$. Vast majority of lamps belonging to this group have maximal *GF* in range $10^{-2}$ to $10^{-1}$. Immunity tests only underlined the very good performance of this class. Sample PH/67/-/1 represents only the average performing sample from its class (judging by its *GF* around $10^{-1}$ in peaks) and still performed best from all tested bulbs across classes.

Class C – The worst performing class. Because of its topology it has high GF over wide frequency ranges. The highest measured *GF* around 3. With rising IH frequency its *GF* does not decline very much. In immunity tests it notably underperforms incandescent bulb. Around 50 Hz it has immunity only 0.07 % of $U_1$ to produce $P_{st} = 1$. It is the lowest measured value across all samples. Its immunity does not rise with rising frequency around 1000 Hz it has immunity with applied IH only 0.23 % of $U_1$.

AC – The mixed class. Flicker sensitivity across this class varies. The most sensitive sample VT/69/-/1 reaches *GF* over 3. And $P_{st}$ over 13 with applied IH with magnitude 2 % of $U_1$. The least sensitive TP/30/-/1 reach *GF* around 0.3 and $P_{st}$ around 1.5 with applied IH with magnitude 2 % of $U_1$. Characteristic for this class is lower *GF* in frequency range 1- 100 Hz but significantly higher in upper frequency ranges. With increasing frequency immunity of tested bulbs do not significantly rise. The worst performing bulb VT/69/-/1 have minimum immunity only 0,08 %. As with the *GF* curves, immunity in frequency range 1-100 Hz is much higher than in frequency regions above.

D – Both samples have the highest *GF* in range 1 to 100 Hz. With rising frequency their sensitivity significantly decreases. To 600 Hz about factor of 10. Highest measured GF has sample VT/84/T/1 with value of 1.1. In the immunity tests by superimposed IH their immunity curves closely resemble incandescent lamp in frequency range 1-100 Hz.

Immunity curves have wide parts with immunity over 25 % of $U_1$ however due to the very unstable luminous flux output, they contain many blank parts without measured value. Especially the VT/84/T/1 sample, which in immunity test with applied rectangular AM modulation does not have a specified immunity much above 150 Hz.

# 6. THE LED LAMP MODEL

Emphasis of previous parts of thesis was on characterization and evaluation of large part of LED lamps parameters related to the flicker performance or spectral composition of their radiated flux. However, from obtained results is complicated to clearly understand which exact parameters of drivers are related to the differences within same class of LED drivers and how to exactly improve their current design to obtain low sensitivity to flicker. To be able to study and better understand influence of wide variety of LED lamps parameters on flicker performance without construction of physical model it is needed to have its mathematical model. Models of LED lamp are even great tool for manufacturers. By simulation of IH GF curves in the preproduction stage they may find out that their design has a flaw which does not manifest as an electrical problem. But, from standpoint of flicker it may create underperforming lamp, sensitive to flicker as for example EM/01/-/1. Which visibly draws same shaped WF of current as the others, but its driver was not able to regulate to constant output which leads to earlier mentioned dips in its luminous flux shown in Figure 30. Therefore, the aim of this chapter is to propose a model of the previously tested LED lamp and its verification based on measured data.

## 6.1 Designing and parametrization of LED lamp model

As a LED lamp model for simulation was chosen sample RE/96/-/1. It belongs to class C so it has CCR driver topology, performing very unsatisfactory across all tests focused on flicker performance. Model of its driver was inspired by [21]. As a SW for simulations Simulink was chosen. Its schematic is shown in Figure 67. Lamps of class C uses on the input DBR followed by CCR regulator which serves as dc/dc converter to limit current through LED chain. In this lamp model CCR is emulated by CCS (Constant current source). Because of nonlinear V-I characteristics of LED string and direct relation of dc to ac current. Real V-I characteristics of LED string has to be incorporated to CCS. So, the LED string is modelled as part of the CCS.

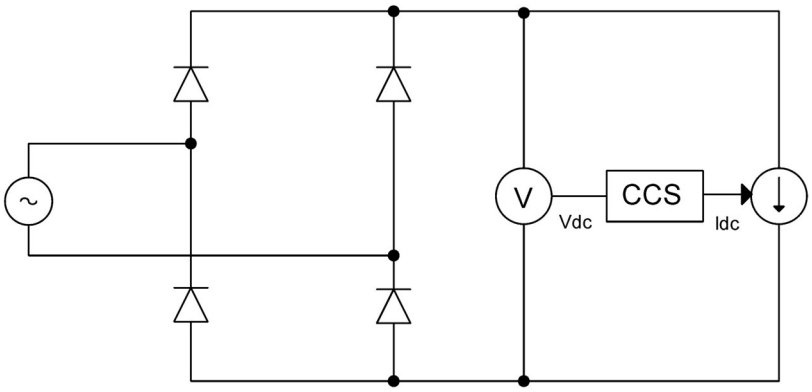


Figure 67 Principial schematic of designed lamp model

Parameters considered in this LED string model are forward voltage $V_F$, thermal potential including nonlinearity factor $V_T$ and $R_F$ on-state resistance.The CCS model realized in Simulink is shown in Figure 68.

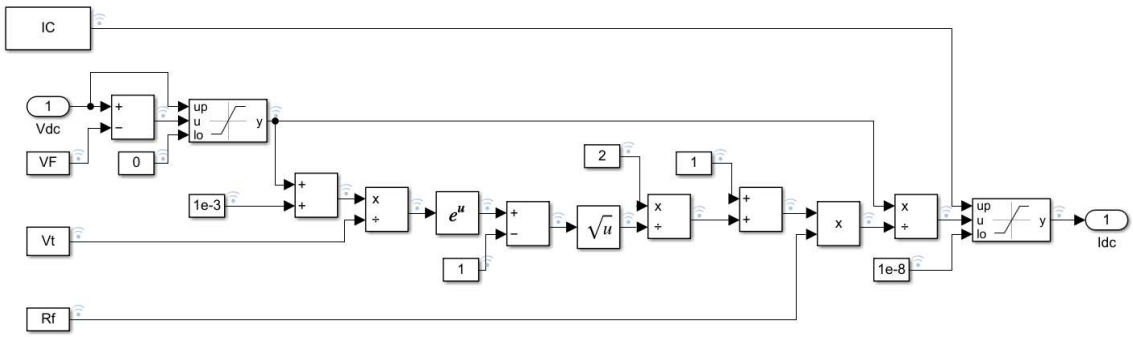


Figure 68 Model of CCS created in Simulink.

At the beginning of the simulation, it was needed to find values of parameters $V_F$, $V_T$, $R_F$, and $IC$, which denotes the maximal current through string. Values were found by the perfect match of simulated current WF and measured WF of current. Results of parametrization are showed in Figure 69. Obtained was perfect match between measured and simulated lamp. Values of used parameters are $V_F$ = 250 V, $V_T$ = 8.25 V, $R_F$ = 1400 Ω and $IC$ = 27,6 mA.

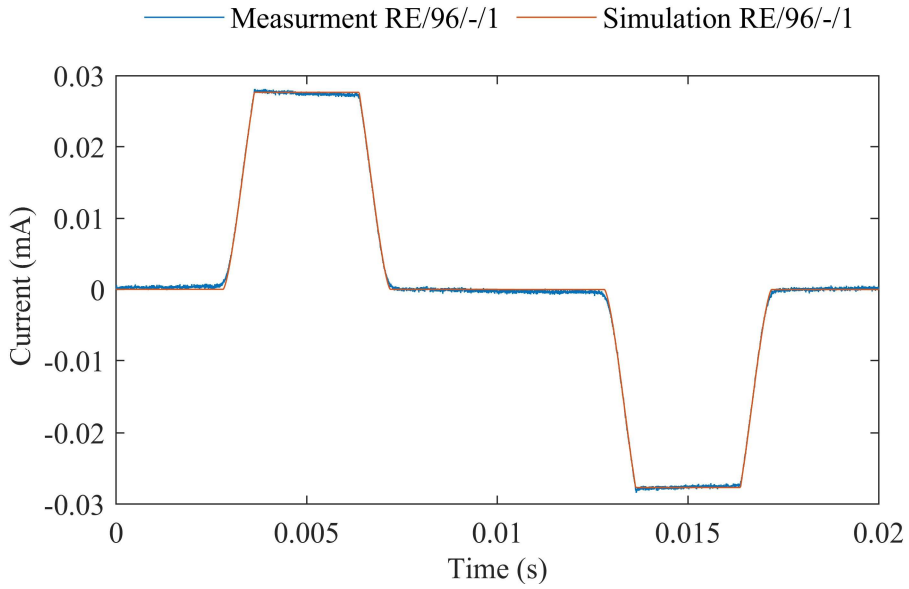


Figure 69 Comparison of measured and simulated WF of current

To evaluate output luminous flux from the model it was needed to create lamp model and follow the procedure shown in Figure 70. From the driver is calculated its instantaneous output power which serves as an input to lamp model. In lamp model is done smoothing and amplifying. On the output of lamp model is then finally luminous flux which should corresponds with measured values.

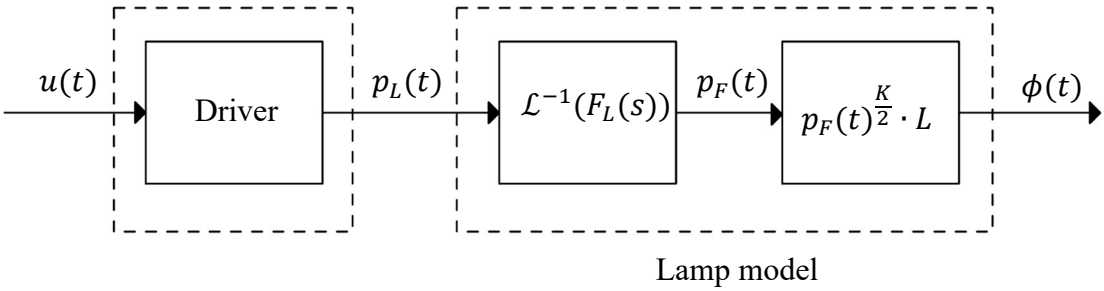


Figure 70 Overview of the simulated lamp model with procedure to obtain output luminous flux

Used smoothing transfer function is defined as:

$$F_L = \frac{1}{\frac{\tau_L}{10^6}s^2 + \tau_L s + 1} \tag{5.1}$$

Values of parameters included in the lamp model have to be figured out by simulation to match desired WF of luminous flux. Their values for simulation of sample RE/96/-/1 are equal to $\tau_L = 40 \cdot 10^{-6}$; $K = 0{,}85$; $L = 144$. Obtained results of simulation in comparison with measured values are depicted in Figure 71. Simulated results of luminous flux very well correspond to the measured luminous flux. And, thus simulation is now fully paramterized to serve as general model for RE/96/-/1.

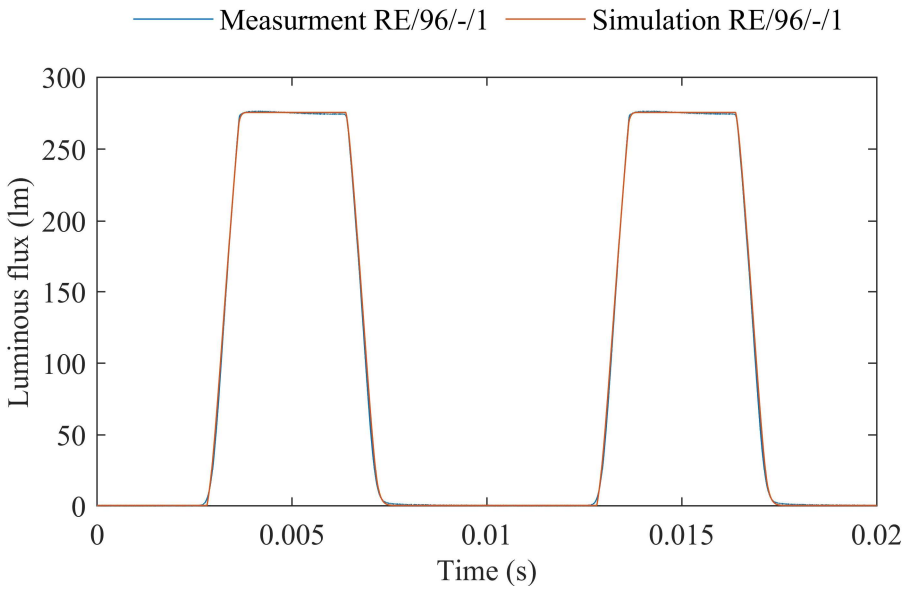


Figure 71 Comparison of measured and simulated WF of luminous flux

## 6.2 LED Lamp model verification

The lamp model described so far has only been validated on steady-state measurements under ideal power supply conditions. Therefore, it is needed to verify its correctness in states which are not specific and include IH components in its supply voltage. For this reason, the proposed model was tested on measurement of the IH GF curve. For this test a Simulink project was created to automatically measure *GF*. its schematic is shown in Figure 72. Model used for these simulations is placed in attachment Nr.5.

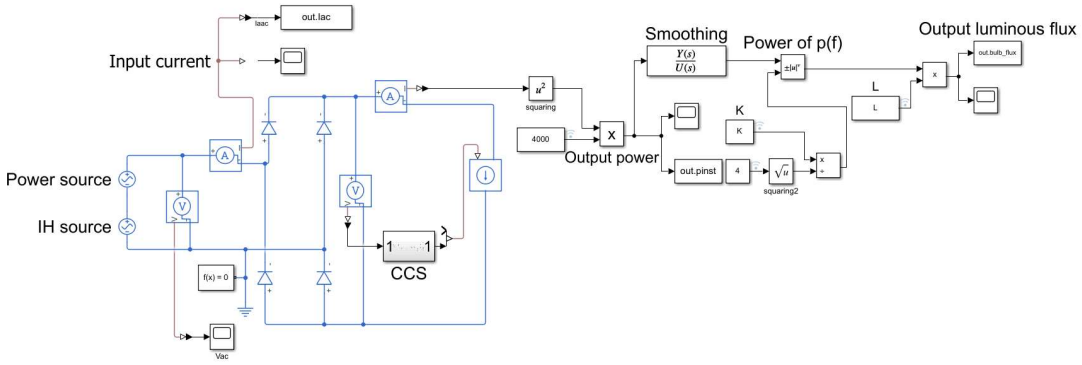


Figure 72 Simulink model for measuring IH GF curves

Similar model was used for previous parametrization tests, however the IH source was not needed. Controlling software in MATLAB automatically measures *GF* and changes frequency of IH source if measuring on a given frequency is over. Results from performed simulation in comparison with measured values of *GF* are shown in Figure 73.

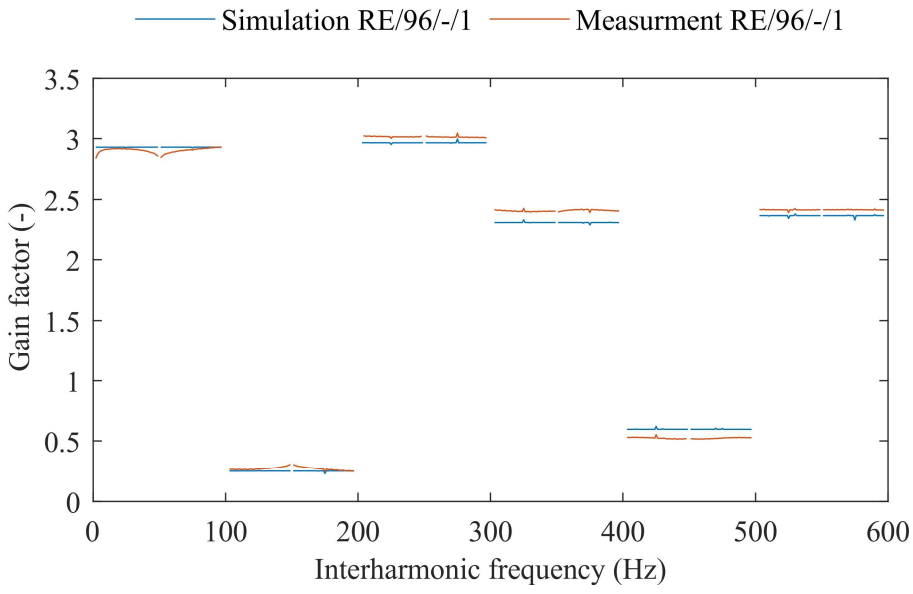


Figure 73 Comparison of measured and simulated IH GF curves of sample RE/96/-/1

It can be seen from Figure 73 that the IH GF curve obtained by simulation agrees very well with the measured IH GF curve. The highest difference between measured and simulated values are in frequency range 300 – 400 Hz. Here the difference is equal to -4.5 %. Thus, it can be concluded that the proposed model is able to provide sufficient accuracy.

## 6.3 Sensitivity analysis

The proposed LED lamp model was further used to analyse the dependence of *GF* on forward voltage $V_F$. Two additional VF values were tested, the first with VF = 125 V, which represents an LED string of half the length compared to the RE/96/-/1 sample, and the second with VF = 275, which represents a longer LED string. All other parameters were unchanged. Simulated drawn currents are depicted in Figure 74. LED lamps with lowest $V_F$ has the longest duration of conduction state because the instantaneous value of input voltage reach its value of $V_F$ as first.

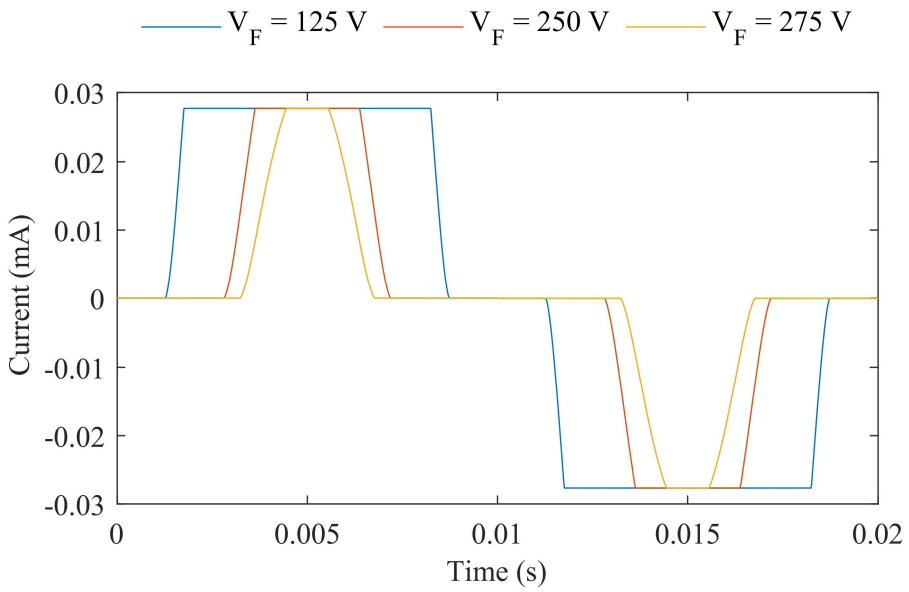


Figure 74 Currents drawn by LED lamps with different forward voltages.

Output luminous flux is then pictured in Figure 75. In comparison with drawn currents there are not so much visible differences. All curves have the same peak values of currents and then consequently the same peak values in luminous flux because their CCRs are set to the same output currents. Edges of curves are smoothed out by used smoothing function (5.1). The final results of analysis are depicted in Figure 76. As it can be seen value of $V_F$ have very high influence on *GF* of lamp. The lower the forward voltage the lower the *GF* and vice versa. LED lamp with $V_F$ of 275 V reached *GF* 7.5 in range from 1 to 100 Hz. This influence of $V_F$ value on overall flicker sensitivity is much likely linked with

time of rising and falling of current. By comparing currents in Figure 74 it can be seen that LED lamp with lowest $V_F$ have duration of their falling and rising edge much lower to their overall conduction time than LED lamps with higher values of $V_F$. Duration of rising and falling edge seems to play crucial role in flicker sensitivity. It is caused because CCRs during the falling and rising edge do not directly regulate output power and input signal is then translated to the output in this case to the luminous flux. For better understanding of this topic, it would be needed to conduct much more analyses with changing even other parameters. However, this analysis shows how even such underperforming lamp topology from the standpoint of flicker performance could be further improved.

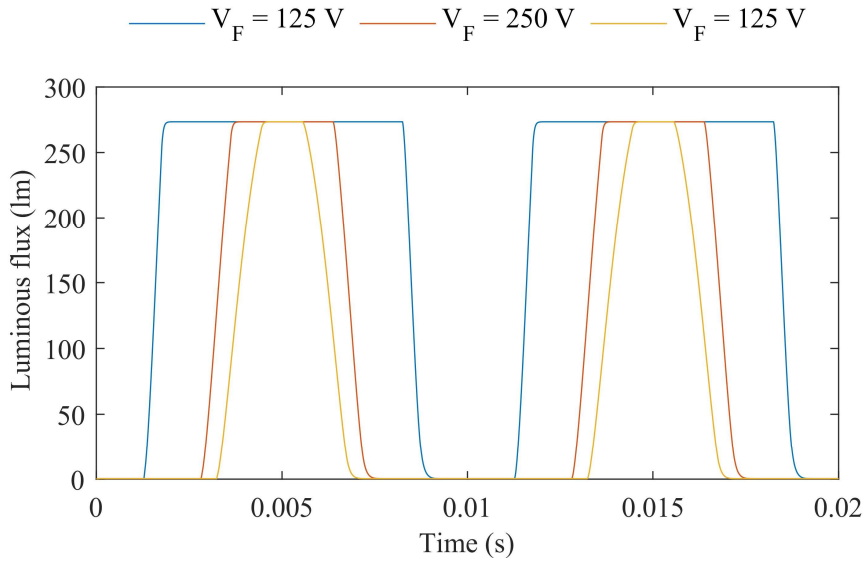


Figure 75 Output luminous flux of LED lamps with different values of forward voltages

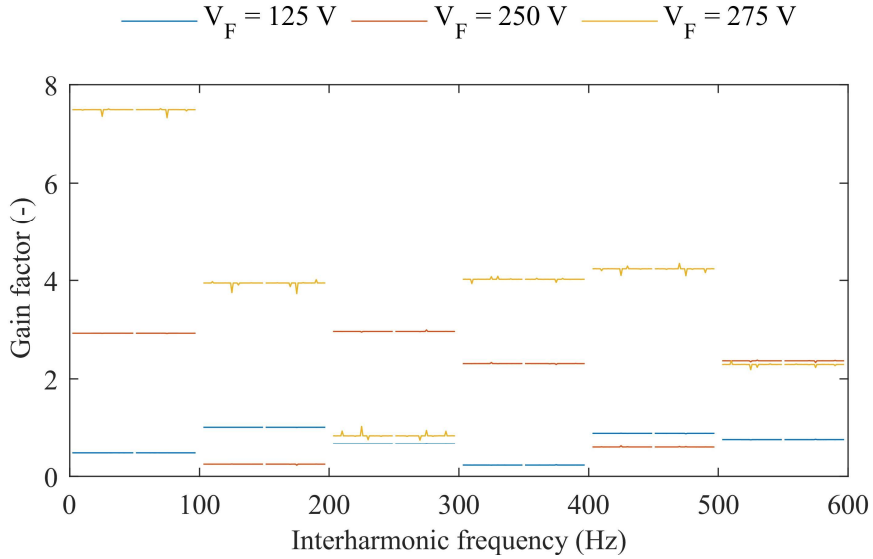


Figure 76 IH GF curves of LED lamps with different forward voltages

# 7. CONCLUSION

The thesis deals with the investigation and description of flicker performance of retrofit LED bulbs used in household applications with common sockets as E14, E27, G10. It categorises LED bulbs into groups according to the topology of their drivers and evaluates their overall flicker performance. In addition, at the end, the thesis propose an LED lamp model for simulation of IH GF curves.

In the first part, thesis mathematically by examples describe light flicker causes and shows voltage fluctuations sources of AM modulation, PM modulation and interharmonic distortion. It shows that AM modulation is mostly caused by variable load, PM modulation by changing configuration of UHV lines (phase jumps) and interharmonic distortion by PV inverters, PWM drivers and HVAC systems. With using EN 50160 it classifies supply voltage variations and rapid voltage changes as cause of light flicker. Further it shows how flicker sensitivity and immunity differs on various types of light sources.

Second part explore main part of the thesis, thus evaluation of various LED lamps parameters, characterisation of LED lamps, LED lamps drivers and designing of LED lamp model. It starts with market analyses. Which finds that the bestselling producers on market are Philips, V-TAC, EMOS with 36 %, 19 %, and 19 % market share respectively. LED technology used inside of bulbs is still by 84 % based on SMD LED chips, 13 % on LED filament and 3 % on SMD RGB chips. The bestselling LED bulbs are with socket E27 with market share 59 % followed by socket E14 with 16 % and G9 with 3 %. LED lamps with CCT in the range 4000-5000 K accounts for 51 % of market share, CCT in the range 2000 – 3000 K accounts for 45 % and CCT in the range 6000 – 6400 accounts for 4 %. Non-dimmable LED lamps prevail on the market with 93 % share followed by dimmable with 4 % and last are color changing with 3 %. With only slights changes described in the thesis the same composition of lamps was obtained for testing. Overall, 31 samples were acquired.

Further thesis examines all selected 31 samples by measuring their WFs of output luminous flux and drawn current under the ideal supply conditions. By current WFs and in some cases by disassembling are all lamps divided to 4 main groups A, C, AC and D. Moreover, on recorded values of drawn current and luminous flux is performed STFT in frequency range 10 - 250 kHz to study differences in switching process of drivers.

LED bulbs in group A have as ac/dc converter DBR followed by bulk capacitor and after the capacitor is dc/dc switch-mode converter to this group overall belong 24

samples. By current WFs, A group is divided intoto subgroups Aa and Ab. In current WF of group Ab is visible conduction in off-state by connected parallel component in ac side, usually it is capacitor in EMI filter. To group Aa belong 16 samples, so Ab is composed of 8 samples. This group exibits lowest measured SVM and $P_{st,LM}$ which indicates stable output of light. Raised percent flicker in this group usually means presence of switching frequency in output luminous flux. In sample TE/40/-/1 because of its short on-state, the highest $THD_I$ was measured from all samples with a value of 176,4 %. Results from STFT shows that this class could be characterised only by 3 different patterns occurring in current spectrograms. Samples in current or luminous flux in the analysed range of STFT contain FM modulated components.

To group C belong only one sample. Topology is composed of DBR which is followed by CCR, bulk capacitor as well as EMI filter is not necessary. Bulb in this group because of its principle of function reached percent flicker of 100 % and SVM 6.231. Its $THD_I$ is relatively low equal to 68 %. Spectrograms from STFT do not have any signs of a switch-mode function of the driver.

To group AC belong LED lamps with DBR at input which is followed by first CCR limiting current through bulk capacitor and by second CCR limiting the current through the LED string. This group is composed of 4 samples. Sample VT/61/-/1 has SVM of 0.617. Spectrograms form STFT look very similar to spectrograms of group C which denotes very close topology. Beside sample TP/30/-/1 no frequencies related to switch-mode driver are visible.

To group D belong 2 LED lamps samples with active PF correction with single stage switch-mode dc/dc converter. STFT shows very similar spectrogram between samples. Both samples have higher SVM of 0.33 and 0.41. This class has specific $THD_I$ in range from 30 to 41 %.

Thesis further evaluates spectral parameters of radiant flux. From measured spectral parameters as *CCT* and *CRI* follows, that measured CCT from nominal on average differs by 1.54 %. And measured *CRI* from nominal is on average higher by 4.84 %.

Then are performed and described flicker sensitivity and immunity measurements. Following their results class, A is the best performing class. Differences between Aa and Ab are not found in those tests. The least sensitive sample across all categories was found in this group it is TE/40/-/1 with *GF* in range 1-600 Hz around $10^{-3}$. Immunity of tested sample PH/67/-/1 is highest among all samples. Class C was found as the worst performing class. The highest measured GF is 3 and around 50 Hz it has

immunity only 0.07 % of $U_1$ for $P_{st}$ = 1. Class AC is mixed by performance. Hovewer even the best performing samples are not comparable to class A. The worst performing bulbs VT/61/-/1 have minimum immunity with applied IH only 0,08 % of $U_1$ for $P_{st}$ = 1. Characteristic for this group is higher immunity and lower gain in range 1 – 100 Hz than on higher frequency ranges. Class D have highest measured *GF* in frequency range 1- 100 Hz. Its GF decline to 600 Hz by a factor of 10. Its immunity curves resembles an incandescent bulb.

In the last part is proposed and verified LED lamp model of sample RE/96/-/1 belonging to class C. Its simulated results are compared with measured IH GF curves. The highest difference between measured and simulated values is only -4.5 %. So the proposed model could be used for simulation of IH *GF* curves of LED lamps belonging to class C. Further were conducted sensitivity analyses. Which analyse the influence of forward voltage of LED lamp on its *GF* performance. It finds out that *GF* performance is directly linked with $V_F$ of LED lamps, and it further discussed its causes.

In the last part, a model of LED lamp sample RE/96/-/1 belonging to class C is proposed and verified. Its simulated results are compared with the measured IH GF curves. The largest difference between measured and simulated values is only -4.5%. Thus, the proposed model can be used to simulate the IH GF curves of LED lamps belonging to class C. Next, sensitivity analyses are performed. Which analyses the effect of the forward voltage of the LED lamp on its IH *GF* curves. The *GF* performance was found to be directly related to the $V_F$ of the LED lamps. In the end it is discussed possible cause of this relation between $V_F$ and *GF*.

Upon exploring the research and analysis in this thesis, it is recommended to further continue to disassemble LED lamps in each group and find how circuits within one topology differ. Found results will help more exactly show differences within one topology and possibly explain various spectrogram patterns occurring within one group. Further it will be needed to explore possible ways of flicker mitigation in LED lamps of class C from results found in sensitivity analyses.

# LITERATURE


[1] KARLICEK, R., SUN, C.-C., GEORGES ZISSIS, MA, R. and Springerlink (Online Service (2019). *Handbook of Advanced Lighting Technology*. Cham: Springer International Publishing.

[2] COLLIN, A.J., DJOKIC, S.Z., DRAPELA, J., LANGELLA, R. AND TESTA, A. (2019). Light Flicker and Power Factor Labels for Comparing LED Lamp Performance. *IEEE Transactions on Industry Applications*, 55(6), pp.7062–7070.

[3] IEEE Recommended Practices for Modulating Current in High-Brightness LEDs for Mitigating Health Risks to Viewers. (2015). *IEEE Std 1789-2015*

[4] CIE TN 006:2016. Visual Aspects of Time-Modulated Lighting Systems – Definitions and Measurement Models

[5] DRAPELA, J., LANGELLA, R., TESTA, A., COLLIN, A.J., ZHENG, S. AND DJOKIC, S.Z. (2018). Experimental evaluation and classification of LED lamps for light flicker sensitivity. *2018 18th International Conference on Harmonics and Quality of Power (ICHQP)*

[6] BAGGINI, A. (2008). *Handbook of Power Quality*. 111 River Street, Hoboken, NJ 07030, USA: John Wiley & Sons, p.611. ISBN: 9780470754238.

[7] DRAPELA, J. (2014). *Kvalita elektricke energie a EMC*. [online] Available at: https://moodle.vut.cz/pluginfile.php/405781/mod_resource/content/0/PQ1_predna sky_KISP_v2022_2.pdf [Accessed 12 Jan. 2023].

[8] F.F., a s (2023). *ČEZ Distribuce připojila do sítě za loňský rok rekordních 21 325 fotovoltaických elektráren.* [online] Skupina ČEZ - O Společnosti. Available at: https://www.cez.cz/cs/pro-media/tiskove-zpravy/cez-distribuce-pripojila-do-site-za-lonsky-rok-rekordnich-21-325-fotovoltaickych-elektraren-173010 [Accessed 23 Jan. 2023].

[9] ARIYA SANGWONGWANICH, YANG, Y., SERA, D. AND FREDE BLAABJERG (2017). Interharmonics from grid-connected PV systems: Mechanism and mitigation. *2017 IEEE 3rd International Future Energy Electronics Conference and ECCE Asia (IFEEC 2017 - ECCE Asia)*.

[10] DEROSA, F., LANGELLA, R., SOLLAZZO, A. AND TESTA, A. (2005). On the Interharmonic Components Generated by Adjustable Speed Drives. *IEEE Transactions on Power Delivery*, 20(4), pp.2535–2543.

[11] IEC 61000-4-15:2010. Electromagnetic compatibility (EMC) - Part 4-15: Testing and measurement techniques - Flickermeter - Functional and design specifications

[12] EN 50160:2021. Voltage characteristics of electricity supplied by public electricity networks

[13] IEEE Std 1453-2015. IEEE Recommended Practice for the Analysis of Fluctuating Installations on Power Systems

[14] DRAPELA, J., LANGELLA, R., SLEZINGR, J. AND ANTONIA CARLA TESTA (2018). Generalized lamp model for light flicker studies. 154, pp.413–422.

[15] KUKACKA, L. AND DRAPELA, J. (2020). A Preliminary Study on Modeling of Voltage Induced Flicker Sensitivity of Fluorescent and LED Lamps with Closed-Loop Control. *2020 19th International Conference on Harmonics and Quality of Power (ICHQP)*.

[16] DRAPELA, J., KRATKY, M., WEIDINGER, L. AND ZAVODNY, M. (2005). Light flicker of fluorescent lamps with different types of ballasts caused by interharmonics. *2005 IEEE Russia Power Tech*.

[17] eur-lex.europa.eu. (n.d.). *Commission Regulation (EU) 2019/2020 of 1 October 2019 layin... - EUR-Lex*. [online] Available at: https://eur-lex.europa.eu/legal-content/en/LSU/?uri=CELEX:32019R2020&qid=1688036695546 [Accessed 15 Jan. 2023].

[18] PRICE, L.L.A. (2017). Can the Adverse Health Effects of Flicker from LEDs and Other Artificial Lighting Be Prevented? *LEUKOS*, 13(4), pp.191–200. doi:https://doi.org/10.1080/15502724.2017.1316669.

[19] IEA. (n.d.). *Global lighting sales in the Net Zero Scenario, 2010-2030 – Charts – Data & Statistics*. [online] Available at: https://www.iea.org/data-and-statistics/charts/global-lighting-sales-in-the-net-zero-scenario-2010-2030 [Accessed 22 Jan. 2023].

[20] DRAPELA, J. AND SLEZINGR, J. (2012). Design and utilization of a light flickermeter. *2012 IEEE International Workshop on Applied Measurements for Power Systems (AMPS) Proceedings*. doi:https://doi.org/10.1109/amps.2012.6344007.

[21] COLLIN, A.J., DJOKIC, S.Z., DRAPELA, J., GUO, Z., LANGELLA, R., TESTA, A. AND WATSON, N.R. (2020). Analysis of Approaches for Modeling the Low Frequency Emission of LED Lamps. *Technology Evolution and Power Quality Issues in Designing Future Lighting Systems*, 13(7), pp.1571–1571. doi:https://doi.org/10.3390/en13071571.

# SYMBOLS AND ABBREVIATIONS

Abbreviations:

| | |
|---|---|
| aPFC | Active power factor correction |
| PFC | Power factor correction |
| LED | Light emitting diode. |
| AM | Amplitude modulation |
| PM | Phase modulation |
| FM | Frequency modulation |
| SVM | Stroboscopic effect visibility measure |
| CFL | Compact fluorescent lamp |
| CCR | Constant current regulator |
| MPPT | Maximum Power Point Tracking |
| RMS | Root mean square |
| UHV | Ultra high voltage |
| LFI | Light flicker index |
| EMI | Electromagnetic interference |
| HV | High voltage |
| WF | Waveform |
| LV | Low voltage |
| PV | Photovoltaics |
| HVAC | Heating, ventilation, and air conditioning |
| PWM | Pulse Width Modulation |
| DBR | Diode bridge rectifier |
| THD | Total harmonic distortion |
| DFT | Dicrete fourier transform |
| STFT | short-time fourier transform |
| FFT | Fast Fourier transform |
| CCS | Constant current source |

Symbols:

| | | |
|---|---|---|
| $GF$ | Gain Factor | (-) |
| $Mod\%$ | Percent flicker | (-) |
| $U_{\mathrm{IH}}$ | Interharmonic component voltage | (V) |
| $\Delta U$ | Voltage drop | (V) |
| $P_{\mathrm{st}}$ | Short term flicker severity index | (-) |
| $P_{\mathrm{lt}}$ | Long-term flicker severity index | (-) |
| $\overline{U}_Z$ | Voltage across load | (V) |
| $\overline{U}_G$ | Supply voltage of grid | (V) |
| $f_{vis}$ | Visible frequency of luminous flux | (Hz) |

| | | |
|---|---|---|
| $\Phi$ | Luminous flux | (lm) |
| $\Delta U$ | Modulation depth | (%) |
| $U_{1,}\ U_{1h}$ | Voltage on fundamental frequency | (V) |
| $V_F$ | Forward voltage | (V) |
| $R_F$ | on-resistance | (Ω) |
| $V_F$ | nonlinearity factor | (V) |
| $IC$ | Maximum current through circuit | (A) |
| $\delta_{CRI}$ | Difference between nominal and measured CRI | (%) |
| $\delta_{CCT}$ | Difference between nominal and measured CCT | (%) |
| $K_p$ | The lamp efficacy | (%) |
| $P_{st,LM}$ | Short term flicker severity index of output light | (-) |
| $THD_I$ | Total harmonic distortion of current | (%) |
| $PF$ | Power factor | (-) |
| $SVM$ | Stroboscopic effect visibility measure | (-) |
| $CCT$ | Correlated Color Temperature | (K) |
| $CRI$ | Color Rendering Index | (-) |
| $CCT_M$ | Measured value of $CCT$ | (K) |
| $CCT_N$ | Nominal value of $CCT$ | (K) |
| $CRI_M$ | Measured value of $CRI$ | (-) |
| $CRI_N$ | Nominal value of $CRI$ | (-) |

# Appendix A - Electronic attachment

| Nr. | NAME |
|---|---|
| 1 | 1_CATALOG_DATA |
| 2 | 2_FREQUENCY_SPECTRA |
| 3 | 3_SPECTROGRAMS |
| 4 | 4_RADIOMETRIC_SPECTRA |
| 5 | 5_LAMP_MODEL |